SLAC–PUB–6304
July 1993
T/E

NEW PERSPECTIVES IN QUANTUM CHROMODYNAMICS*

STANLEY J. BRODSKY

Stanford Linear Accelerator Center

Stanford University, Stanford, California 94309

Invited Lectures presented at the Symposium/Workshop
"Particle Physics at the Fermi Scale"
Beijing, People's Republic of China
May 27–June 4, 1993

* Work supported by the Department of Energy, contract DE–AC03–76SF00515.

NEW PERSPECTIVES IN QUANTUM CHROMODYNAMICS

STANLEY J. BRODSKY

Stanford Linear Accelerator Center
Stanford University, Stanford, California 94309

ABSTRACT In these lectures I will discuss three central topics in quantum chromodynamics: (1) the use of light cone quantization and Fock space methods to determine the long and short-distance structure of quark and gluon distributions within hadrons; (2) the role of spin, heavy quarks, and nuclei in unraveling fundamental phenomenological features of QCD; and (3) a new approach to understanding the scale and scheme dependence of perturbative QCD predictions.

1. INTRODUCTION

One of the most challenging problems in theoretical high energy physics is to compute the bound-state structure of the proton and other hadrons from quantum chromodynamics (QCD), the field theory of quarks and gluons. The goal is to not only calculate the spectrum of hadron masses from first principles, but also to derive the momentum and spin distributions of the quarks and gluons which control high energy hadron interactions. In the first chapter, I will discuss new methods based on "light-cone" quantization which have been proposed as alternatives to lattice theory for solving non-perturbative problems in QCD and

other field theories. The basic idea is a generalization of Heisenberg's pioneering matrix formulation of quantum mechanics: if one could numerically diagonalize the matrix of the Hamiltonian representing the underlying QCD interaction, then the resulting eigenvalues would give the hadron spectrum, while the corresponding eigenstates would describe each hadron in terms of its quark and gluon degrees of freedom.

The new ingredient which appears to make this method tractable is quantization on the light-cone—which sets boundary conditions as if the observer were travelling at the speed of light! For example, if one shines a laser directed along the z-axis on an atom, the scattered photons determine the coordinates of each electron at a fixed value of $t - z/c$. One then can use the equations of motion of quantum electrodynamics QED to predict the coordinates of the electrons at later values of $t - z/c$.

The foundations of light-cone quantization date back to Dirac, who in 1949 showed that there are remarkable advantages in quantizing relativistic field theories at fixed "light-cone time" $t - z/c$ rather than ordinary time. In the traditional formulation, handling a moving bound state is as complicated as diagonalizing the Hamiltonian itself. On the other hand, quantization on the light-cone can be formulated without having to choose a specific frame of reference. Thus a light-cone QCD Hamiltonian describes bound states of confined relativistic quarks and gluons of arbitrary four-momentum. It also provides a precise definition of hadron structure in terms of quarks and gluons and a general calculus for computing relativistic scattering amplitudes, form factors, electroweak transitions, and other hadronic phenomena.

The problem of computing the hadronic spectrum and the corresponding light-cone wavefunctions of QCD can thus be reduced to the diagonalization of a matrix representation of the light- cone Hamiltonian. This method, called "discretized light-cone quantization" (DLCQ), has now been successfully applied to a number of quantum field theories in one-space and one-time dimension, including QCD, quantum electrodynamics, Yukawa models, and the two-dimensional matrix models of superstring theory. For QCD(1+1), complete numerical solutions for the spectrum and light-cone wavefunctions can be obtained as a function of the coupling strength, the quark masses, and the number of flavors and colors.

Light-cone quantization of QCD in physical space-time is a highly

challenging numerical computational problem. In the DLCQ method, developed by H. C. Pauli and myself, the size of the quark and gluon basis and the discretization of the transverse momenta quickly leads to very large matrices. In addition, the Hamiltonian must be supplemented by renormalization terms. Approximate methods have been developed which use effective light-cone Hamiltonians and a truncation of the quark and gluon basis states (the "Light-Front Tamm-Dancoff method") or a combination of light-cone quantization with traditional lattice gauge theory in the transverse dimensions. In the case of quantum electrodynamics in 3+1 dimensions, the positronium spectrum has been obtained at large coupling strength ($\alpha = 0.3$) by solving an integral equation derived from the truncated QED light-cone Hamiltonian.

The most subtle problem now confronting light-cone quantization methods is how to understand the spontaneous symmetry breaking normally associated with the structure of the vacuum. In light-cone quantization the momentum-independent "zero modes" of the quantum fields are determined from constraint equations derived from the equations of motion of the theory. Although the vacuum is simple in light-cone quantization, the values of the zero modes determine the phase and physics of the theory. There are other fundamental renormalization and gauge invariance issues that still have to be completely understood, such as how symmetries lost in the truncation to a finite basis of free quark and gluon states can be restored, how to deal consistently with massless particles, and how to control singularities. All of these problems make the field quite exciting and challenging.

In addition to its potential for solving QCD problems, light-cone quantization has already led to many new insights into the quantization of gauge theories. Light-cone quantization not only provides a consistent language for representing hadrons as QCD bound-states of relativistic quarks and gluons, but it also provides a novel method for simulating quantum field theory on a computer and understanding non-perturbative features of QCD.

In the second chapter, I will discuss a number of interesting spin, heavy quark, and nuclear effects which test fundamental features of perturbative and non-perturbative QCD. These include constraints on the shape and normalization of the polarized quark and gluon structure functions of the proton; the principle of hadron helicity retention in high x_F inclusive reactions; predictions based on total hadron he-

licity conservation in high momentum transfer exclusive reactions; the dependence of nuclear structure functions and shadowing on virtual photon polarization; and general constraints on the magnetic moment of hadrons. I also will discuss the implications of several measurements which are in striking conflict with leading-twist perturbative QCD predictions, such as the extraordinarily large spin correlation A_{NN} observed in large angle proton-proton scattering, the anomalously large $\rho\pi$ branching ratio of the J/ψ, and the rapidly changing polarization dependence of both J/ψ and continuum lepton pair hadroproduction observed at large x_F.

In the third chapter, which is based on recent work with Hung Jung Lu, I will discuss a crucial problem in perturbative quantum chromodynamics: the setting of the renormalization scale in perturbative QCD predictions. First I discuss the use of generalized renormalization group equations which allow a careful analysis of the theoretical error when the scale is unspecified. I also discuss difficulties encountered when one uses various scale setting procedures. I then discuss the validity and use of the automatic scale fixing procedure developed by Lepage and Mackenzie and myself.

2. LIGHT-CONE QUANTIZATION AND QCD

A primary goal of particle physics is to understand the structure of hadrons in terms of their fundamental quark and gluon degrees of freedom. It is important to predict not only the spectrum of the hadrons, but also to derive from first principles the hadron structure functions that control inclusive reactions, the form of the hadron distribution amplitudes that control exclusive processes, and the behavior of the fragmentation functions which control the transition between quark and gluon jets and hadrons. Such questions will evidently require an understanding of confinement and other properties of non-perturbative quantum chromodynamics at the amplitude level. The first, but non-trivial, step toward this goal is to give a consistent definition of hadron wavefunctions, the amplitudes which describe a composite system consisting of an arbitrary number of confined relativistic quarks and gluons.

There are many reasons why detailed information on hadron wavefunctions in QCD is critical for future progress in particle physics. For

example, in electroweak theory, the central unknown required for reliable calculations of weak decay amplitudes are the hadronic matrix elements: the computation of the B meson decay into particular hadron channels requires detailed knowledge of both the light and heavy hadron wavefunctions. The coefficient functions in the operator product expansion needed to compute leading and higher twist structure functions and other inclusive cross sections are also essentially unknown. Form factors and exclusive scattering processes depend in detail on the basic amplitude structure of the scattering hadrons in a general Lorentz frame. Even the calculation of the proton magnetic moment requires an understanding of hadron wavefunctions in a boosted frame.

In this chapter I will discuss the light-cone quantization of gauge theories from two perspectives: as a language for representing hadrons as QCD bound-states of relativistic quarks and gluons, and also as a novel method for simulating quantum field theory on a computer. The light-cone Fock state expansion of wavefunctions at fixed light-cone time in fact provides a precise definition of the parton model and a general calculus for hadronic matrix elements. The Hamiltonian formulation of quantum field theory quantized at fixed light-cone time has led to new non-perturbative calculational tools for numerically solving quantum field theories.[1] In particular, the "discretized light-cone quantization," method (DLCQ)[2] has been successfully applied to several gauge theories, including QCD in one-space and one-time dimension, and quantum electrodynamics in physical space-time at large coupling strength. Other non-perturbative methods based on light-cone quantization, such as the transverse lattice[3] and the Light-Front Tamm-Dancoff method[4] are also being developed as new alternatives to conventional lattice gauge theory.

There have been relatively few calculations of the wavefunctions of hadrons from first principles in QCD. The most interesting progress has come from QCD sum rule calculations,[5] and lattice gauge theory[6,7] both of which have provided predictions for the lowest moments $\langle x_i^n \rangle$ of the proton's distribution amplitude, $\phi_p(x_i, Q)$. The distribution amplitude is the fundamental gauge invariant wavefunction which describes the fractional longitudinal momentum distributions of the valence quarks in a hadron integrated over transverse momentum up to the scale Q.[8] However, the results from the two analyses are in strong

disagreement: the QCD sum rule analysis predicts a strongly asymmetric three-quark distribution (see Fig. 1), whereas the lattice results,[7] obtained in the quenched approximation, favor a symmetric distribution in the x_i. Models of the proton distribution amplitude based on a quark–di-quark structure suggest strong asymmetries and strong spin-correlations in the baryon wavefunctions.[9] Even less is known from first principles in non-perturbative QCD about the gluon and non-valence quark contributions to the proton wavefunction, although data from a number of experiments now suggest non-trivial spin correlations, a significant strangeness content, and a large x component to the charm quark distribution in the proton.[10]

It is also interesting to note that light-cone wavefunctions of the projectile hadron in large measure control the distributions of final state hadrons produced in the fragmentation region of inclusive processes $AB \to CX$. At high energies, the Fock states of large invariant mass $\mathcal{M}$ survive for times $T = 2P_{\rm lab}/\mathcal{M}^2$ and are materialized by the interactions of the slowest parton spectators in the target. Because of color screening, small color singlet configurations in the projectile Fock state can penetrate the target with minimal QCD interactions whereas large transverse size color fluctuations interact strongly in the target. These considerations can help explain many of the features of Feynman-scaling distributions, including the nuclear dependence on x_F and the size of the multiplicity fluctuations and leading charm production. Further details may be found in Ref. 11.

By far the simplest and most intuitive representation of relativistic bound state wavefunctions is the light-cone Fock expansion. In 1949 Dirac[12] showed that there are remarkable advantages of quantizing relativistic field theories at fixed "light-cone time" $\tau = t + z/c$ rather than ordinary time. In the traditional equal-time Hamiltonian formulation none of the Poincare operators that generate Lorentz boosts commute with the Hamiltonian; thus computing a boosted wavefunction is as complicated a dynamical problem as diagonalizing the Hamiltonian itself. On the other hand, quantization on the light-cone can be formulated without reference to the choice of a specific Lorentz frame; the eigensolutions of the light-cone Hamiltonian, the generator of translations in τ, describe bound states of arbitrary four-momentum, allowing the computation of scattering amplitudes and other dynamical quantities. Another remarkable feature of this formalism is the apparent

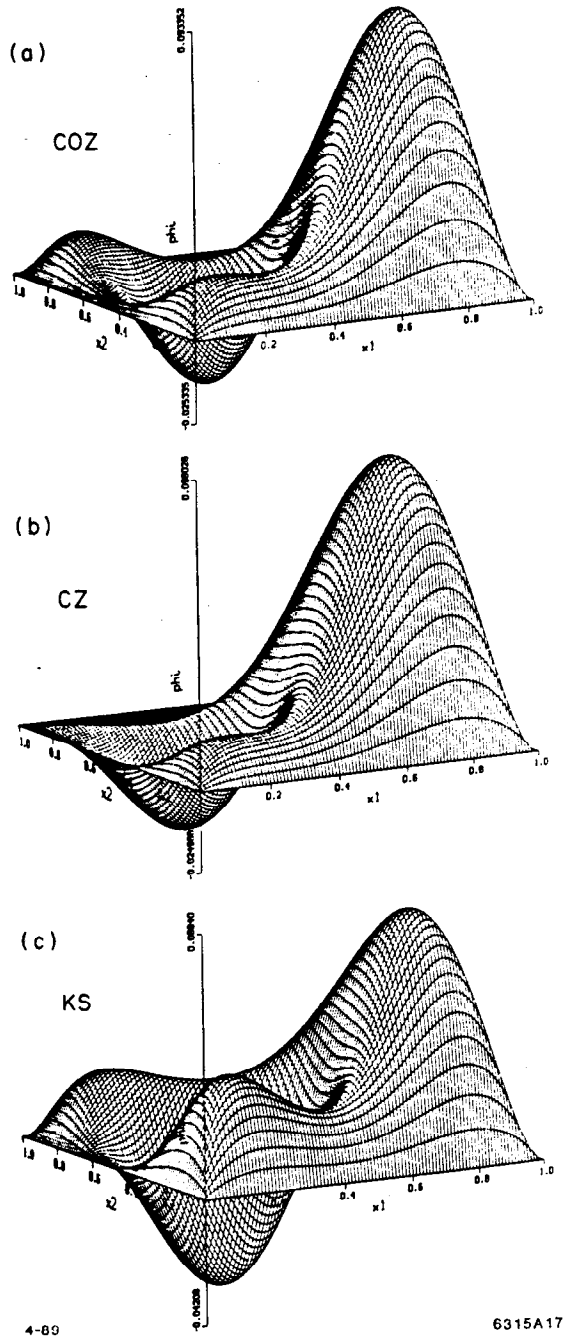

Figure 1. The proton distribution amplitude $\phi_P(x_i, \mu)$ evaluated at the scale $\mu \sim 1$ GeV from QCD sum rules.[5] The enhancement at large x_1 corresponds to a strong positive correlation when the u quark with spin parallel to that of the proton has a high momentum fraction.

simplicity of the light-cone vacuum. In many theories the vacuum state of the free Hamiltonian is an eigenstate of the total light-cone Hamiltonian. In principle, the Fock expansion constructed on this vacuum state provides a complete relativistic many-particle basis for diagonalizing the full theory.

There are advantages of light-cone quantization even in ordinary quantum mechanics. Consider an experiment which could specify the initial wavefunction of a multi-electron atom. Determining $\Psi(\vec{r}_i, t = 0)$, $i = 1, \ldots n$ would require the simultaneous measurement of the positions of the n bound electrons. In principle this could be carried out by the simultaneous Compton scattering of n independent laser beams on the atom. In contrast, determining the initial wavefunction at a fixed light-cone time τ requires only the scattering of one plane-wave laser beam since the signal reaching each of the electrons is received along the light front at the same light-cone time $\tau = t_i + z_i/c$.

In the case of perturbation theory, light-cone quantization has overwhelming advantages over standard time-ordered perturbation theory. In order to calculate a Feynman amplitude of order g^n in TOPTH one must suffer the calculation of n time-ordered graphs, each of which is a non-covariant function of energy denominators which, in turn, consist of sums of complicated square roots $p_i^0 = \sqrt{\vec{p}_i^2 + m_i^2}$. On the other hand, in light-cone perturbation theory (LCPTH), only a relatively few graphs give non-zero contributions, and those that are non-zero have light-cone energy denominators which are simple sums of rational forms $p^- = (\vec{p}_{\perp i}^2 + m_i^2)/p_i^+$. An analog of light-cone perturbation theory has in fact been used to calculate the anomalous magnetic moment to two loops in QED.[13]

In light-cone quantization, a free particle is specified by its four momentum $k^\mu = (k^+, k^-, k_\perp)$ where $k^\pm = k^0 \pm k^3$. Since it has positive energy, its light-cone energy is also positive: $k^- = (k_\perp^2 + m^2)/k^+ > 0$. In perturbation theory, transverse momentum $\sum k_\perp$ and the plus momentum $\sum k^+$ are conserved at each vertex. The light-cone bound-state wavefunction thus describes constituents which are on their mass shell, but off the light-cone energy shell: $P^- < \sum k_i^-$.

In principle, the problem of computing the spectrum in QCD and the corresponding light-cone wavefunctions for each hadron can be reduced to the diagonalization of the Fock state matrix representation

of the QCD light-cone Hamiltonian in analogy to Heisenberg quantum mechanics. Any hadron state must be an eigenstate of the light-cone Hamiltonian. (For convenience we will work in the "standard" frame where $\underline{P}_\pi \equiv (P^+, P_\perp) = (1, 0_\perp)$ and $P_\pi^- = M_\pi^2$.) Thus the state $|\pi\rangle$ satisfies an equation

$$\left(M_\pi^2 - H_{LC}\right)|\pi\rangle = 0. \tag{1}$$

Projecting this onto the various Fock states $\langle q\bar{q}|$, $\langle q\bar{q}g|\ldots$ results in an infinite number of coupled integral eigenvalue equations,[8]

$$\left(M_\pi^2 - \sum_i \frac{\vec{k}_{\perp i}^2 + m_i^2}{x_i}\right)\begin{bmatrix}\psi_{q\bar{q}/\pi}\\ \psi_{q\bar{q}g/\pi}\\ \vdots\end{bmatrix} \tag{2}$$

$$= \begin{bmatrix}\langle q\bar{q}|V|q\bar{q}\rangle & \langle q\bar{q}|V|q\bar{q}g\rangle & \cdots\\ \langle q\bar{q}g|V|q\bar{q}\rangle & \langle q\bar{q}g|V|q\bar{q}g\rangle & \cdots\\ \vdots & \vdots & \ddots\end{bmatrix}\begin{bmatrix}\psi_{q\bar{q}/\pi}\\ \psi_{q\bar{q}g/\pi}\\ \vdots\end{bmatrix}$$

where V is the interaction part of H_{LC}. Diagrammatically, V involves completely irreducible interactions—*i.e.* diagrams having no internal propagators—coupling Fock states. (See Fig. 2.) The explicit forms of each matrix element of V are given in Ref. 2. In principle,the solutions to these equations determine not only the hadronic spectrum of QCD but also the light-cone wavefunctions needed to compute hadronic amplitudes.

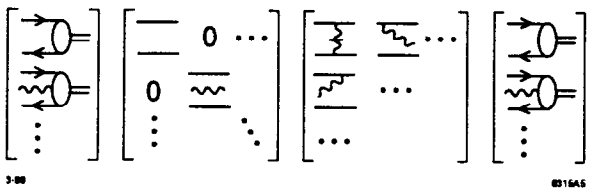

Figure 2. Coupled eigenvalue equations for the light-cone wavefunctions of a pion.

Recently a new numerical method, discretized light-cone quantization (DLCQ), has been developed to diagonalize the light-cone Hamiltonian on a covariantly regulated discrete basis.[2] By imposing periodic or anti-periodic boundary conditions of the fields in x^- and $x_\perp$, and an upper bound on the invariant mass of the particles in the Fock space

$$\mathcal{M}_0^2 = \sum_{i=1}^{n} \left(\frac{k_\perp^2 + m^2}{x} \right)_i < \Lambda^2$$

(the "global cutoff"), one obtains a discrete momentum space matrix representation of the light-cone Hamiltonian. The DLCQ method thus provides a new type of computer simulation of quantum field theories in momentum space. Since only relative coordinates appear, the formulation is completely independent of the total momentum p^+ and $\vec{p}_\perp$ of the system. By using light-cone gauge, only the minimum number of physical degrees of freedom appear in the simulation. Unlike lattice gauge theory, DLCQ has no fermion doubling problem.

The DLCQ method thus converts the problem of solving a quantum field theory to the diagonalization of the light-cone Hamiltonian on a discrete Fock-space basis

$$\langle n \,|\, H_{LC} \,|\, m \rangle \;\; \langle m \,|\, \psi \rangle = \mathcal{M}^2 \, \langle n \,|\, \psi \rangle \;\; .$$

Its most dramatic success has been the applications to quantum field theories in one-space and one-time dimensions. The DLCQ method was first used to obtain the mass spectrum and wavefunctions of Yukawa theory, $\overline{\psi}\psi\phi$, in one-space and one-time dimensions.[14] This success led to further applications including QED(1+1) for general mass fermions and the massless Schwinger model by Eller *et al.*,[15] ϕ^4 theory in 1+1 dimensions by Harindranath and Vary,[16] and QCD(1+1) for N_C = 2,3,4 by Hornbostel *et al.*[17] Complete numerical solutions have been obtained for the meson and baryon spectra as well as their respective light-cone Fock state wavefunctions for general values of the coupling constant, quark masses, and color. Similar results for QCD(1+1) were also obtained by Burkardt[18] by solving the coupled light-cone integral equation in the low particle number sector. Burkardt was also able to study

non-additive nuclear effects in the structure functions of nuclear states in QCD(1+1). In each of these applications, the mass spectrum and wavefunctions were successfully obtained, and all results agree with previous analytical and numerical work, where they were available. More recently, Hiller[19] has used DLCQ and the Lanczos algorithm for matrix diagonalization to compute the annihilation cross section, structure functions and form factors in 1+1 theories. Although these are just toy models, they do exhibit confinement and are excellent tests of the light-cone Fock methods.

In the case of gauge theories in one-space and one-time dimension, there are no physical gluon degrees of freedom in light-cone gauge. The computational problem is thus tractable, and it is possible to explicitly diagonalize the light-cone Hamiltonian and solve these theories numerically. In the work of Hornbostel *et al.*,[17] complete numerical solutions for the spectrum and light-cone wavefunctions in QCD(1+1) can be obtained for any value of the coupling strength and quark masses and any number of flavor and color.

A related approach, the light-front Tamm-Dancoff method (LFTD)[4] has also been proposed to solve the light-cone equation of motion. As in the traditional Tamm-Dancoff method, the light-cone Fock space is truncated to a fixed particle number, and cutoffs are imposed on the maximum transverse momentum and minimum k_i^+. Renormalization counterterms are then introduced to restore the QCD symmetries violated by the Fock space truncation.

The application of the DLCQ and LFTD methods to QCD in physical space-time is a highly challenging problem. The size of the quark and gluon Fock space and the discretization of the transverse momenta leads quickly to very large matrices. A more subtle difficulty is the necessity to include zero mode contributions enforced by the equations of motion and the imposed boundary conditions. The effective Hamiltonian must also be supplemented by terms specified by the ultraviolet renormalization procedure. Despite these challenges, the light-cone methods have been successfully been applied to QED(3+1)[20,21,22] at couplings $\alpha \sim 0.3$. For example, Kaluza and Pauli[21] have computed the structure functions of QED bound states, the lepton and photon light-cone momentum distributions of positronium.

It is thus natural to employ the light-cone Fock expansion as the

basis for representing the physical states of QCD. For example, a pion with momentum $\underline{P} = (P^+, \vec{P}_\perp)$ is described by expansion over color-singlet eigenstates of the free QCD light-cone Hamiltonian:

$$|\pi : \underline{P}\rangle$$

$$= \sum_{n,\lambda_i} \int \overline{\prod_i} \frac{dx_i d^2\vec{k}_{\perp i}}{\sqrt{x_i} 16\pi^3} \left| n : x_i P^+, x_i \vec{P}_\perp + \vec{k}_{\perp i}, \lambda_i \right\rangle \psi_{n/\pi}(x_i, \vec{k}_{\perp i}, \lambda_i) \tag{3}$$

where the sum is over all Fock states and helicities, and where

$$\overline{\prod_i} dx_i \equiv \prod_i dx_i \, \delta \left(1 - \sum_j x_j \right)$$

$$\overline{\prod_i} d^2\vec{k}_{\perp i} \equiv \prod_i d^2\vec{k}_{\perp i} \, 16\pi^3 \, \delta^2 \left(\sum_j \vec{k}_{\perp j} \right). \tag{4}$$

The wavefunction $\psi_{n/\pi}(x_i, \vec{k}_{\perp i}, \lambda_i)$ is the amplitude for finding partons in a specific light-cone Fock state n with momenta $(x_i P^+, x_i \vec{P}_\perp + \vec{k}_{\perp i})$ in the pion. The Fock state is off the light-cone energy shell: $\sum k_i^- > P^-$. The light-cone momentum coordinates x_i, with $\sum_{i=1}^n x_i = 1$ and $\vec{k}_{\perp i}$, with $\sum_{i=1}^n \vec{k}_{\perp i} = \vec{0}_\perp$, are actually relative coordinates; *i.e.* they are independent of the total momentum P^+ and $P_\perp$ of the bound state. The special feature that light-cone wavefunctions do not depend on the total momentum is not surprising, since x_i is the longitudinal momentum fraction carried by the i^{th}-parton ($0 \leq x_i \leq 1$), and $\vec{k}_{\perp i}$ is its momentum "transverse" to the direction of the meson. Both of these are frame-independent quantities. The ability to specify wavefunctions simultaneously in any frame is a special feature of light-cone quantization.

The coefficients in the light-cone Fock state expansion thus are the parton wavefunctions $\psi_{n/H}(x_i, \vec{k}_{\perp i}, \lambda_i)$ which describe the decomposition of each hadron in terms of its fundamental quark and gluon degrees of freedom. The light-cone variable x_i is often identified with

the constituent's longitudinal momentum fraction $x_i = k_i^z/P^z$, in a frame where the total momentum $P^z \to \infty$. However, in light-cone Hamiltonian formulation of QCD, x_i is the boost-invariant light-cone fraction,

$$x_i \equiv \frac{k_i^+}{P+} = \frac{k_i^0 + k_i^z}{P^0 + P^z} \,, \tag{5}$$

independent of the choice of Lorentz frame.

Given the light-cone wavefunctions, $\psi_{n/H}(x_i, \vec{k}_{\perp i}, \lambda_i)$, one can compute virtually any hadronic quantity by convolution with the appropriate quark and gluon matrix elements. For example, the leading-twist structure functions measured in deep inelastic lepton scattering are immediately related to the light-cone probability distributions:

$$2M\, F_1(x,Q) = \frac{F_2(x,Q)}{x} \approx \sum_a e_a^2\, G_{a/p}(x,Q) \tag{6}$$

where

$$G_{a/p}(x,Q) = \sum_{n,\lambda_i} \int \prod_i \frac{dx_i d^2\vec{k}_{\perp i}}{16\pi^3}\, |\psi_n^{(Q)}(x_i, \vec{k}_{\perp i}, \lambda_i)|^2 \sum_{b=a} \delta(x_b - x) \tag{7}$$

is the number density of partons of type a with longitudinal momentum fraction x in the proton. This follows from the observation that deep inelastic lepton scattering in the Bjorken-scaling limit occurs if x_{bj} matches the light-cone fraction of the struck quark. (The $\sum_b$ is over all partons of type a in state n.) However, the light-cone wavefunctions contain much more information for the final state of deep inelastic scattering, such as the multi-parton distributions, spin and flavor correlations, and the spectator jet composition.

The spacelike form factor is the sum of overlap integrals analogous to the corresponding nonrelativistic formula:[23]

$$F(Q^2) = \sum_{n,\lambda_i} \sum_a e_a \int \prod_i \frac{dx_i\, d^2\vec{k}_{\perp i}}{16\pi^3}\, \psi_n^{(\Lambda)*}(x_i, \vec{\ell}_{\perp i}, \lambda_i)\, \psi_n^{(\Lambda)}(x_i, \vec{k}_{\perp i}, \lambda_i). \tag{8}$$

Here e_a is the charge of the struck quark, $\Lambda^2 \gg \vec{q}_\perp^{\,2}$, and

$$\vec{\ell}_{\perp i} \equiv \begin{cases} \vec{k}_{\perp i} - x_i \vec{q}_\perp + \vec{q}_\perp & \text{for the struck quark} \\ \vec{k}_{\perp i} - x_i \vec{q}_\perp & \text{for all other partons.} \end{cases} \tag{9}$$

The general rule for calculating an amplitude involving wavefunction $\psi_n^{(\Lambda)}$, describing Fock state n in a hadron with $\underline{P} = (P^+, \overrightarrow{P}_\perp)$, has the form[8] (see Fig. 3):

$$\sum_{\lambda_i} \int \prod_i \frac{dx_i d^2\vec{k}_{\perp i}}{\sqrt{x_i} 16\pi^3} \, \psi_n^{(\Lambda)}(x_i, \vec{k}_{\perp i}, \lambda_i) \; T_n^{(\Lambda)}(x_i P^+, x_i \overrightarrow{P}_\perp + \vec{k}_{\perp i}, \lambda_i) \tag{10}$$

where $T_n^{(\Lambda)}$ is the irreducible scattering amplitude in LCPTH with the hadron replaced by Fock state n. The light-cone Fock expansion thus allows a definition of the parton model and wavefunctions. By using the light-cone gauge, $A^+ = 0$, only physical non-ghost degrees of freedom appear in the Fock expansion even for non-Abelian theories. Furthermore in this gauge, the numerator couplings of soft gluons inserted into hard scattering expansions remain finite in the high momentum transfer limit. Thus this formalism is ideal for proving factorization theorems, *i.e.* the isolation of hard and soft contributions at high momentum transfer.

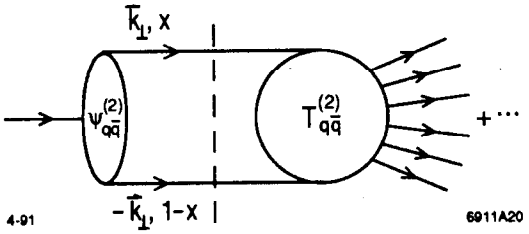

Figure 3. Calculation of hadronic amplitudes in the light-cone Fock formalism.

Exclusive Processes and Light-cone Wavefunctions

The dynamics of exclusive reactions reflects not only the behavior of quark-gluon scattering processes at the amplitude level, but also the fundamental structure of the hadron wavefunctions themselves. In a relativistic quantum field theory, a bound state cannot be described in terms of a fixed number of constituents. However, in the case of exclusive reactions at large momentum transfer, there is an enormous simplification: only the lowest valence-quark light-cone Fock state of each hadron contributes to a high momentum transfer exclusive scattering process. It is easy to show that in the light-cone gauge, $A^+ = 0$, higher Fock state contributions involving extra gluons are always suppressed by powers of the momentum transfer Q.[24] Furthermore, the absence of gluon radiation into the final state demands that the valence quarks in the hadron wavefunction must be at relative transverse separation $b_\perp^i$ of order $1/Q$; so that small color-dipole configurations of the hadron wavefunction control large momentum transfer exclusive processes.[25,24] Thus at high momentum transfer exclusive reactions provide an important testing ground for light-cone wavefunctions since in the light-cone gauge only the simplest valence wavefunction is involved.

On the other hand, many properties of large momentum transfer exclusive reactions can be calculated without explicit knowledge of the form of the non-perturbative light-cone wavefunctions. The main ingredients of this analysis are asymptotic freedom, and the power-law scaling relations and quark helicity conservation rules of perturbative QCD. For example, consider the light-cone convolution formula for the meson form factor at high momentum transfer Q^2. If the internal momentum transfer is large then one can iterate the gluon-exchange term in the effective potential for the light-cone wavefunctions. The result is the hadron form factors can be written in a factorized form as a convolution of quark "distribution amplitudes" $\phi(x_i, Q)$, one for each hadron involved in the amplitude, with a hard-scattering amplitude T_H.[8,26] The distribution amplitude is the fundamental gauge invariant wavefunction which describes the fractional longitudinal momentum distributions of the valence quarks in a hadron integrated over transverse momentum up to the scale Q.[8] The pion's electromagnetic form factor, for example, can be written as[8,26,27]

$$F_\pi(Q^2) = \int_0^1 dx \int_0^1 dy\, \phi_\pi^*(y,Q)\, T_H(x,y,Q)\, \phi_\pi(x,Q) \left(1 + \mathcal{O}\left(\frac{1}{Q}\right)\right). \tag{11}$$

Here T_H is the scattering amplitude for the form factor but with the pions replaced by collinear $q\bar{q}$ pairs—*i.e.* the pions are replaced by their valence partons. We can also regard T_H as the free particle matrix element of the order $1/Q^2$ term in the effective Lagrangian for $\gamma^* q\bar{q} \to q\bar{q}$.[10]

The process-independent distribution amplitude[8] $\phi_\pi(x,Q)$ is the probability amplitude for finding the $q\bar{q}$ pair in the pion with $x_q = x$ and $x_{\bar{q}} = 1-x$. It is directly related to the light-cone valence wavefunction:

$$\phi_\pi(x,Q) = \int \frac{d^2\vec{k}_\perp}{16\pi^3}\, \psi^{(Q)}_{q\bar{q}/\pi}(x,\vec{k}_\perp) = P^+_\pi \int \frac{dz^-}{4\pi}\, e^{ixP^+_\pi z^-/2}$$

$$\times \langle 0|\, \overline{\psi}(0)\, \frac{\gamma^+\gamma_5}{2\sqrt{2n_c}}\, \psi(z)\, |\pi\rangle^{(Q)} \Big|_{z^+ = \vec{z}_\perp = 0}.$$

The $\vec{k}_\perp$ integration in the above equation is cut off by the ultraviolet cutoff $\Lambda = Q$ implicit in the wavefunction; thus only Fock states with invariant mass squared $\mathcal{M}^2 \leq Q^2$ contribute.

The above result for exclusive amplitudes is in the form of a factorization theorem; all of the non-perturbative dynamics is factorized into the non-perturbative distribution amplitudes, which sums all internal momentum transfers up to the scale Q^2. On the other hand, all momentum transfers higher than Q^2 appear in T_H, which, because of asymptotic freedom, can be computed perturbatively in powers of the QCD running coupling constant $\alpha_s(Q^2)$.

Isgur and Llewellyn Smith[28] and also Radyushkin[29] have raised the concern that important contributions to exclusive processes could arise from non-factorizing end-point contributions of the hadron wavefunctions with $x \sim 1$ even at very large momentum transfer. However, recent work by Botts, Li, and Sterman[30] has now shown that such soft physics contributions are effectively eliminated due to Sudakov suppression. I will briefly review this work below. In addition, Kronfeld and Nizic[31] have shown how one can consistently integrate over on-shell

singularities in the hard-scattering amplitude for Compton processes involving baryons. Thus the QCD predictions based on the factorization of long and short distance physics are reliable and should be valid for momentum transfers in the experimentally accessible domain beyond a few GeV. It is clearly important to test these predictions as precisely as possible.

Given the factorized structure of exclusive amplitudes at large momentum transfer, one can read off a number of general features of the PQCD predictions; *e.g.* the dimensional counting rules, hadron helicity conservation, color transparency, etc.[24] In addition, the scaling behavior of the exclusive amplitude is modified by the logarithmic dependence of the distribution amplitudes in Q^2 which is in turn determined by QCD evolution equations.[8]

Because of asymptotic freedom, the nominal power-law fall-off $\mathcal{M} \sim Q^{4-n}$ of an exclusive amplitude at large momentum transfer reflects the elementary scaling of the lowest-order connected quark and gluon tree graphs obtained by replacing each of the external hadrons by its respective collinear quarks. Here n is the total number of initial state and final state lepton, photon, or quark fields entering or leaving the hard scattering subprocess. The empirical success of the dimensional counting rules for the power-law fall-off of form factors and general fixed center-of-mass angle scattering amplitudes has given important evidence for scale-invariant quark and gluon interactions at short distances.[32] QCD also predicts calculable corrections to the nominal dimensional counting power-law behavior due to the running of the strong coupling constant, higher order corrections to the hard scattering amplitude, Sudakov effects, pinch singularities, as well as the evolution of the hadron distribution amplitudes, $\phi_H(x_i, Q)$, the basic factorizable non-perturbative wavefunctions needed to compute exclusive amplitudes.[24,5]

The fundamental non-perturbative quantities which control large momentum transfer exclusive reactions in quantum chromodynamics are the hadron distribution amplitudes[8]: $\phi_B(x_i, \lambda_i, Q)$, for the baryons with $x_1 + x_2 + x_3 = 1$, and $\phi_M(x_i, \lambda_i, Q)$, for the mesons with $x_1 + x_2 = 1$. The distribution amplitudes are the hadron wavefunctions which interpolate between the QCD bound state and their valence quarks. The constituents have longitudinal light-cone momentum fractions $x_i = (k^0 + k^z)_i/(p^0 + p^z)$, helicities λ_i, and transverse separation $b^i_\perp \simeq 1/Q$. If

one can calculate the distribution amplitude at an initial scale Q_0, then one can determine $\phi(x_i, Q)$ at higher momentum scales via evolution equations in $\log Q^2$ or equivalently, the operator product expansion. Thus far the most important experimental constraints on the hadron distribution amplitudes has come from the normalization and scaling of form factors at large momentum transfer.

The data for hadron form factors is consistent with the onset of PQCD scaling at a momentum transfers of a few GeV, as expected from the parameters which determine the mass scales of QCD. Recently Stoler[33] has shown that the measurements of the transition form factors of the proton to the $N(1535)$ and $N(1680)$ resonances are consistent with the predicted PQCD Q^{-4} scaling to beyond $Q^2 = 20\ GeV^2$. The normalization is also in reasonable agreement with that predicted from QCD sum rule constraints on the nucleon distribution amplitudes, allowing for uncertainties from higher order QCD corrections. In the case of the proton to $\Delta(1232)$ transition, the form factor falls faster that Q^{-4}. This anomalous behavior is in fact predicted by the QCD sum rule analysis since unlike the proton, the Δ has a highly symmetric distribution amplitude with a small coupling to the QCD hard scattering amplitude. The observed scaling pattern of the transition form factors gives strong support to the QCD sum rule predictions and PQCD factorization.

The hadron distribution amplitudes can also be used for calculating weak decay transitions, structure functions at $x \sim 1$, fragmentation distributions at large z, and higher twist correlations.[34] For example, strong higher twist effects are observed in the angular and Q^2 dependence of Drell-Yan processes and deep inelastic scattering at $x \sim 1$.[35] In each of these applications, one can use factorization theorems to separate the perturbative quark and gluon dynamics which involves momentum transfer higher than Q from the non-perturbative long-distance physics contained in $\phi(x_i, Q)$. These analyses parallel the developments in leading-twist inclusive reactions, where one factorizes hard-scattering quark-gluon subprocess cross sections from the long-distance physics contained in the hadron structure functions. However, in the case of exclusive processes at large momentum transfer, the scale-separation and factorization are done at the amplitude level.

Exclusive reactions involving two real or virtual photons provide a particularly interesting testing ground for QCD because of the rela-

tive simplicity of the couplings of the photons to the underlying quark currents and the absence of significant initial state interactions—any remnant of vector-meson dominance contributions is suppressed at large momentum transfer. The angular distributions for the hadron pair production processes $\gamma\gamma \to H\overline{H}$ are sensitive to the shapes of the hadron wavefunctions.[36] Lowest order predictions for meson pair production in two photon collisions using this formalism are given in Refs. 36 and 5; the analysis of the $\gamma\gamma$ to meson pair process has been carried out to next to leading order in $\alpha_s(Q^2)$ by Nizic.[37]

The simplest example of two-photon exclusive reactions is the $\gamma^*(q)\gamma \to M^0$ process which is measurable in tagged $e^+e^- \to e^+e^-M^0$ reactions. The photon to neutral meson transition form factor $F_{\gamma\to M^0}(Q^2)$ is predicted to fall as $1/Q^2$—modulo calculable logarithmic corrections from the evolution of the meson distribution amplitude. The QCD prediction reflects the scale invariance of the quark propagator at high momentum transfer, the same scale-invariance which gives Bjorken scaling of the deep inelastic lepton-nucleon cross sections. The existing data from the TPC/$\gamma\gamma$ experiment are consistent with the predicted scaling and normalization of the transition form factors for the π^0, η_0, and η'. The Mark II and TPC/$\gamma\gamma$ measurements of $\gamma\gamma \to \pi^+\pi^-$ and $\gamma\gamma \to K^+K^-$ reactions are also consistent with PQCD expectations. A review of this work is given in Ref. 38.

Compton Scattering in Perturbative QCD

Compton scattering $\gamma p \to \gamma p$ at large momentum transfer and the s-channel crossed reactions $\gamma\gamma \to \overline{p}p$ and $\overline{p}p \to \gamma\gamma$ are classic tests of the perturbative QCD formalism for exclusive reactions. At leading twist each helicity amplitude has the factorized form,[24] (see Fig. 4)

$$\mathcal{M}^{\lambda\lambda'}_{hh'}(s,t) = \sum_{d,i} \int [dx][dy]\phi_i(x_1,x_2,x_3;\widetilde{Q})$$

$$\times\, T_i^{(d)}(x,h,\lambda;y,h',\lambda';s,t)\phi_i(y_1,y_2,y_3;\widetilde{Q})\ .$$

The index i labels the three contributing valence Fock amplitudes at the renormalization scale $\widetilde{Q}$. The index d labels the 378 connected Feynman diagrams which contribute to the eight-point hard scattering amplitude

$qqq\gamma \to qqq\gamma$ at the tree level; *i.e.* at order $\alpha\alpha_s^2(\widehat{Q})$. The arguments $\widehat{Q}$ of the QCD running coupling constant can be evaluated amplitude by amplitude using the method of Ref. 39. The evaluation of the hard scattering amplitudes $T_i^{(d)}(x, h, \lambda; y, h', \lambda'; s, t)$ has now been done by several groups.[40,41,31,42]

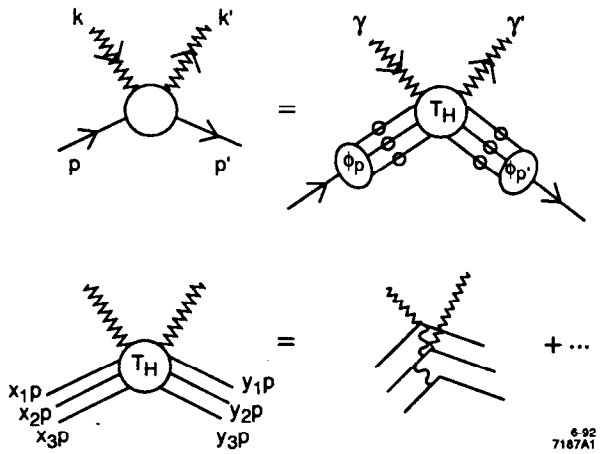

Figure 4. Factorization of the Compton amplitude in QCD.

An important simplification of Compton scattering in PQCD is the fact that pinch singularities are readily integrable and do not change the nominal power-law behavior of the basic amplitudes.[31] Physically, the pinch singularities correspond to the existence of potentially on-shell intermediate states in the hard scattering amplitudes, leading to a non-trivial phase structure of the Compton amplitudes. Such phases can in principle be measured by interfering the virtual Compton process in $e^{\pm}p \to e^{\pm}p\gamma$ with the purely real Bethe-Heitler bremmstrahlung amplitude.[43] A careful analytic treatment of the integration over the on-shell intermediate states is given by Kronfeld and Nizic.[31]

The most characteristic feature of the PQCD predictions is the scaling of the differential Compton cross section at fixed t/s or θ_{CM}.

$$s^6 \frac{d\sigma}{dt}(\gamma p \to \gamma p) = F(t/s).$$

The power s^6 reflects the fact that 8 elementary fields enter or leave

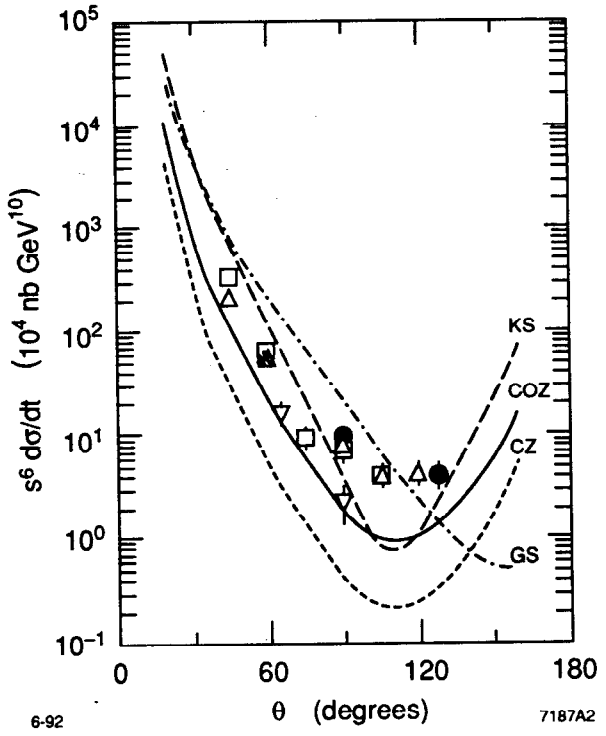

Figure 5. Comparison of the QCD prediction for the scaled unpolarized proton Compton scattering differential cross section $s^6 d\sigma/dt(\gamma p \to \gamma p)$ with experiment. The experimental data[44] are at $s = 4.63\ GeV$ (circles) $s = 6.51\ GeV$ (triangles), $s = 8.38\ GeV$ (squares) and $s = 10.26\ GeV$ (asterisk). The QCD prediction is from the calculation of Kronfeld and Nizic.[31] The QCD sum rule distribution amplitudes are listed in Ref. 5.

the hard scattering subprocess.[32] The scaling of the existing data[44] as shown in Fig. 5 is remarkably consistent with the PQCD power-law prediction, but measurements at higher energies and momentum transfer are needed to test the predicted logarithmic corrections to this scaling behavior and determine the angular distribution of the scaled cross section over as large a range as possible.

The predictions for the normalization of the Compton cross section and the shape of its angular distribution are sensitive to the shape of the proton distribution amplitude $\phi_p(x_i, Q)$. The forms predicted for the proton distribution amplitude by QCD sum-rules by Chernyak, Oglobin, and Zhitnitskii, and also King and Sachrajda, shown in Fig. 1, appear to give a reasonable representation of the existing data. These

distributions, which predict that 65% of the proton's momentum is carried by the u quark with helicity parallel to the proton's helicity also provide reasonable predictions for the normalization of the proton's form factor and the $J/\psi \to p\bar{p}$ decay rate. Kronfeld and Nizic have also given detailed predictions for the helicity and phase structure of the PQCD predictions for both proton and neutrons. The crossing behavior from the Compton scattering to the annihilation channels will also provide important tests and constraints on the PQCD formalism and the shape of the proton distribution amplitudes. Predictions for the timelike processes have been made by Farrar *et al.*,[40] Millers and Gunion[41], and Hyer.[42]

It should be emphasized that the theoretical uncertainties from finite nucleon mass corrections, the magnitude of the QCD running coupling constant, and the normalization of the proton distribution amplitude largely cancel out in the ratio of differential cross sections

$$R_{\gamma\gamma/e^+e^-}(s,\theta_{cm}) = \frac{d\sigma(\bar{p}p \to \gamma\gamma)/dt}{d\sigma(\bar{p}p \to e^+e^-)/dt},$$

which is predicted by QCD to be essentially independent of s at large momentum transfer. (See Fig. 6.) If this scaling is confirmed, then the center-of-mass angular dependence of $R_{\gamma\gamma/e^+e^-}(s,\theta_{cm})$ will be one of the best ways to determine the shape of $\phi_p(x_i,Q)$. The measurement of this ratio appears to well-suited to the Fermilab antiproton accumulator experiment $E760$ and SuperLear.

Another important characteristic of the leading-twist QCD predictions for exclusive processes is hadron-helicity conservation.[45] Because of chiral invariance, the hard-scattering amplitude is non-zero only for amplitudes that conserve quark helicity. Since the distribution amplitude projects only $L_z = 0$, this implies that the proton helicity is conserved in $\gamma p \to \gamma p$. Similarly, the baryon and anti-baryon helicities must be opposite in the crossed reactions $\gamma\gamma \to \overline{BB}$ and $\bar{p}p \to \gamma\gamma$ at large momentum transfer. Detailed predictions for each of the leading power Compton scattering helicity amplitudes are also given by Kronfeld and Nizic.[31]

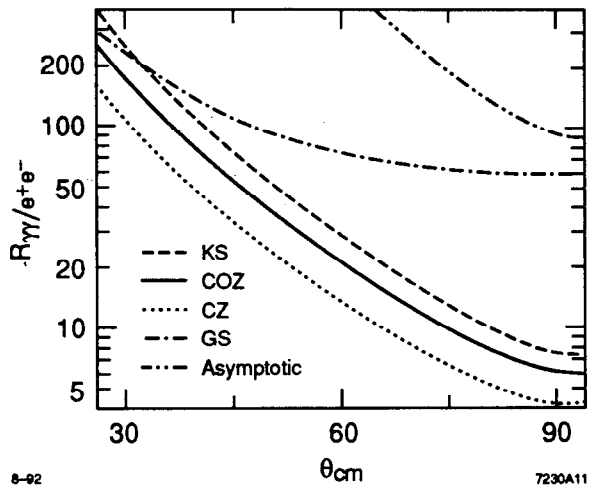

Figure 6. PQCD predictions for the ratio of the timelike Compton cross section for $\bar{p}p \to \gamma\gamma$ to the cross section for $\bar{p}p \to e^+e^-$ annihilation assuming different model forms for the proton distribution amplitude at $s = 25\ GeV^2$.[42] The predictions include the effect of Sudakov suppression in the endpoint region using the Li-Sterman formalism.

The Domain of Validity of PQCD Predictions for Exclusive Processes

The factorized predictions for the Compton amplitude are rigorous predictions of QCD at large momentum transfer. However, it is important to understand the kinematic domain where the leading twist predictions become valid. As emphasized by Isgur and Llewellyn Smith,[28] this question is non-trivial because of the possibility of significant contributions to the scattering amplitude at the endpoint regions $x_i \to 1$ where the PQCD factorization could break down. Because of the denominator structure of the hard scattering amplitudes, *e.g.*, $T_H \propto \alpha_s/[(1-x)(1-y)Q^2]$ for the meson form factor, the endpoint integration region at $x \sim 1$ and $y \sim 1$ will be enhanced. Of more concern is the fact that such endpoint regions are further emphasized when one assumes the strongly asymmetric forms for the nucleon distribution amplitude derived from QCD sum rules.

It is important to note that the end-point regime corresponds to scattering processes where one quark carries nearly all of the proton's momentum and is at a fixed transverse separation $b_\perp$ from the spectator quarks. However, if a quark which is isolated in space receives a

large momentum transfer $x_i Q$, it will normally strongly radiate gluons into the final state due to the displacement of both its initial and final self-field, contrary to the requirements of exclusive scattering.[30] For example, in QED the radiation from the initial and final state charged lines is controlled by the coherent sum $\sum_i \frac{\epsilon \cdot p_i}{k \cdot p_i} \eta_i q_i$ where q_i and p_i are the charges four-momenta of the charged lines, ϵ and k are polarization and four-momentum of the radiation, and $\eta_i = \pm 1$ for initial and final state particles, respectively. Radiation will occur for any finite momentum transfer scattering as long as the photon's wavelength is less than the size of the initial and final neutral bound states.

The radiation from the colored lines in QCD have similar coherence properties:[46] because of the destructive color interference of the radiators, the momentum of the radiated gluon in a QCD hard scattering process only ranges from k of order $1/b_\perp$, where color screening occurs, up to the momentum transfer $x_i Q$ of the scattered quarks. The one-gluon correction to the wavefunction is thus proportional to

$$\frac{C_F}{\pi} \int^Q \frac{\mathrm{d}^2 q_\perp}{q_\perp^2} \Big[3 - \sum_{i<j} \exp\big(-i(b_i - b_j) \cdot q_\perp\big) \Big] \frac{\alpha_s(q_\perp^2)}{2\pi} \int_{q_\perp}^Q \frac{\mathrm{d}q_+}{q_+}.$$

This result[30,42] and unitarity allows one to compute the probability that no radiation occurs during the hard scattering. It is given by a rapidly falling exponentiated Sudakov form factor $S = S(x_i Q, b_{\perp_i}, \Lambda_{QCD})$; thus at large Q and fixed impact separation, the Sudakov factor strongly suppresses the endpoint contribution. On the other hand, when $b_\perp = \mathcal{O}(x_i Q)^{-1}$, the Sudakov form factor is of order 1, and the radiation leads to logarithmic evolution and contributions of higher order in $\alpha_s(Q^2)$ corrections already contained in the PQCD predictions.[8,47,48] This is the starting point of the detailed analysis of the suppression of endpoint contributions to meson and baryon form factors and its quantitative effect on the PQCD predictions recently presented by Li and Sterman.[30] This analysis has now also been applied to two-photon reactions and the timelike proton form factor by Hyer.[42]

It should be emphasized that the standard PQCD contributions to large momentum transfer exclusive reactions derive from wavefunction configurations where the valence quarks are at small transverse separation $b_\perp \simeq \mathcal{O}(1/Q)$, the regime where there is no Sudakov suppression.

However, as noted by Li and Sterman, the hard scattering amplitude loses its singular end-point structure if one retains the valence quark transverse momenta in the denominators. For example, in the case of the pion form factor, the hard scattering amplitude is effectively modified to the form

$$T_H \propto \frac{\alpha_s}{(1-x)(1-y)Q^2 + (\mathbf{k}_1^\perp + \mathbf{k}_2^\perp)^2}. \tag{12}$$

Li and Sterman thus find that the pion form factor becomes relatively insensitive to soft gluon exchange at momentum transfers beyond 20 Λ_{QCD}. In the case of the proton Dirac form factor, the corresponding analysis by Li[30] is in good agreement with experiment at momentum transfers greater than 3 GeV.

The Botts, Li, and Sterman analysis of the Sudakov suppression of endpoint contributions makes it understandable why PQCD factorization and its predictions for exclusive processes are already applicable at momentum transfers of a few GeV, thus accounting for the empirical success of quark counting rules in exclusive process phenomenology. The Sudakov effect suppression also enhances "color transparency" phenomena, since only small color singlet wavefunction configurations can scatter at large momentum transfer.[25] Color transparency in Compton scattering can be tested by checking for the absence of final state absorption in quasi-elastic $\gamma p \to \gamma p$ scattering in heavy nuclei. QCD color transparency also implies that there will be diminished initial state absorption of the antiproton for large-angle quasi-elastic $\bar{p}p \to \gamma\gamma$ annihilation in heavy nuclear targets.

In the case of large angle proton-proton scattering, the perturbative predictions for color transparency and the spin-spin correlation A_{NN} appear to fail at $E_{CM} \sim 5\ GeV$; this effect has been attributed to the effect of the threshold for charm production in intermediate states.[49] A similar breakdown of the perturbative predictions may also occur at the corresponding energy threshold in $\bar{p}p \to \gamma\gamma$ at large angles due to charmed hadron intermediate states.

Recently Luke, Manohar, and Savage[50] have shown that the QCD trace anomaly leads to a strong, attractive, scalar potential which dominates the interaction of heavy quarkonium states with ordinary matter at low relative velocity. The scalar attraction is sufficiently strong to

produce nuclear-bound quarkonium.[51] Thus it will be interesting to look for strong threshold enhancements for charm production near threshold in two-photon reactions, particularly in exclusive channels such as $\rho^0 J/\psi$ as well as $D\overline{D}$. Predictions for the threshold production of charmed mesons has also been given in Ref. 52. Evidence for excess inclusive production of charmed mesons in photon-photon collisions has been reported by the JADE collaboration.[53]

Exclusive processes, particularly two-photon reactions, thus provide one of the most important, but least explored frontiers in particle physics. The recent analyses by Botts, Li, and Sterman and by Kronfeld and Nizic have shown that the predictions based on QCD factorization theorems are applicable to measurements at present-day accelerators. It is clearly crucial for a fundamental understanding of both the perturbative and non-perturbative aspects of QCD that the predictions for exclusive amplitudes be tested as carefully as possible.

Exclusive Weak Decays of Heavy Hadrons

An important application of PQCD factorization is to exclusive decays of heavy hadrons to light hadrons, such as $B^0 \to \pi^+\pi^-$, K^+, K^-.[54] To a good approximation, the decay amplitude $\mathcal{M} = \langle B|H_{Wk}|\pi^+\pi^-\rangle$ is caused by the transition $\overline{b} \to W^+\overline{u}$; thus $\mathcal{M} = f_\pi p_\pi^\mu \frac{G_F}{\sqrt{2}} \times \langle \pi^-|J_\mu|B^0\rangle$ where J_μ is the $\overline{b} \to \overline{u}$ weak current. The problem is then to recouple the spectator d quark and the other gluon and possible quark pairs in each B^0 Fock state to the corresponding Fock state of the final state π^-. (See Fig. 7.) The kinematic constraint that $(p_B - p_\pi)^2 = m_\pi^2$ demands that at least one quark line is far off shell: $p_{\overline{u}}^2 = (yp_B - p_\pi)^2 \sim -\mu m_B \sim -1.5\ GeV^2$, where we have noted that the light quark takes only a fraction $(1-y) \sim \sqrt{(k_\perp^2 + m_d^2)}/m_B$ of the heavy meson's momentum since all of the valence quarks must have nearly equal velocity in a bound state. In view of the successful applications[55] of PQCD factorization to form factors at momentum transfers in the few GeV^2 range, it is reasonable to assume that $\langle |p_{\overline{u}}^2| \rangle$ is sufficiently large that we can begin to apply perturbative QCD methods.

The analysis of the exclusive weak decay amplitude can be carried out in parallel to the PQCD analysis of electroweak form factors[56] at large Q^2. The first step is to iterate the wavefunction equations of

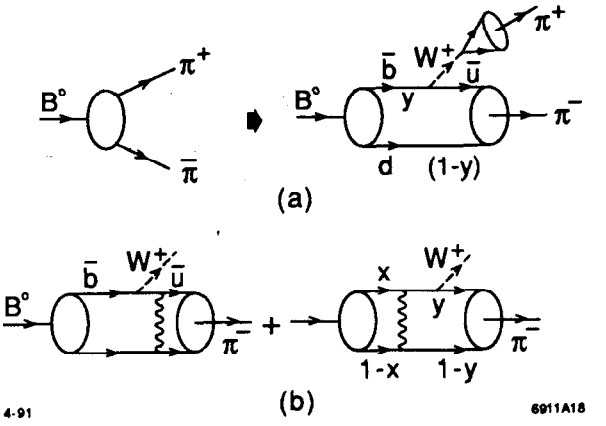

Figure 7. Calculation of the weak decay $B \to \pi\pi$ in the PQCD formalism of Ref. 54. The gluon exchange kernel of the hadron wavefunction is exposed wherever a hard momentum transfer is required.

motion so that the large momentum transfer through the gluon exchange potential is exposed. The heavy quark decay amplitude can then be written as a convolution of the hard scattering amplitude for $Q\bar{q} \to W^+ q\bar{q}$ convoluted with the B and π distribution amplitudes. The minimum number valence Fock state of each hadron gives the leading power law contribution. Thus T_H contains all perturbative virtual loop corrections of order $\alpha_s(\Lambda^2)$. The result is the factorized form:

$$\mathcal{M}(B \to \pi\pi) = \int_0^1 dx \int_0^1 dy \phi_B(y,\Lambda) T_H \phi_\pi(x,\Lambda) \; . \tag{13}$$

All of the non-perturbative corrections with momenta $|k^2| < \Lambda^2$ are summed in the distribution amplitudes.

An interesting example of this analysis is "atomic alchemy"[57] *i.e.*, the exclusive decays of muonic atoms to electronic atoms plus neutrinos. In this case the calculation requires the very high momentum tail of the atomic wavefunctions, which in turn can be obtained via the iteration of the relativistic atomic bound-state equations. Again one obtains a factorization theorem for exclusive atomic transitions where the atomic wavefunction at the origin plays the role of the distribution amplitude.

Discretized Light-cone Quantization: Applications to QCD

QCD dynamics takes a rather simple form when quantized at equal light-cone "time" $\tau = t + z/c$. In light-cone gauge $A^+ = 0$, the QCD light-cone Hamiltonian

$$H_{\rm QCD} = H_0 + gH_1 + g^2H_2 \tag{14}$$

contains the usual 3-point and 4-point interactions plus induced terms from instantaneous gluon exchange and instantaneous quark exchange diagrams. The perturbative vacuum serves as the lowest state in constructing a complete basis set of color-singlet Fock states of H_0 in momentum space. Solving QCD is then equivalent to solving the eigenvalue problem:

$$H_{\rm QCD}|\Psi >= M^2|\Psi > \tag{15}$$

as a matrix equation on the free Fock basis. The set of eigenvalues $\{M^2\}$ represents the spectrum of the color-singlet states in QCD. The Fock projections of the eigenfunction corresponding to each hadron eigenvalue gives the quark and gluon Fock state wavefunctions $\psi_n(x_i, k_{\perp i}, \lambda_i)$ required to compute structure functions, distribution amplitudes, decay amplitudes, etc. For example, the e^+e^- annihilation cross section into a given $J = 1$ hadronic channel can be computed directly from its $\psi_{q\bar{q}}$ Fock state wavefunction.

The key step in obtaining a discrete representation of the light-cone Hamiltonian in a form amenable to numerical diagonalization, is the construction of a complete, countable, Fock state basis,

$$\sum_n |n\rangle \langle n| = I \ . \tag{16}$$

This can be explicitly done in QCD by constructing a complete set of color-singlet eigenstates of the free Hamiltonian as products of representations of free quark and gluon fields. The states are chosen as eigenstates of the constants of the motion, P^+, $\vec{P}_\perp$, J_z, and the conserved charges. In addition, one can pre-diagonalize the Fock representation by classifying the states according to their discrete symmetries, as described in the previous section. This step alone reduces the size of the matrix representations by as much as a factor of 16.

The light-cone Fock representation can be made discrete by choosing periodic (or, in the case of fermions, anti-periodic) boundary conditions on the fields: $\psi(z^-) = \pm\psi(z^- - L)$, and $\psi(x_\perp) = \psi(x_\perp - L_\perp)$. Thus in each Fock state, $P^+ = \frac{2\pi}{L}K$, and each constituent $k_i^+ = \frac{2\pi}{L}n_i$, where the positive integers n_i satisfy $\sum_i n_i = K$. Similarly $\vec{k}_{\perp i} = \frac{\pi}{L_\perp}\vec{n}_{\perp i}$, where the vector integers sum to $\overrightarrow{0}_\perp$ in the standard frame.

The positive integer K is called the "harmonic resolution." For a given choice of K, there are only a finite number of partitions of the plus momenta; thus only a finite set of rational values of $x_i = k_i^+/P^+ = n_i/K$ appear: $x_i = \frac{1}{K}, \quad \frac{2}{K}, \ \ldots \ \frac{K-1}{K}$. Thus eigensolutions obtained by diagonalizing H_{LC} on this basis determine the deep inelastic structure functions $F_I(x)$ only at the set of rational discrete points x_i. The continuum limit thus requires extrapolation to $K \to \infty$. Note that the value of L is irrelevant, since it can always be scaled away by a Lorentz boost. Since H_{LC}, P^+, $\overrightarrow{P}_\perp$, and the conserved charges all commute, H_{LC} is block diagonal.

The DLCQ program becomes especially simple for gauge theory in one-space one-time dimensions not only because of the absence of transverse momenta, but also because there are no gluon degrees of freedom. In addition, for a given value of the harmonic resolution K the Fock basis becomes restricted to finite dimensional representations. The dimension of the representation corresponds to the number of partitions of the integer K as a sum of positive integers n. The eigenvalue problem thus reduces to the diagonalization of a finite Hermitian matrix. The continuum limit is clearly $K \to \infty$.

Since continuum scattering states as well as single hadron color-singlet hadronic wavefunctions are obtained by the diagonalization of H_{LC}, one can also calculate scattering amplitudes as well as decay rates from overlap matrix elements of the interaction Hamiltonian for the weak or electromagnetic interactions. In principle, all higher Fock amplitudes, including spectator gluons, can be kept in the light-cone quantization approach; such contributions cannot generally be neglected in decay amplitudes involving light quarks.

DLCQ has been used to successfully obtain the complete color-singlet spectrum of QCD in one-space and one-time dimension for $N_C = 2, 3, 4$.[17] The hadronic spectra are obtained as a function of quark mass and QCD coupling constant (see Fig. 8). Where they are available, the

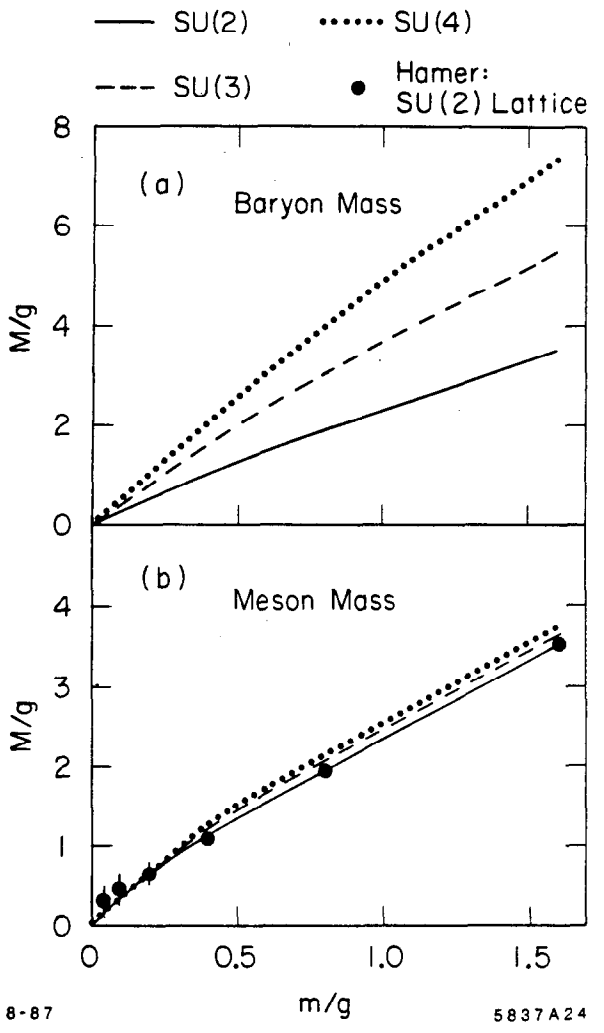

Figure 8. The baryon and meson spectrum in QCD(1+1) computed in DLCQ for $N_C = 2, 3, 4$ as a function of quark mass and coupling constant.

spectra agree with results obtained earlier; in particular, the lowest meson mass in SU(2) agrees within errors with lattice Hamiltonian results. The meson mass at $N_C = 4$ is close to the value predicted by 't Hooft in the large N_C limit. The DLCQ method also provides the first results for the baryon spectrum in a non-Abelian gauge theory. The lowest baryon mass is shown in Fig. 8 as a function of coupling constant. The ratio of meson to baryon mass as a function of N_C also agrees at strong coupling with results obtained by bosonization

methods.[58] Precise values for the mass eigenvalue can be obtained by extrapolation to large K by fitting to forms with the correct functional dependence in $1/K$.

When the light-cone Hamiltonian is diagonalized at a finite resolution K, one gets a complete set of eigenvalues corresponding to the total dimension of the Fock state basis. A representative example of the spectrum is shown in Fig. 9 for baryon states ($B = 1$) as a function of the dimensionless variable $\lambda = 1/(1+\pi m^2/g^2)$. Notice that spectrum automatically includes continuum states with $B = 1$.

The structure functions for the lowest meson and baryon states in SU(3) at two different coupling strengths $m/g = 1.6$ and $m/g = 0.1$ are shown in Figs. 10 and 11. Higher Fock states have a very small probability; representative contributions to the baryon structure functions are shown in Fig. 12. Although these results are for one-time one-space theory they do suggest that the sea quark distributions in physical hadrons may be highly structured.

The Heavy Quark Content of the Proton

The DLCQ results for sea quark distributions in QCD(1+1) may have implications for the heavy quark content of physical hadrons. One of the most intriguing unknowns in nucleon structure is the strange and charm quark structure of the nucleon wavefunction.[59] The EMC spin crisis measurements indicate a significant $s\bar{s}$ content of the proton, with the strange quark spin strongly anti-correlated with the proton spin. Just as striking, the EMC measurements[60] of the charm structure function of the Fe nucleus at large $x_{bj} \sim 0.4$ appear to be considerably larger than that predicted by the conventional photon-gluon fusion model, indicating an anomalous charm content of the nucleon at large values of x. The probability of intrinsic charm has been estimated[60] to be 0.3%.

Figure 13 shows recent results obtained by Hornbostel[61] for the structure functions of the lowest mass meson in QCD(1+1) wavefunctions for $N_C = 3$ and two quark flavors. As seen in the figure, the heavy quark distribution arising from the $q\bar{q}Q\overline{Q}$ Fock component has a two-hump character. The second maximum is expected since the constituents in a bound state tend to have equal velocities. The result is insensitive to the value of the Q^2 of the deep inelastic probe. Thus intrinsic charm is a feature of exact solutions to QCD(1+1). Note that

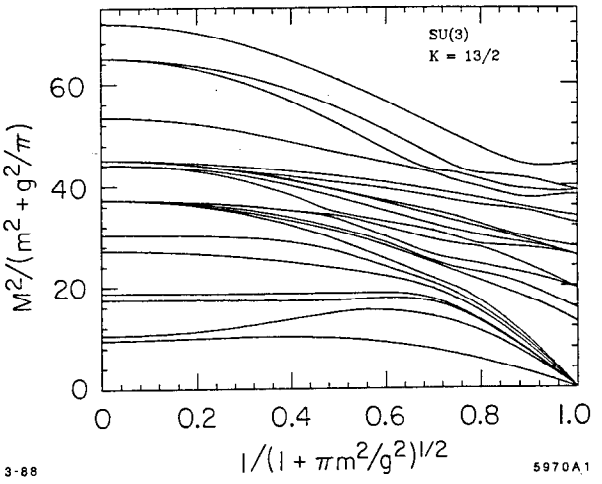

Figure 9. Representative baryon spectrum for QCD in one-space and one-time dimensions.

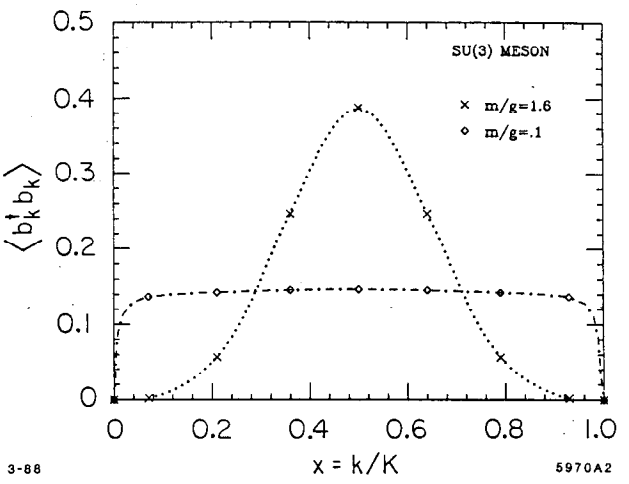

Figure 10. The meson quark momentum distribution in QCD(1+1) computed using DLCQ.

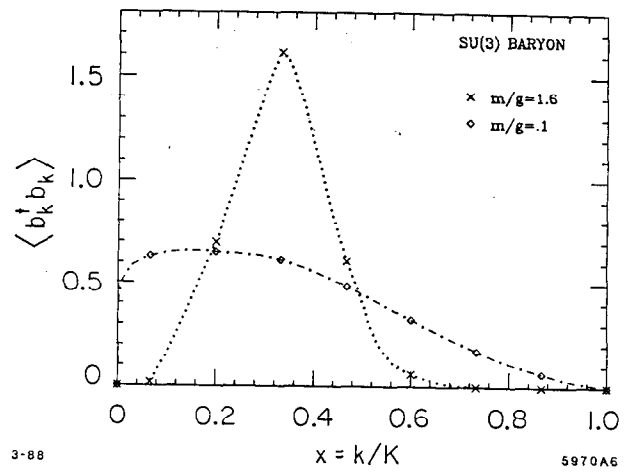

Figure 11. The baryon quark momentum distribution in QCD(1+1) computed using DLCQ.

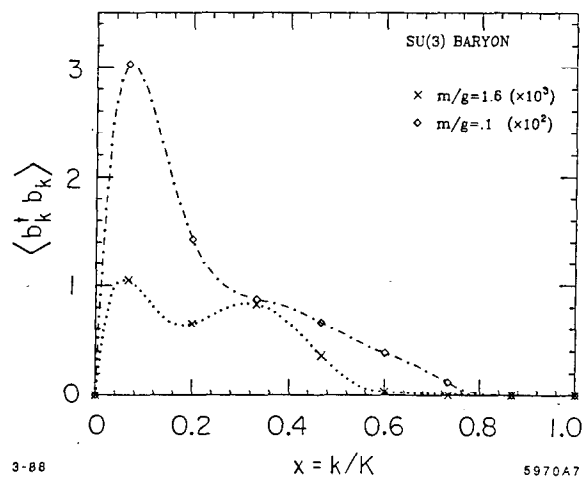

Figure 12. Contribution to the baryon quark momentum distribution from $qqq\overline{qq}$ states for QCD(1+1).

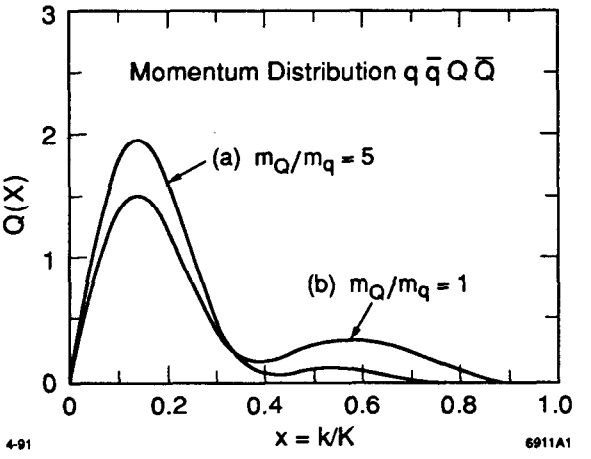

Figure 13. The heavy quark structure function $Q(x) = G_{Q/M}(x)$ of the lightest meson in QCD(1+1) with $N_c = 3$ and $g/m_q = 10$. Two flavors are assumed with (a) $m_Q/m_q = 1.001$ and (b) $m_Q/m_q = 5$. The curves are normalized to unit area. The probability of the $q\bar{q}Q\overline{Q}$ state is 0.56×10^{-2} and 0.11×10^{-4}, respectively. The DLCQ method for diagonalizing the light-cone Hamiltonian is used with anti-periodic boundary conditions. The harmonic resolution is taken at $K = 10/2$. (From Ref. 17.)

the integrated probability for the Fock states containing heavy quarks falls nominally as g^2/m_Q^4 in this super-renormalizable theory, compared to g^2/m_Q^2 dependence expected in renormalizable theories.

In the case of QCD(3+1), we also expect a two-component structure for heavy-quark structure functions of the light hadrons. The low x_F enhancement reflects the fact that the gluon-splitting matrix elements of heavy quark production favor low x. On the other hand, the $Q\overline{Q}q\bar{q}$ wavefunction also favors equal velocity of the constituents in order to minimize the off-shell light-cone energy and the invariant mass of the Fock state constituents. In addition, the non-Abelian effective Lagrangian analysis discussed above allows a heavy quark fluctuation in the bound state wavefunction to draw momentum from all of the hadron's valence quarks at order $1/m_Q^2$. This implies a significant contribution to heavy quark structure functions at medium to large momentum fraction x. The EMC measurements of the charm structure function of the nucleon appear to support this picture.[60]

It is thus useful to distinguish *extrinsic* and *intrinsic* contributions

to structure functions. The extrinsic contributions are associated with the substructure of a single quark and gluon of the hadron. Such contributions lead to the logarithmic evolution of the structure functions and depend on the momentum transfer scale of the probe. The intrinsic contributions involve at least two constituents and are associated with the bound state dynamics independent of the probe. The intrinsic gluon distributions[62] are closely related to the retarded mass-dependent part of the bound-state potential of the valence quarks.[63] In addition, because of asymptotic freedom, the hadron wavefunction has only an inverse power $\mathcal{M}^{-2}$ suppression for high mass fluctuations, whether one is considering heavy quark pairs or light quark pairs at high invariant mass $\mathcal{M}$. This "intrinsic hardness" of QCD wavefunctions leads to a number of interesting phenomena, including a possible explanation for "cumulative production," high momentum components of the nuclear fragments in nuclear collisions. This is discussed in detail in Ref. 64.

Renormalization and Ultra-violet Regulation of Light-cone-quantized Gauge Theory

An important element in the light-cone Hamiltonian formulation of quantum field theories is the regulation of the ultraviolet region. In order to define a renormalizable theory, a covariant and gauge invariant procedure is required to eliminate states of high virtuality. The physics beyond the scale Λ is contained in the normalization of the mass $m(\Lambda)$ and coupling constant $g(\Lambda)$ parameters of the theory, modulo negligible corrections of order $1/\Lambda^n$ from the effective Lagrangian. The logarithmic dependence of these input parameters is determined by the renormalization group equations. In Lagrangian field theories the ultraviolet cut-off is usually introduced via a spectrum of Pauli-Villars particles or dimensional regulation.

In the case of QCD (3+1), the renormalization of the light-cone Hamiltonian in light-cone gauge is not yet completely understood, but a number of methods are now under consideration. In Ref. 8 Lepage and I showed that by using invariant cutoffs for both the interactions in the light-cone Hamiltonian and the Fock space, one could verify the renormalization group behavior of the gauge-invariant distribution amplitude. The result is consistent with results obtained from the Bethe-Salpeter equation or the operator product expansion. Thus one has a reason to believe that a properly regulated and truncated

light-cone Hamiltonian can be constructed consistent with the known renormalization group structure of QCD.

In DLCQ, one needs to provide *a priori* some type of truncation of the Fock state basis. Since wavefunctions and Green's functions decrease with virtuality, one expects that states very far off the light-cone energy shell will have no physical effect on a system, except for renormalization of the coupling constant and mass parameters. Thus it is natural to introduce a "global" cut-off such that a Fock state $|n\rangle$ is retained only if

$$\sum_{i\epsilon n} \frac{\vec{k}_{\perp i}^2 + m_i^2}{x_i} - M^2 < \Lambda^2 \ . \tag{17}$$

Here M is the mass of the system in the case of the bound state problem, or the total invariant mass $\sqrt{s}$ of the initial state in scattering theory. One can also regulate the ultraviolet region by introducing a "local" cutoff on each matrix element $\langle n|H_{LC}|m\rangle$ by requiring that the change in invariant mass squared

$$\left| \sum_{i\epsilon n} \frac{\vec{k}_{\perp i}^2 + m_i^2}{x_i} - \sum_{i\epsilon m} \frac{\vec{k}_{\perp i}^2 + m_i^2}{x_i} \right| < \Lambda^2 \ . \tag{18}$$

This avoids spectator-dependent renormalization counterterms.[20] Similarly, one can use a lower cutoff on the invariant mass difference to regulate the infrared region.[65] Global and local cutoff methods were used in Ref. 8 to derive factorization theorems for exclusive and inclusive processes at large momentum transfer in QCD. In particular, the global cut-off defines the Fock-state wavefunctions $\psi^{\Lambda}(x, \vec{k}_{\perp}, \lambda)$ and distribution amplitude $\phi(x, \Lambda)$, the non-perturbative input for computing hadronic scattering amplitudes. The renormalization group properties of the light-cone wavefunctions and the resulting evolution equations for the structure functions and distribution amplitudes are also discussed in Ref. 8. The calculated anomalous dimensions γ_n for the moments of these quantities agree with results obtained using the operator product expansion.[66]

In general, light-cone quantization using the global or local cutoff can lead to terms in H_{LC}^{Λ} of the form $\delta m \overline{\psi} \frac{\gamma^+}{i\partial^+} \psi$. Such terms arise in order g^2 as a result of normal-ordering of the four-point interaction terms. Although such a term is invariant under the large class of light-cone Lorentz transformations, it is not totally invariant. Burkardt and Langnau[67] have suggested that the extra counterterms can be fixed by *a posteriori* imposing rotational symmetry on the bound state solutions, so that all Lorentz symmetries are restored.

The Zero-mode Problem in Light-cone-quantized Gauge Theory

The role of zero modes in the light-cone quantization of 1+1 gauge theories has now been greatly clarified by the work of Heinzl, Kruschke, and Werner,[68] McCartor and Robertson,[69] Griffin[70] and Hornbostel.[71] In general, zero mode (field excitations with $k^+ = 0$) must be retained consistent with the constraints imposed by the field equations of motion and the imposed boundary conditions. In the case of massless QED (1+1) (the Schwinger model), one needs to retain the zero mode at the A^+ field, since this degree of freedom leads to the labeling of the degenerate θ-vacua of the theory and the corresponding fermion condensates. In the case of theories such as $\phi^4(1+1)$, the zero mode of the ϕ field provides the degree of freedom usually associated with the spontaneous breaking of the vacuum. It is also clear that zero modes play an important role in implementing the correct degrees of freedom in the effective light-cone Hamiltonian for quantum field theories in 3+1 dimensions. Again, one must allow for quantum excitations with $k^+ = 0$ and any value of $\vec{k}_\perp$ so that the equations of motion and the boundary conditions are fulfilled. In the case of DLCQ, the assumed anti-periodic boundary conditions automatically exclude zero modes for the fermion fields, but zero modes are generally needed to describe the boson fields. Hiller and Wivoda[72] have shown that in the $\lambda\phi\psi\overline{\psi}$ theory, the convergence of the DLCQ solutions to the known Wick-Cutkowsky solutions is greatly increased by the inclusion of the $\phi(k^+ = 0)$ modes.

Zero modes are also required for the implementation of the light-cone gauge ($A^+ = 0$) in gauge theories in 1+1 dimensions. One of the most serious complications of the light-cone gauge quantization of QED (3+1) is the appearance of an apparently unregulated $1/k^+$ singularity

in the expression for electron-electron scattering due to the $1/(k \cdot \eta)$ terms in the photon propagator. Although this singularity vanishes for on-shell scattering, it confounds the proper interpretation of the effective potential for positronium in the effective light-cone potential. However, Soper[73] has now shown that the Leibbrandt-Mandelstam prescription for the light-cone propagator with

$$\frac{1}{k^+} \Rightarrow \frac{k^-}{k^+k^- + i\epsilon} \tag{19}$$

automatically generates a subtraction term in the QED effective Hamiltonian which eliminates the gauge singularity at $k^+ = 0$. This solution corresponds to a ghost zero mode, first identified by Bassetto[74] to be necessary for the consistent implementation of the light-cone gauge with periodic boundary conditions. A similar subtraction at $k^+ = 0$ also occurs in the definition of the evolution kernel for the distribution amplitude.[8]

Advantages of Light-cone Quantization

As I have discussed in this chapter the method of discretized light-cone quantization provides a relativistic, frame-independent discrete representation of quantum field theory amenable to computer simulation. In principle, the method reduces the light-cone Hamiltonian to diagonal form and has the remarkable feature of generating the complete spectrum of the theory: bound states and continuum states alike. DLCQ is also useful for studying relativistic many-body problems in relativistic nuclear and atomic physics. In the nonrelativistic limit the theory is equivalent to the many-body Schrödinger theory. DLCQ has been successfully applied to a number of field theories in one-space and one-time dimension, providing not only the bound-state spectrum of these theories, but also the light-cone wavefunctions needed to compute structure functions, intrinsic sea-quark distributions, and the e^+e^- annihilation cross section.

Although the primary goal has been to apply light-cone methods to non-perturbative problems in QCD in physical space-time, it is important to validate these techniques for the much simpler Abelian theory of QED. The discretized quantization of quantum electrodynamics on

the light-cone in principle allows practical numerical solutions for obtaining its spectrum and wavefunctions at arbitrary coupling strength α. We also have discussed a frame-independent and approximately gauge-invariant particle number truncation of the Fock basis which is useful both for computational purposes and physical approximations. In this method[20] ultraviolet and infrared regularizations are kept independent of the discretization procedure, and are identical to that of the continuum theory. One thus obtains a finite discrete representation of the gauge theory which is faithful to the continuum theory and is completely independent of the choice of Lorentz frame.

Light-cone quantization appears to have the potential for solving important non-perturbative problems in gauge theories. It has a number of intrinsic advantages:

- The formalism is independent of the Lorentz frame—only relative momentum coordinates appear. The computer does not know the Lorentz frame!
- Fermions and derivatives are treated exactly; there is no fermion-doubling problem.
- The ultraviolet and infrared regulators can be introduced as frame independent momentum space cut-offs of the continuum theory, independent of the discretization.
- The field theoretic and renormalization properties of the discretized theory are faithful to the continuum theory. No non-linear terms are introduced by the discretization.
- One can use the exact global symmetries of the continuum Lagrangian to pre-diagonalize the Fock sectors.
- The discretization is denumerable; there is no over-counting. The minimum number of physical degrees of freedom are used because of the light-cone gauge. No Gupta-Bleuler or Faddeev-Popov ghosts occur and unitarity is explicit.
- Gauge invariance is lost in a Hamiltonian theory. However, the truncation can be introduced in such a way as to minimize explicit breaking of the gauge symmetries.[20]
- The output of H_{LC} matrix diagonalization is the full color-singlet spectrum of the theory, both bound states and continuum, together with their respective light-cone wavefunctions.

There are, however, a number of difficulties that need to be resolved:

- The number of degrees of freedom in the representation of the light-cone Hamiltonian increases rapidly with the maximum number of particles in the Fock state. Although heavy quark bound states probably only involve a minimal number of gluons in flight, this is most likely not true for light hadrons.
- Some problems of ultraviolet and infrared regulation remain. Although Pauli-Villars ghost states and finite photon mass can be used to regulate Abelian theories, it is not suitable method in non-Abelian theories.[65]
- The renormalization procedure is not completely understood in the context of non-perturbative problems. However, a non-perturbative recursive representation for electron mass renormalization has been successfully tested in QED(3+1).[20]
- The Coulomb singularity in the effective gluon-exchange potential is poorly approximated in the discrete form. An analytic trick must be used to speed convergence. Such a method has been tested successfully in the case of the positronium spectrum in QED(3+1).[22]
- The vacuum in QCD is not likely to be trivial since the four-point interaction term in $g^2 G_{\mu\nu}^2$ can introduce new zero-mode color-singlet states which mix with the free vacuum state. Thus a special treatment of the QCD vacuum is required. In the case of zero mass quarks, there may be additional mixing of the perturbative vacuum with fermion zero-modes.

In addition to its potential for solving the problems of the hadronic spectrum and wavefunctions of QCD, light-cone quantization has already led to many new insights into the quantization of gauge theories. It has also brought a refocus of both theory and experiment to the novel features of QCD phenomena at the amplitude level.

3. NOVEL SPIN, HEAVY QUARK, AND SPIN EFFECTS IN QCD

In this section I will discuss a number of interesting hadronic spin effects which test fundamental features of perturbative and non-perturbative QCD. These include constraints on the shape and normalization

of the polarized quark and gluon structure functions of the proton; the principle of hadron helicity retention in high x_F inclusive reactions; predictions based on total hadron helicity conservation in high momentum transfer exclusive reactions; the dependence of nuclear structure functions and shadowing on virtual photon polarization; and general constraints on the magnetic moment of hadrons. I also will discuss the implications of several measurements which are in striking conflict with leading-twist perturbative QCD predictions, such as the extraordinarily large spin correlation A_{NN} observed in large angle proton-proton scattering, the anomalously large $\rho\pi$ branching ratio of the J/ψ, and the rapidly changing polarization dependence of both J/ψ and continuum lepton pair hadroproduction observed at large x_F.

Polarization effects and spin correlations often provide the most sensitive tests of the underlying structure and dynamics of hadrons. The basic measures of the spin structure of the proton are its magnetic moment, which gives a global measure of the quark spin content of the proton, and the spin-dependent structure functions, which register the local distribution of the quark helicity currents as a function of their light-cone momentum fraction x.[75] The SLAC-Yale and EMC measurements show a strong positive helicity correlation between the helicity of the $u-$ and $\overline{u}$ quarks with that of the proton; the helicity of the $d-$ and $s-$quark and antiquarks are negatively correlated. Most remarkably, the net correlation of the quark plus antiquark helicity with that of the proton Δq is consistent with zero. Since the total spin projection $\frac{1}{2}\Delta q + \Delta g + L_z = \frac{1}{2}$, there must be a significant fraction of Fock states in the proton containing gluons, and there must be a non-trivial correlation of the gluon helicity with that of the proton.

Although the net correlation of the quark helicity with the proton helicity in inclusive reactions is small, the spin correlations of large angle elastic pp scattering nevertheless display a dramatic structure at the highest measured energies $\sqrt{s} \sim 5\ GeV$.[76] These measurements are in strong conflict with the expectations of perturbative QCD which predicts a smooth power-law fall-off for exclusive helicity amplitude with increasing momentum transfer.[77] The strong polarization correlations observed in pp scattering are clearly of fundamental interest, since the microscopic QCD mechanisms that underlie the spin correlations between the incident and final hadrons must involve the coherent transfer of helicity information through their common quark and gluon con-

stituents. The implications of the spin correlation measurements will be discussed below.

In this chapter I shall emphasize a basic but non-trivial prediction of the gauge couplings of PQCD, "hadron helicity retention": a projectile hadron tends to transfer its helicity to its leading particle fragments. A particularly interesting consequence is the prediction that the J/ψ and the continuum lepton pairs produced in pion-nucleus collisions will be longitudinally polarized at large x_F. Helicity retention also provides important constraints on the shape of the gluon and quark helicity distributions. In the large x_F domain, with $Q^2(1-x)$ fixed, leading twist and multi-parton higher twist processes can be of equal importance.[78] In the case of large momentum transfer exclusive reactions, the underlying chiral structure of perturbative QCD predicts that sum of hadron helicities in the initial state must equal that of the final state.[45] Although hadron helicity conservation appears to be empirically satisfied in most reactions, the most interesting cases are its dramatic failures such as the large branching ratio for $J/\psi \to \rho\pi$. I will discuss these predictions and their experimental tests below.

Although most of the topics discussed in this chapter are concerned with quark or gluon helicity, there are also interesting linear polarization predicted by the theory, such as in Υ decays, or in the planar correlations of four-jet events in e^+e^- annihilation. In addition, the oblateness[79] of a gluon jet can be used to determine its axis of linear polarization.

The Magnetic Moment of Hadrons in QCD

Much of our understanding of the helicity structure of hadrons comes from rigorous constraints, such as the Bjorken Sum Rule for the integral of the spin dependent structure functions, and the Drell-Hearn-Gerasimov sum rule, which relates the anomalous magnetic moment of a composite system to an integral over the photoabsorption cross section. In fact Burkert and Ioffe[80] have shown that the DHG and Bjorken sum rules can be regarded as low and high Q^2 limits of the same sum rule.

One of the most interesting consequences of the DHG sum rule occurs if we take a point-like limit such that the threshold for inelastic excitation becomes infinite while the mass of the system is kept finite.

Since the integral over the photoabsorption cross section vanishes in this limit, the DHG sum rule implies that the anomalous moment must also vanish. Thus in the point-like limit, the magnetic moment of a spin-half system must approach the Dirac value $\mu \to \mu_D = e/2M$ up to structure corrections of order M/Λ, [or $(M/\Lambda)^2$ if the underlying theory is chiral].[81] Hiller and I have recently derived a generalization of the DHG sum rule for spin-one composite systems. In the point-like limit, both the magnetic moment and quadrupole moment of any spin-one system must approach the canonical values predicted by electroweak theory for the W.[82]

The Drell-Hearn sum rule also has important consequences for the computation of the magnetic moments of baryons in QCD. Magnetic moments are often computed using the quark model formula $\vec{\mu} = \sum_{i=1}^{3} \vec{\mu}_i$. This formula is correct in the case of atoms where the mass of the nucleus can be taken as infinite. However, magnetic moment additivity cannot be correct in general: the DHG sum rule shows that in the limit of strong binding where the constituents become very massive and the hadron becomes point-like, its magnetic moment must equal the Dirac value, not zero as predicted by quark moment additivity. The flaw in the conventional quark model formula is that it does not take into account the fact that the moment of a system H is derived from the electron scattering amplitude $eH \to e'H'$ at non-zero momentum transfer q. The Dirac value in the point-like limit actually arises from the Wigner boost of the wavefunction from p to $p+q$. A detailed discussion of this and the resulting relativistic corrections to the moment are given Ref. 83. On the other hand, the overlap of light-cone Fock wavefunctions does provide a general method for the evaluation of hadronic magnetic moments and form factors.[81]

The Gluon Helicity Distribution

One of the most interesting questions in QCD spin physics is the distribution of gluon polarization in the proton. The gluon distribution of a hadron is usually assumed to be radiatively generated from the QCD evolution of the quark structure functions beginning at an initial scale Q_0^2. The evolution is incoherent; *i.e.* each quark in the hadron radiates gluons independently. However, as can be seen in the light-cone Hamiltonian approach, the higher Fock components of a bound state in QCD contain gluons at any resolution scale. Furthermore, the

exchange of gluon quanta between the bound-state constituents provides an interaction potential whose energy–dependent part generates a non-trivial non-additive contribution to the full gluon distribution $G_{g/H}(x, Q_0^2)$. The physics of gluon helicity distributions clearly involves the nonperturbative structure of the proton. Nevertheless, there are constraints which we can use to limit the possible form of the helicity–aligned and anti–aligned gluon distributions: $G^+(x) = G_{g\uparrow/N\uparrow}(x)$ and $G^-(x) = G_{g\downarrow/N\uparrow}(x)$[84]:

1. In order to insure positivity of fragmentation functions, the distribution functions $G_{a/b}(x)$ must behave as an odd or even power of $(1-x)$ at $x \to 1$ according to the relative statistics of a and b.[85] Thus the gluon distribution of a nucleon must have the behavior: $G_{g/N}(x) \sim (1-x)^{2k}$ at $x \to 1$ to ensure correct crossing to the fragmentation function $D_{N/g}(z)$.

2. In the $x \to 1$ limit, a gluon constituent of the proton is far off–shell and the leading behavior in the hadron wavefunctions is dominated by perturbative QCD contributions to the interaction kernel. We thus may use the minimally connected tree-graphs to characterize the threshold dependence of the structure functions. We find for a three quark plus one gluon Fock state, $\lim_{x\to 1} G^+(x) \to C(1-x)^{2N_q-2} = C(1-x)^4$. The gauge theory couplings of gluons to quarks also imply $\lim_{x\to 1} G^-(x)/G^+(x) \to (1-x)^2$. Thus $G^-(x) \sim (1-x)^6$ at $x \sim 1$. QCD evolution does not change these powers appreciably since the available phase-space for secondary gluon emission is limited to $k_\perp^2 < (1-x)Q^2$.
3. In the low x domain the quarks in the hadron radiate gluons coherently. Define $\Delta G(x) = G^+(x) - G^-(x)$ and $G(x) = G^+(x) + G^-(x)$. One then finds that the asymmetry ratio $\Delta G(x)/G(x)$ vanishes linearly with x.
4. In a simplest three quark plus one-gluon Fock state model the generated gluon distribution in the nucleon at low x has the normalization[84] $\Delta G(x)/G(x) = (x/3)\langle 1/y \rangle$, where y is the quark momentum fraction in the three quark state. The factor of $1/3$ is due to the fact that all of the quarks contribute positively to $G(x)$, but are proportional to the sign of their helicity in $\Delta G(x)$.

If we assume equal quark momentum partition $\langle 1/y \rangle = 3$, then the

above constraints are satisfied by the simple form[84]:

$$\begin{aligned} \Delta G(x) &= (N/x)[1-(1-x)^2](1-x)^4, \\ G(x) &= (N/x)[1+(1-x)^2](1-x)^4 \ . \end{aligned} \tag{20}$$

This gives $\Delta G/\langle x_g \rangle = 77/72 = 1.07$ for the ratio of the gluon helicity to its momentum fraction in the nucleon. Since the gluon momentum fraction is ~ 0.5, we predict the total gluon helicity correlation $\Delta G = 0.54$, which by itself saturates the proton spin sum rule. It is expected that these results should provide a good characterization of the gluon distribution at the resolution scale $Q_0^2 \simeq M_p^2$. Clearly the model could be improved by taking into account higher Fock states and QCD evolution.

A determination of the unpolarized gluon distribution of the proton at $Q^2 \sim 2\ GeV^2$ using direct photon and deep inelastic data has been given in Ref. 86. The best fit over the interval $0.05 \leq x \leq 0.75$ assuming the form $xG(x, Q^2 = 2\ GeV^2) = A(1-x)^{\eta_g}$ gives $\eta_g = 3.9 \pm 0.11(+0.8 - 0.6)$, where the errors in parenthesis allow for systematic uncertainties. This result is compatible with the prediction $\eta_g = 4$ for the gluon distribution at the bound–state scale, allowing for the small effects due to QCD evolution.

Quark Helicity Distributions and Hadron Helicity Retention in Inclusive Reactions at Large x_F

Consider a general inclusive reaction $AB \to CX$ at large x_F where the helicities λ_C and λ_A are measured. To be precise, we shall use the boost-invariant light-cone momentum fraction $x_C = \frac{k_C^+}{k_A^+} = \frac{(k^0+k^z)_C}{(k^0+k^z)_A}$. Hadron helicity retention implies that the difference between λ_C and λ_A tends to a minimum at $x_C \to 1$. Hadron helicity retention follows from the helicity structure of the gauge theory interactions, and it is applicable to hadrons, quarks, gluons, leptons, or photons. For example, in QED photon radiation in lepton scattering has the well-known distribution $dN/dx \propto [1+(1-x)^2]/x$. The first term corresponds to the case where the photon helicity has the same sign as the lepton helicity; opposite sign helicity production is suppressed by a factor $(1-x)^2$ at $x \to 1$[87]: the projectile helicity tends to be transferred by the leading fragment at each step in perturbation theory. It is a nontrivial step

to show that hadron helicity also holds for hadrons in QCD; e.g.: the structure functions of the leading quarks in the proton have the nominal power behavior: $G_{q/p}(x) \sim (1-x)^3$ for $\lambda_q = \lambda_p$ and $G_{q/p}(x) \sim (1-x)^5$ if $\lambda_q = -\lambda_p$. This result follows from the fact that at $x \to 1$ the struck quark is far off-shell and spacelike: $k^2 \sim -\mu^2/(1-x)$ where μ is a typical hadron mass scale; the leading fall-off of structure functions at $x \to 1$ can thus be computed from the minimally-connected tree-graphs.

These considerations have the immediate consequence that the down and anti-down quark distribution $\Delta d(x)$ has a zero as a function of x. At large x PQCD predicts that the helicity-antiparallel distribution $d^+(x)$ is suppressed relative to the helicity-parallel distribution $d^+(x)$ by two powers of $(1-x)$. At very small x the two distributions must have equal magnitude to ensure convergence of sum rules. However, measurements imply that the integral $\Delta d = \int_0^1 dx[d^+(x) - d^-(x)]$ is negative. Thus one expects that $\Delta d(x)$ changes sign as a function of x.[84]

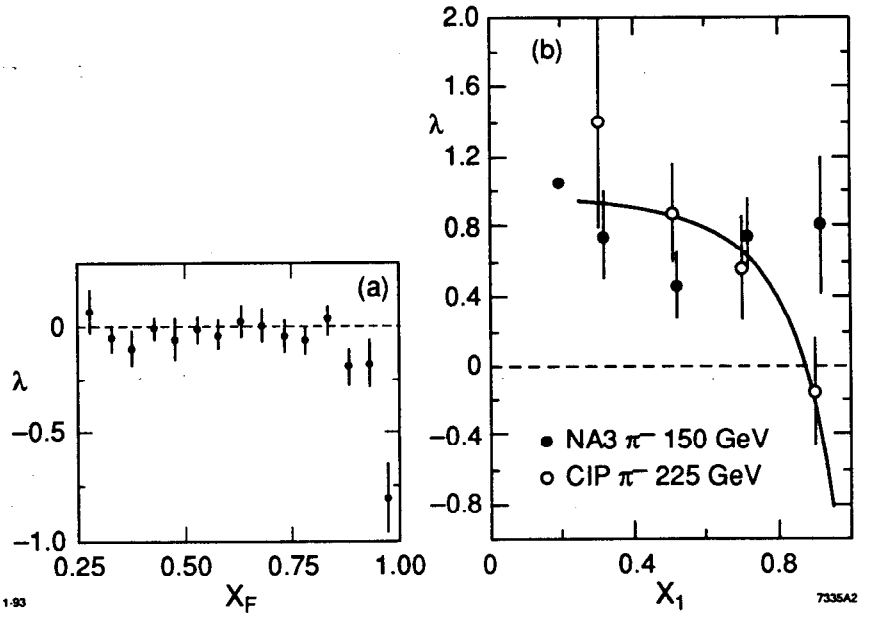

Figure 14. The x_F dependence of the polarization parameter λ for (a) J/ψ production[88] and (b) continuum lepton pair production[89] in $\pi - N$ collisions as a function of x_F.

One of the most important testing grounds for hadron helicity retention is J/ψ production in $\pi - N$ collisions. The helicity of the J/ψ can be measured from the angular distribution $1 + \lambda \cos^2 \theta_\mu$ of one of the muons in the leptonic decay of the J/ψ. At low to medium values of x_F the Chicago-Iowa-Princeton Collaboration[88] finds that $\lambda \sim 0$, which is consistent with expectations from the gluon-gluon fusion subprocess. However, at large $x_F > 0.9$ the angular distribution changes markedly to $\sin^2 \theta_\mu$; *i.e.*, the J/ψ is produced with longitudinal polarization. [See Fig. 14(a).] Note that the expectation of quark anti-quark fusion is $1 + \cos^2 \theta_\mu$ ($\lambda = +1$), as in the Drell-Yan process. The sudden change to longitudinal polarization must mean that a new heavy quark production mechanism is present at large x_F.[90] In fact, it is easy to guess the relevant process which can produce high momentum charm quark pairs. [See Fig. 15(a).] Since nearly all of the pion's momentum is transferred to the charmonium system, one needs to consider diagrams where each valence quark in the incoming pion emits a fast gluon. The two gluons then fuse to make a fast $c\bar{c}$ pair. At large momentum fraction x, each gluon's helicity tends to be parallel to the helicity of its parent quark. Thus the angular momentum J_z of the gluon pair is transferred to the $c\bar{c}$ pair. The angular momentum tends to be preserved by any subsequent gluon radiation or gluon interaction from the heavy quarks. The J/ψ then tends to have the same helicity as the projectile at high light-cone momentum fraction.

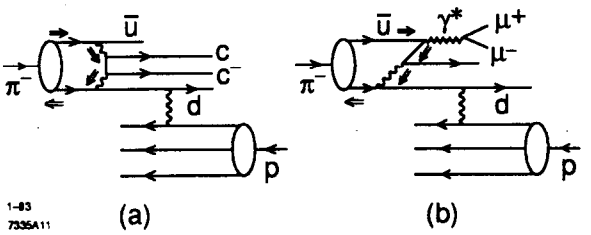

Figure 15. Higher twist mechanisms for producing (a) J/ψ and (b) massive lepton pairs at high x_F in meson-nucleon collisions.

Thus there is a natural mechanism in QCD which produces the J/ψ in the same helicity as the incoming beam hadron; the essential feature is the involvement of all of the valence quarks of the incoming hadron directly in the heavy quark production subprocess. Since such

diagrams involve the correlation between the partons of the hadron, it can be classified as a higher-twist "intrinsic charm" amplitude; the production cross section is suppressed by powers of $f_\pi/M_{Q\overline{Q}}$ relative to conventional fusion processes. Although nominally higher twist, such diagrams provide an efficient way to transfer the beam momentum to the heavy quark system while stopping the valence quarks.

The intrinsic charm mechanism also can explain other features of the J/ψ hadroproduction.[91,92,93] The observed cross section persists to high x_F in excess of what is predicted from gluon fusion or quark anti–quark annihilation subprocesses; furthermore the cross section at high x_F has a strongly suppressed nuclear dependence, $A^{\alpha(x_F)} \sim 0.7$. The nuclear dependence actually depends on x_F not x_2 which rules out leading twist mechanisms. The higher-twist intrinsic charm *e.g.* $|uudc\bar{c}\rangle$ Fock state wavefunctions have maximum probability when all of the quarks have equal velocities, *i.e.* when $x_i \propto \sqrt{m_i^2 + k_{\perp_i}^2}$. This implies that the charm and anti–charm quarks have the majority of the momentum of the proton when they are present in the hadronic wavefunction. In a high energy proton–nucleus collision, the small transverse size, high–x intrinsic $c\bar{c}$ system can penetrate the nucleus, with minimal absorption and can coalesce to produce a charmonium state at large x_F. Since the soft quarks expand rapidly in impact space, the main interaction in the target of the intrinsic charm Fock state is with the slow valence quarks rather than the compact $c\bar{c}$ system.[78] Thus at large x_F the interaction in the nucleus should have the A-dependence of normal hadron nucleus cross sections: $\sim A^{0.7}$. Note that at high energies, the formation of the charmonium state occurs far outside the nucleus. Thus one predicts similar $A^{\alpha(x_F)}$–dependence of the J/ψ and ψ' cross sections. These predictions are in agreement with the results reported by the E–772 experiment at Fermilab.[92]

In the case of continuum pair production, the lepton pair produced via the leading-twist Drell-Yan fusion mechanism $q\bar{q}\to\mu^+\mu^-$ has transverse polarization ($\lambda = 1$). However, at large x_F the muon angular distribution is observed to change to $\sin^2\theta_\mu$.[89] [See Fig. 14(b).] This result was predicted[34] from the dominance of higher twist $\pi q\to\mu^+\mu^- q$ subprocess contributions at high x_F. A detailed calculation shows subprocess amplitude can be normalized to the same integral over the pion distribution amplitude $\int dx\phi(x,Q)/(1-x)$ that controls the pion form

factor.[94]

In the higher-twist subprocess diagram, Fig. 15(b), the lepton pair tends to have the same helicity as the beam hadron at large x_F. For example, consider $\pi^- N \to \mu^+ \mu^- X$ at high x_F. The valence d quark emits a fast gluon which in turn makes a fast-u, slow-$\bar{u}$ pair. Because of the QCD couplings, the fast u then carries the helicity of the d. The valence $\bar{u}$ then annihilates with the fast u to make the lepton pair at $x_F \sim 1$. The lepton pair thus tends to have the helicity ($J_z = 0$) of the pion, in agreement with hadron helicity retention.

Hadron Helicity Conservation in Hard Exclusive Reactions

There are also strong helicity constraints on form factors and other exclusive amplitudes which follow from perturbative QCD.[77] At large momentum transfer, each helicity amplitude contributing to an exclusive process at large momentum transfer can be written as a convolution of a hard quark-gluon scattering amplitude T_H which conserves quark helicity with the hadron distribution amplitudes $\phi(x_i, Q)$, which are the $L_z = 0$ projections of the hadron's valence Fock state wavefunction: $\phi(x_i, \lambda_i, Q) = \int [d^2 k_\perp]\ \psi(x_i, \vec{k}_{\perp i}, \lambda_i) \theta(k_{\perp i}^2 < Q^2)$ where $\psi(x_i, \vec{k}_{\perp i}, \lambda_i)$ is the valence wavefunction. Since ϕ only depends logarithmically on Q^2, the main dynamical dependence of $F_B(Q^2)$ is the power behavior $(Q^2)^{-2}$ derived from the scaling behavior of the elementary propagators in T_H.

As shown by Botts, Li, and Sterman,[95] the virtual Sudakov form factor suppresses long distance contributions from Landshoff multiple scattering and $x \sim 1$ integration regions, so that the leading high momentum transfer behavior of hard exclusive amplitudes are generally controlled by short-distance physics. Thus quark helicity conservation of the basic QCD interactions leads to a general rule concerning the spin structure of exclusive amplitudes[45]: to leading order in $1/Q$, the total helicity of hadrons in the initial state must equal the total helicity of hadrons in the final state. This selection rule is independent of any photon or lepton spin appearing in the process. The result follows from (a) neglecting quark mass terms, (b) the vector coupling of gauge particles, and (c) the dominance of valence Fock states with zero angular momentum projection. The result is true in each order of perturbation theory in α_s.

For example, PQCD predicts that the Pauli Form factor $F_2(Q^2)$ of a baryon is suppressed relative to the helicity-conserving Dirac form factor $F_1(Q^2)$. A recent experiment at SLAC carried out by the American-University/SLAC collaboration is in fact consistent with the prediction $Q^2F_2(Q^2)/F_1(Q^2) \rightarrow$ const.[96] Helicity conservation holds for any baryon to baryon vector or axial vector transition amplitude at large spacelike or timelike momentum. Helicity non-conserving form factors should fall as an additional power of $1/Q^2$.[45] Measurements[97] of the transition form factor to the $J = 3/2$ $N(1520)$ nucleon resonance are consistent with $J_z = \pm 1/2$ dominance, as predicted by the helicity conservation rule.[45] One of the most beautiful tests of perturbative QCD is in proton Compton scattering, where there are now detailed predictions available for each hadron helicity-conserving amplitude for both the spacelike and timelike processes.[98] In the case of spin-one systems such as the ρ or the deuteron, PQCD predicts that the ratio of the three form factors have the same behavior at large momentum transfer as that of the W in the electroweak theory.[82]

Hadron helicity conservation in large momentum transfer exclusive reactions is a general principle of leading twist QCD. In fact, in several outstanding cases, it does not work at all, particularly in single spin asymmetries such as A_N in pp scattering, and most spectacularly in the two-body hadronic decays of the J/ψ. The inference from these failures is that non-perturbative or higher twist effects must be playing a crucial role in the kinematic range of these experiments.

The J/ψ decays into isospin-zero final states through the intermediate three-gluon channel. If $PQCD$ is applicable, then the leading contributions to the decay amplitudes preserve hadron helicity. In the case of e^+e^- annihilation into vector plus pseudoscalar mesons, Lorentz invariance requires that the vector meson will be produced transversely polarized. Since this amplitude does not conserve hadron helicity, $PQCD$ predicts that it will be dynamically suppressed at high momentum transfer. Hadron helicity conservation appears to be severely violated if one compares the exclusive decays J/ψ and $\psi' \rightarrow \rho\pi, K^*\overline{K}$ and other vector-pseudoscalar combinations. The predominant two-body hadronic decays of the J/ψ have the measured branching ratios

$$
\begin{aligned}
BR(J/\psi \to K^+K^-) &= 2.37 \pm 0.31 \times 10^{-4} \\
BR(J/\psi \to \rho\pi) &= 1.28 \pm 0.10 \times 10^{-2} \\
BR(J/\psi \to K^+K^{-*}) &= 5.0 \pm 0.4 \times 10^{-3} \ .
\end{aligned}
\tag{21}
$$

Thus the vector-pseudoscalar decays are not suppressed, in striking contrast to the PQCD predictions. On the other hand, for the ψ':

$$
\begin{aligned}
BR(\psi' \to K^+K^-) &= 1.0 \pm 0.7 \times 10^{-4} \\
BR(\psi' \to \rho\pi) &< 8.3 \times 10^{-5} \ \ (90\%\ CL) \\
BR(\psi' \to K^+K^{-*}) &< 1.8 \times 10^{-5} \ \ (90\%\ CL) \ .
\end{aligned}
\tag{22}
$$

From the standpoint of perturbative QCD, the observed suppression of ψ' to vector-pseudoscalar mesons is expected; it is the J/ψ that is anomalous.[99] What can account for the apparently strong violation of hadron helicity conservation? One possibility is that the overlap of the $c\bar{c}$ system with the wavefunctions of the ρ and π is an extremely steep function of the pair mass, as discussed by Chaichian and Tornqvist.[100] However, this seems unnatural in view of the similar size of the J/ψ and ψ' branching ratios to K^+K^-. Pinsky[101] has suggested that the ψ' decays predominantly to final states with excited vector mesons such as $\rho'\pi$, in analogy to the absence of configuration mixing in nuclear decays. However, this long-distance decay mechanism would not be expected to be important if the charmonium state decays through $c\bar{c}$ annihilation at the Compton scale $1/m_c$.

Another way in which hadron helicity conservation might fail for $J/\psi \to$ gluons $\to \pi\rho$ is if the intermediate gluons resonate to form a gluonium state $\mathcal{O}$. If such a state exists, has a mass near that of the J/ψ, and is relatively stable, then the subprocess for $J/\psi \to \pi\rho$ occurs over large distances and the helicity conservation theorem need no longer apply. This would also explain why the J/ψ decays into $\pi\rho$ and not the ψ'. Tuan, Lepage, and I[99] have thus proposed, following Hou and Soni,[102] that the enhancement of $J/\psi \to K^*\overline{K}$ and $J/\psi \to \rho\pi$ decay modes is caused by a quantum mechanical mixing of the J/ψ with a $J^{PC} = 1^{--}$ vector gluonium state $\mathcal{O}$ which causes the breakdown of the QCD helicity theorem. The decay width for $J/\psi \to \rho\pi$ via the sequence $J/\psi \to \mathcal{O} \to \rho\pi$ must be substantially larger than the

decay width for the (non-pole) continuum process $J/\psi \rightarrow 3$ gluons $\rightarrow \rho\pi$. In the other channels the branching ratios of the $\mathcal{O}$ must be so small that the continuum contribution governed by the QCD theorem dominates over that of the $\mathcal{O}$ pole. A gluonium state of this type was first postulated by Freund and Nambu[103] based on OZI dynamics soon after the discovery of the J/ψ and ψ' mesons. The most direct way to search for the $\mathcal{O}$ is to scan $\bar{p}p$ or e^+e^- annihilation at $\sqrt{s}$ within ~ 100 MeV of the J/ψ, triggering on vector/pseudoscalar decays such as $\pi\rho$ or $\overline{K}K^*$ and look for enhancements relative to K^+K^-. Such a search has recently been proposed for the BEPC by Chen Yu, Gu Yifan, and Wang Ping.

Anomalous Spin Correlations and Color Transparency Effects in Proton-Proton Scattering

The perturbative QCD analysis of exclusive amplitudes assumes that large momentum transfer exclusive scattering reactions are controlled by short distance quark-gluon subprocesses, and that corrections from quark masses and intrinsic transverse momenta can be ignored. Since hard scattering exclusive processes are dominated by valence Fock state wavefunctions of the hadrons with small impact separation and small color dipole moments, one predicts that initial and final state interactions are generally suppressed at high momentum transfer. In particular, since the formation time is long at high energies, one predicts that the attenuation of quasi-elastic processes due to Glauber inelastic scattering in a nucleus will be reduced. This is the color transparency prediction of perturbative QCD.[25] A test of color transparency in large momentum transfer quasielastic pp scattering at $\theta_{\rm cm} \simeq \pi/2$ has been carried out at BNL using several nuclear targets (C, Al, Pb).[104] The attenuation at $p_{\rm lab} = 10$ GeV/c in the various nuclear targets was observed to be in fact much less than that predicted by traditional Glauber theory. The expectation from perturbative QCD is that the transparency effect should become even more apparent as the momentum transfer rises. However, the data at $p_{\rm lab} = 12$ GeV/c shows normal nuclear attenuation and thus a violation of color transparency.

An even more serious challenge to the PQCD predictions for exclusive scattering is the observed behavior of the normal spin-spin correlation asymmetry $A_{NN} = [d\sigma(\uparrow\uparrow) - d\sigma(\uparrow\downarrow)]/[d\sigma(\uparrow\uparrow) + d\sigma(\uparrow\downarrow)]$ measured in large momentum transfer pp elastic scattering. At $p_{\rm lab} = 11.75$

GeV/c and $\theta_{cm} = \pi/2$, A_{NN} rises to $\simeq$ 60%, corresponding to four times more probability for protons to scatter with their incident spins both normal to the scattering plane and parallel, rather than normal and opposite.[76] In contrast, the unpolarized data is to first approximation consistent with the fixed angle scaling law $s^{10}d\sigma/dt(pp \to pp) = f(\theta_{CM})$ expected from the perturbative analysis. The onset of new structure at $s \simeq 23$ GeV^2 suggests new degrees of freedom in the two-baryon system.

Guy De Teramond and I[49] have noted that the onset of strong spin-spin correlations, as well as the breakdown of color transparency, can be explained as the consequence of a strong threshold enhancement at the open-charm threshold for $pp \to \Lambda_c Dp$ at $\sqrt{s} = 5.08\ GeV$ or $p_{lab} \sim 12\ GeV/c$. At this energy the charm quarks are produced at rest in the center of mass. Since all eight quarks have zero relative velocity, they can resonate to give a strong threshold effect in the $J = L = S = 1$ partial wave. (The orbital angular momentum of the pp state must be odd since the charm and anti-charm quarks have opposite parity.) The $J = L = S = 1$ partial wave has maximal spin correlation $A_{NN} = 1$. A charm production cross section of the order of 1 μb in the threshold region can have, by unitarity, a large effect on the large angle elastic $pp \to pp$ amplitude since the competing perturbative QCD hard-scattering amplitude at large momentum transfer is very small at $\sqrt{s} = 5\ GeV$. In fact as recently shown by Manohar, Luke, and Savage,[50] the QCD trace anomaly predicts that the scalar charmonium-nucleus interaction is strongly amplified at low velocities and can lead to nuclear-bound charmonium.[51]

An analytic model which contains all of these features is given in Ref. 49. The background component of the model is the perturbative QCD amplitude with s^{-4} scaling of the $pp \to pp$ amplitude at fixed θ_{cm} and the dominance of those amplitudes that conserve hadron helicity.[45] A comparison[105] of the magnitude of cross sections for different exclusive two-body scattering channels indicate that quark interchange amplitudes[106] dominate quark annihilation or gluon exchange contributions. The most striking test of the model is its prediction for the spin correlation A_{NN} shown in Fig. 16. The rise of A_{NN} to $\simeq$ 60% at $p_{lab} = 11.75$ GeV/c is correctly reproduced by the high energy J=1 resonance interfering with ϕ(PQCD). The narrow peak which appears

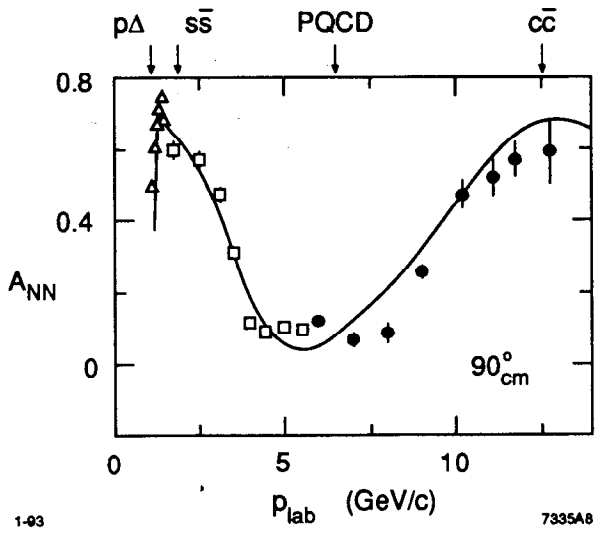

Figure 16. A_{NN} as a function of $p_{\rm lab}$ at $\theta_{cm} = \pi/2$. The data[76] are from Crosbie *et al.* (solid dots), Lin *et al.* (open squares) and Bhatia *et al.* (open triangles). The peak at $p_{\rm lab} = 1.26$ GeV/c corresponds to the $p\Delta$ threshold. The data are well reproduced by the interference of the broad resonant structures at the strange ($p_{\rm lab} = 2.35$ GeV/c) and charm ($p_{\rm lab} = 12.8$ GeV/c) thresholds, interfering with a PQCD background. The value of A_{NN} from PQCD alone is 1/3.

in the data of Fig. 16 corresponds to the onset of the $pp \rightarrow p\Delta(1232)$ channel which can be interpreted as a $uuuuddq\bar{q}$ $^3F_3$ resonance. The heavy quark threshold model also provides a good description of the s and t dependence of the differential cross section, including its "oscillatory" dependence[107] in s at fixed $\theta_{\rm cm}$, and the broadening of the angular distribution near the resonances. Most important, it gives a consistent explanation for the striking behavior of both the spin-spin correlations and the anomalous energy dependence of the attenuation of quasielastic pp scattering in nuclei. A threshold enhancement or resonance couples to hadrons of conventional size. Unlike the perturbative amplitude, the protons coupling to the resonant amplitude will have normal absorption in the nucleus. Thus the nucleus acts as a filter, absorbing the non–perturbative contribution to elastic pp scattering, while allowing the hard-scattering perturbative QCD processes to occur additively throughout the nuclear volume.[108] Conversely, in the momentum range $p_{\rm lab} = 5$ to 10 GeV/c one predicts that the per-

turbative hard-scattering amplitude will be dominant at large angles. It is thus predicted that color transparency should reappear at higher energies ($p_{\rm lab} \geq 16$ GeV/c), and also at smaller angles ($\theta_{\rm cm} \approx 60°$) at $p_{\rm lab} = 12$ GeV/c where the perturbative QCD amplitude dominates. If the resonance structures in A_{NN} are indeed associated with heavy quark degrees of freedom, then the model predicts inelastic pp cross sections of the order of 1 mb and 1μb for the production of strange and charmed hadrons near their respective thresholds. In fact, the neutral strange inclusive pp cross section measured at $p_{\rm lab} = 5.5$ GeV/c is 0.45 ± 0.04 mb.[109] Thus the crucial test of the heavy quark hypothesis for explaining A_{NN} is the observation of significant charm hadron production at $p_{\rm lab} \geq 12$ GeV/c.

Ralston and Pire[108] have suggested that the oscillations of the pp elastic cross section and the apparent breakdown of color transparency are associated with the dominance of the Landshoff pinch contributions at $\sqrt{s} \sim 5$ *GeV*. The oscillating behavior of $d\sigma/dt$ is then due to the energy dependence of the relative phase between the pinch and hard-scattering contributions. They assume color transparency will disappear whenever the pinch contributions are dominant since such contributions could couple to wavefunctions of large transverse size. However, the large spin correlation in A_{NN} is not readily explained in the Ralston-Pire model unless the Landshoff diagram itself has $A_{NN} \sim 1$.

Polarization-Dependent Nuclear Shadowing

Another interesting spin effect in QCD is the prediction that nuclear shadowing depends on the virtual photon polarization. In models where shadowing is due to the deformation of nucleon structure functions in the nucleus, one would not expect such any dependence on photon polarization. In Refs. 110 and 111 one sees that nuclear shadowing (in the target rest frame) arises from the destructive interference of the multiple scattering of a quark (or antiquark) in the nucleus. The quark comes from the upstream dissociation of the virtual photon. The $q\bar{q}$ pair is formed at a formation time (coherence length) $\tau \propto 1/x_{\rm bj}M$ before the target. In order to get significant multiple scattering and interference one needs a coherence length comparable to the nuclear size. However, Hoyer, Del Duca and I found[111] that the coherence length is significantly shorter (by a factor of $1/\sqrt{3}$) for the longitudinally polarized photon than the transverse case. The reason for this is that the

internal transverse momentum and hence the virtual mass and energy of the $q\bar{q}$ pair is larger by a nearly constant factor in the longitudinal case, thus shortening its lifetime. Thus the nuclear attenuation is delayed to smaller values of $x_{\rm bj}$ in the longitudinal compared to the transverse cross section. Nikolaev[112] has also recently discussed the possibility of smaller nuclear shadowing of σ_L on the grounds that the $q\bar{q}$ system has a smaller transverse size in the case of a longitudinally polarized photon, and it is thus more color transparent. In this case diminished longitudinal shadowing would persist for all $x_{\rm bj}$.

4. THE SCALE AND SCHEME DEPENDENCE OF PERTURBATIVE QCD

One of the most difficult problems in perturbative QCD is how to reliably estimate the theoretical error due to the choice of the renormalization scale and scheme.[113,114,39] Although all physical predictions in QCD should in principle be invariant under the change of both scale and scheme, in practice this invariance is only approximate due to the truncation of the perturbative series.

The ambiguities due to renormalization scale and scheme choice will be alleviated as one computes higher order contributions.[115,116,117,118] In the cases where there are large disparate scales in the problem, resummation techniques also promise to reduce the theoretical uncertainties. However, two questions still remain:

1. How can we give a reliable error estimate which correctly assesses the validity of high order PQCD predictions?
2. Is there a reliable way to choose the renormalization scale in relation to the physical scales? This problem is particularly important in the case of processes in which only low order calculations are available, and in processes with multiple physical scales. Commonly used scale-setting strategies include the Principle of Minimum Sensitivity (PMS)[113] (which also optimizes the choice of scheme), the Fastest Apparent Convergence (FAC) criterion,[114] and the "automatic scale-fixing method" (BLM).[39]

It has been traditional to consider the scale-scheme ambiguity as intrinsically unavoidable and to interpret the numerical fluctuations

coming from different scale and scheme choices as the error in the theoretical prediction. This point of view, aside from being overly pessimistic, is also very unsatisfactory. First of all, in general we do not know how wide a range the scale and scheme parameters should vary in order to give a correct error estimate. Secondly, besides the error due to scale-scheme uncertainties there is also the error from the omitted higher-order terms. In such an approach, it is not clear whether these errors are independent or correlated. The error analysis in this context can become quite arbitrary and unreliable.

For example, in their recent analysis of PQCD predictions for bottom quark production at hadron colliders, Berger, Meng, and Tung,[119] found that the predicted inclusive cross section $\sigma(p\bar{p}\rightarrow bX)$ at $\sqrt{s} = 1.8$ TeV for central rapidities $|y| < 1$ and $p_T > p_T^{min} = 30$ GeV actually varies by more than a factor of 10 within the arbitrary range $0.1M_T < \mu < 4M_T$. Since there is no *a priori* range for μ, the uncertainty due to the scale choice is actually even worse.

Recently Hung Jung Lu and I have shown that reliable error estimates in PQCD can be obtained from an analysis of the Stückelberg-Peterman extended renormalization group equations in perturbative QCD, which express the invariance of physical observables under renormalization-scale and scheme-parameter transformations. In this general framework, one can introduce a universal coupling function that covers all possible choices of scale and scheme. In fact any perturbative series in QCD is equivalent to a particular point in this function. The universal coupling function can be computed from a set of first-order differential equations involving extended beta functions. By using these evolution equations for the numerical evaluation of physical observables, we obtain a formalism that is free of scale-scheme ambiguity and a reliable error analysis of higher-order corrections. This method also leads to a precise definition for $\Lambda_{\overline{MS}}$ as the pole in the associated 't Hooft scheme.

Consider the N-th order expansion series of a physical observable R in terms of a coupling constant $\alpha_S(\mu)$ given in scheme S and at a scale μ:

$$R_N = r_0\alpha_S^p(\mu) + r_1(\mu)\alpha_S^{p+1}(\mu) + \cdots + r_N(\mu)\alpha_S^{p+N}(\mu) \ . \qquad (23)$$

The infinite series R_∞ is renormalization scale-scheme invariant. How-

ever, at any finite order, the scale and scheme dependencies from the coupling constant $\alpha_S(\mu)$ and from the coefficient functions $r_i(\mu)$ do not exactly cancel, which leads to a remnant dependence in the finite series. Different choices of scale and scheme then lead to different theoretical predictions.

In the extended renormalization group method, a perturbative series only serves as an intermediate device for the identification of scale and scheme parameters. The ultimate prediction is obtained through evolution equations in the scale- and scheme-parameter space. This approach provides both a reliable error analysis a precise definition for $\Lambda_{\overline{\rm MS}}$. Renormalization scheme invariant methods have been previously studied by Grunberg, Dhar and Gupta,[114,120] and our approach is essentially a reformulation of these methods in the language of a universal coupling function by using the Stückelberg-Peterman equations.

Power Series vs. Renormalization Group

It is important to emphasize that the goal of PQCD predictions is to relate measured observables. The most natural procedure would be to use one canonical process such as the annihilation cross section ratio $R_{e^+e^-}$ or the heavy quark potential to define $\alpha_s(Q^2)$, and then express other observables in terms of that "effective charge."[114] For example, in QED, Coulomb scattering is used to define the on-shell scheme and to normalize $\alpha(0)$. In the case of QCD it is more convenient to calculate using dimensional regularization, and to use the $\overline{\rm MS}$ scheme as an intermediate coupling; but at any stage, it should be possible to eliminate the dependence on $\alpha_{\overline{MS}}$ in favor of a couplng based on an observable.

To be more definite, let us consider the case of QCD with n_f massless quarks. We will limit ourselves to perturbative quantities that allow series expansion in the strong coupling constant. Given this premise, a physical observable R in QCD can be expanded in a power series like:

$$R = r_0\alpha_o^N + r_1\alpha_o^{N+1} + r_2\alpha_o^{N+2} + \cdots , \qquad (24)$$

where α_o is the bare coupling constant. In general, R can depend on several momentum scales: $R = R(\{k_i\})$. We will consider the $\{k_i\}$ to be fixed for the moment. In the above equation, r_0 is the tree-level

coefficient and N is the tree-level exponent. It is well-known that for a renormalizable theory like QCD, all higher-order coefficients $\{r_i\}_{i\geq 1}$ are divergent and ill-defined, hence the power series in bare coupling constant should be considered purely formal. In other words, QCD alone does not give a direct prediction for R.

Consider now another physical quantity:

$$S = s_0\alpha_o^M + s_1\alpha_o^{M+1} + s_2\alpha_o^{M+2} + \cdots . \tag{25}$$

As in the case of R, QCD does not provide a direct prediction for S since the coefficients $\{s_i\}_{i\geq 1}$ are also divergent. However, QCD does allow us to relate S to R. The procedure is simple. We first invert Eq. (24) to obtain α_o in terms of R,

$$\alpha_o = \left(\frac{R}{r_0}\right)^{1/N} - \frac{r_1}{Nr_0}\left(\frac{R}{r_0}\right)^{2/N} + \cdots, \tag{26}$$

then we substitute this last equation into Eq. (25) to obtain:

$$S = s_0\left(\frac{R}{r_0}\right)^{M/N} + \left[s_1 - \frac{Ms_0}{Nr_0}r_1\right]\left(\frac{R}{r_0}\right)^{(M+1)/N} + \cdots . \tag{27}$$

For a renormalizable theory like QCD, the expansion coefficients in this new series are expected to be finite and well-defined. That is, the infinities in the divergent coefficients like r_1 and s_1 will conspire to cancel each other, yielding a finite result.

Given a third physical quantity

$$T = t_0\alpha_o^P + t_1\alpha_o^{P+1} + t_2\alpha_o^{P+2} + \cdots , \tag{28}$$

we can similarly expand it in terms of R or S, or vice versa. We do not have a direct prediction for R, S or T. However, if one of them is measured, QCD allow us to predict the other two.

Notice that in Eq. (27), the quantity $(R/r_0)^{1/N}$ appears repeatedly. It is convenient to give a symbol to this quantity:

$$\alpha_R \equiv \left(\frac{R}{r_0}\right)^{1/N} . \tag{29}$$

This quantity is known as the effective charge[114] or the effective coupling in the scheme R at the scales $\{k_i\}$. If R is a single scale process, then α_R will depend on only one scale, but in general R and α_R can depend on more than one scale.

Similarly, we can define the effective charges of S and T (or effective coupling in the schemes S and T) as

$$\begin{aligned} \alpha_S &\equiv \left(\frac{S}{s_0}\right)^{1/M} , \\ \alpha_T &\equiv \left(\frac{T}{t_0}\right)^{1/P} . \end{aligned} \tag{30}$$

Since the tree-level coefficients (r_0, s_0, t_0) and exponents (M, N, P) are finite and well-defined, the effective charges α_R, α_S and α_T are therefore also well-defined.

QCD allows us to relate one effective charge to another. For instance, Eq. (27) in terms of effective charges will have the form

$$\alpha_S = \alpha_R + f\alpha_R^2 + g\alpha_R^3 + \cdots , \tag{31}$$

where the expansion coefficients $f, g, \ldots$ are expected to be finite.

More conventional coupling constants like $\alpha_{\overline{\rm MS}}(\mu)$ can also be regarded as effective charges. In fact, in dimensional regularization we have

$$\alpha_{\overline{\rm MS}}(\mu) = \alpha_o - \left(\frac{\beta_0}{4\pi\hat{\epsilon}} + \frac{\beta_0}{4\pi}\ell n\mu^2\right)\alpha_o^2 + \cdots . \tag{32}$$

(Where $1/\hat{\epsilon} = 1/\epsilon + \gamma_E - \ell n 4\pi, \epsilon = (D-4)/2, \beta_0 = 11 - 2n_f/3$. The bare coupling constant α_o is dimension-full in dimensional regularization. In

this formula, α_o and μ have been expressed in a pre-established mass unit.) We can regard this last equation as describing an "observable" with unit tree-level coefficient and exponent. We can expand $\alpha_{\overline{\rm MS}}$ in terms of α_R, α_S or α_T, or vice versa. In this context, there is no distinction between effective charges coming from physical observables or effective charges coming from more conventional coupling constants. Stretching this language, one can in fact refer to $\alpha_{\overline{\rm MS}}$ as the effective charge of the "$\overline{\rm MS}$ process".

Our discussion so far is valid to all orders. Realistically, we can only compute a finite number of terms in an expansion series. The direct evaluation by using a truncated series may not be the best strategy under these circumstances. Suppose we have a physical process R with $\alpha_R(Q) = 0.2$ at $Q = 3$ GeV, and we wish to evaluate the effective charge $\alpha_S(P)$ of another single-scale process $S(P)$ at some large scale, say, $P = 10^5$ GeV. The truncated series

$$\alpha_S(P) = \alpha_R(Q) + f(P,Q)\alpha_R^2(Q) \tag{33}$$

will have a large value of $f(P,Q)$ and higher-order contributions cannot be neglected. In fact, it is known that for large enough value of P, this truncated series will give a negative value for $\alpha_S(P)$.

What if $S = R$ in the above discussion? That is, what if we want to evaluate $\alpha_R(10^5$ GeV) from $\alpha_R(3$ GeV)? The answer is clear: we can the renormalization group equation to evolve $\alpha_R(Q)$ from $Q = 3$ GeV to $Q = 10^5$ GeV. More specifically, given the beta function:

$$\beta_R(\alpha_R) = \frac{d}{d\ell nQ^2}\left(\frac{\alpha_R}{4\pi}\right) = -\beta_0\left(\frac{\alpha_R}{4\pi}\right)^2 + \cdots , \tag{34}$$

we can use it for the evolution of α_R. To first order we obtain

$$\alpha_R(P) = \frac{\alpha_R(Q)}{1 + \frac{\beta_0}{4\pi}\alpha_R(Q)\ell n(P^2/Q^2)} . \tag{35}$$

This result is much more reliable than the one given by the truncated series. In fact, $\alpha_R(P)$ now remains positive for arbitrarily large values of P.

Why is the renormalization group method better than the direct evaluation of the truncated series? The answer is that along the evolution trajectory the scale is changed in a continuous fashion, thus avoiding the presence of dissimilar scales and large coefficients.

Let us return to the case of two different processes. Given two effective charges $\alpha_R(Q)$ and $\alpha_S(P)$. Each one of them can be characterized by its respective beta function:

$$\beta_R(\alpha_R) = \frac{d}{d\ell nQ^2}\left(\frac{\alpha_R}{4\pi}\right) = -\beta_0\left(\frac{\alpha_R}{4\pi}\right)^2 - \beta_1\left(\frac{\alpha_R}{4\pi}\right)^3 - \beta_2^R\left(\frac{\alpha_R}{4\pi}\right)^4 + \cdots ,$$
$$\beta_S(\alpha_S) = \frac{d}{d\ell nP^2}\left(\frac{\alpha_S}{4\pi}\right) = -\beta_0\left(\frac{\alpha_S}{4\pi}\right)^2 - \beta_1\left(\frac{\alpha_S}{4\pi}\right)^3 - \beta_2^S\left(\frac{\alpha_S}{4\pi}\right)^4 + \cdots . \tag{36}$$

The universality of the first two beta function coefficients β_0 and β_1 is a well-known fact. Stevenson[113] has shown that a scheme can be parametrized by its higher-order beta coefficients. Therefore, the R-scheme is characterized by $\{\beta_n^R\}_{n\geq 2}$, and the S-scheme by $\{\beta_n^S\}_{n\geq 2}$. In the expansion series of $\alpha_S(Q)$ in terms of $\alpha_R(P)$:

$$\alpha_S(P) = \alpha_R(Q) + f(P,Q)\alpha_R^2(Q) + g(P,Q)\alpha_R^3(Q) + \cdots , \tag{37}$$

we know that we need a scale $P \sim Q$ to have a reasonable expansion coefficient $f(P,Q)$. However, this may not be enough to guarantee a good convergence if S and R are very different schemes. That is, if the beta function coefficients β_2^R and β_2^S are very different, then the expansion coefficients like $g(P,Q)$ can still be large, rendering the truncated series useless.

The strategy to follow is now clear. We should evolve $\alpha_R(P)$ "adiabatically" into $\alpha_R(Q)$, not only in scale but also in scheme. Along the evolution trajectory, no dissimilar scales or schemes are involved, thus we can expect the result to be more reliable. We need new equations and beta functions that allow us to evolve the scheme parameters $\{\beta_n^R\}$ into $\{\beta_n^S\}$. This will be the subject of the next section.

Let us conclude this section with a comment on error estimation. Conventionally one can estimate the error of a finite series by estimating the next-order coefficient. However, when the power series is unreliable due to largely mismatched scales and schemes, so will be the

corresponding error estimate. We will see that in the extended renormalization group method, we can first estimate the next-order scheme parameter, and then translate the scheme uncertainty into the error estimate for the physical observable.

The Universal Coupling Function in QCD

In this section we will set up the appropriate notation and define the universal coupling function. Given an effective charge $\alpha_R = \alpha_R(\{k_i\})$, we define its fundamental beta function (or scale beta function) to be

$$\begin{aligned} \beta_R(\alpha_R) &= \frac{d}{d\log\lambda^2}\left(\frac{\alpha_R(\{\lambda k_i\})}{4\pi}\right) \\ &= -\beta_0\left(\frac{\alpha_R}{4\pi}\right)^2 - \beta_1\left(\frac{\alpha_R}{4\pi}\right)^3 - \beta_2^R\left(\frac{\alpha_R}{4\pi}\right)^4 + \cdots . \end{aligned} \tag{38}$$

The first two coefficients β_0 and β_1 are universal, whereas all higher-order coefficients $\{\beta_n^R\}_{n\geq 2}$ are process dependent. It will be very convenient to use the first two coefficients of the beta functions to rescale the coupling constant and the scale parameter $\ell n\lambda^2$. (The quantity λ effectively parametrizes the overall scale of a process. For single scale processes, the derivative with respect to the scale parameter can be replaced by the derivative with respect to the scale of the process, as given in Eq. (36).)

Let us define the rescaled coupling constant and the rescaled scale parameter as

$$a_R = \frac{\beta_1}{\beta_0}\frac{\alpha_R}{4\pi} , \qquad \tau = \frac{\beta_0^2}{\beta_1}\ell n\lambda^2 . \tag{39}$$

The rescaled beta function takes the canonical form:

$$\beta_R(a_R) = \frac{da_R}{d\tau} = -a_R^2(1 + a_R + c_2^R a_R^2 + c_3^R a_R^3 + \cdots) , \tag{40}$$

with $c_n^R = \beta_n^R\beta_0^{n-1}/\beta_1^n$ for $n = 2, 3, \cdots$. This rescaling process serves to "unitarize" the expansion coefficients.

For a well-behaved scheme in QCD, we would expect its beta-function expansion to roughly resemble a geometrical series, at least for the first few coefficients. In fact, for the $\overline{\rm MS}$ scheme we have $c_2^{\overline{\rm MS}} = \beta_2^{\overline{\rm MS}}\beta_0/\beta_1^2$, where[121]

$$\begin{aligned} \beta_0 &= 11 - \frac{2}{3}n_f \ , \\ \beta_1 &= 102 - \frac{38}{3}n_f \ , \\ \beta_2^{\overline{\rm MS}} &= \frac{2857}{2} - \frac{5033}{18}n_f + \frac{325}{54}n_f^2 \ , \end{aligned} \tag{41}$$

and for $n_f = 0, 1, 2, 3, 4, 5, 6$ we have respectively $c_2^{\overline{\rm MS}} = 1.5103, 1.4954, 1.4692, 1.4147, 1.2851, 0.92766, -0.33654$. We can clearly see that indeed $c_2^{\overline{\rm MS}}$ is of order of magnitude unity.

The universal coupling function $a(\tau, \{c_i\})$ is the extension of an ordinary coupling constant to include the dependence on scheme parameters. It is required to satisfy the scale evolution equation:

$$\beta(a, \{c_i\}) = \frac{\delta a}{\delta \tau} = -a^2(1 + a + c_2 a^2 + c_3 a^3 + \cdots) \tag{42}$$

for all values of $\{c_i\}$.

The scheme beta functions are defined as:

$$\beta_{(n)}(a, \{c_i\}) \equiv \frac{\delta a}{\delta c_n} \ . \tag{43}$$

As shown by Stevenson,[113] these extended beta functions can be defined in terms of the fundamental beta function. Indeed, the commutativity of second partial derivatives

$$\frac{\delta^2 a}{\delta \tau \delta c_n} = \frac{\delta^2 a}{\delta c_n \delta \tau} \tag{44}$$

implies

$$\frac{\delta \beta_{(n)}}{\delta \tau} = \frac{\delta \beta}{\delta c_n} \ , \tag{45}$$

$$\beta\beta'_{(n)} = \beta_{(n)}\beta' - a^{n+2} \ , \tag{46}$$

where $\beta'_{(n)} = \partial\beta_{(n)}/\partial a$ and $\beta' = \partial\beta/\partial a$. From here

$$\beta^2 \left(\frac{\beta_{(n)}}{\beta}\right)' = -a^{n+2} \ ; \tag{47}$$

therefore

$$\beta_{(n)}(a,\{c_i\}) = \frac{\delta a}{\delta c_n} = -\beta(a,\{c_i\}) \int_0^a dx \frac{x^{n+2}}{\beta^2(x,\{c_i\})} \ , \tag{48}$$

where the lower limit of the integral has been set to satisfy the boundary condition

$$\beta_{(n)} \sim O(a^{n+1}) \ . \tag{49}$$

That is, a change in the scheme parameter c_n can only affect terms of order a^{n+1} and higher in the evolution of the universal coupling function.[113]

We define the universal coupling function $a(\tau,\{c_i\})$ as the solution to the evolution Eqs. (42) and (48) with the boundary condition

$$a(0,\{0\}) = \infty. \tag{50}$$

Notice that the evolution equations contain no explicit reference to QCD parameters such as the numbers of colors or the number of flavors. Therefore, aside from its infinite dimensional character, $a(\tau,\{c_i\})$ is just a mathematical function like, say, Bessel functions or any other special function. Truncation of the fundamental beta function simply corresponds to evaluating $a(\tau,\{c_i\})$ in a subspace where higher order c_i are zero.

Any physical quantity R and hence any given effective charge a_R can be expressed in terms of the universal coupling function. The invariance of R with respect to change of scale and scheme parameters is

described by the equations:

$$\begin{aligned} \frac{\delta R}{\delta \tau} &= 0 \ , \\ \frac{\delta R}{\delta c_n} &= 0 \ . \end{aligned} \tag{51}$$

These equations were first proposed and studied by Stückelberg and Peterman.[122]

Since any two effective charges, *e.g.*, $a_R(\{k_i\})$ and $a(\tau, \{c_i^R\})$, satisfy the same scale evolution equation (compare Eq. (40) to Eq. (42)), there exists a value of $\tau = \tau_R$ for which

$$a_R = a(\tau_R, \{c_i^R\}) \ . \tag{52}$$

We will call τ_R the scale parameter of R. Notice that, although the scheme parameters $\{c_i^R\}$ can be obtained from QCD by computing the coefficients in the fundamental beta function, the value of the scale parameter τ_R is not provided by the theory. This is expected since we know QCD alone does not give a prediction for a_R. A measurement of a_R will allow us to obtain τ_R.

Once a_R (and therefore τ_R) is measured, QCD allows us to predict the value of other effective charges. In order to evolve the universal coupling function from a_R to, say, a_S, we need to know the scale and scheme parameters $(\tau_S, \{c_i^S\})$ of a_S. As we know, the expansion series

$$a_S = a_R + f_2 a_R^2 + f_3 a_R^3 + \cdots \ , \tag{53}$$

is unreliable for evaluating a_S directly. However, this series will allow us to obtain the scale and scheme parameters of a_S from those of a_R.

To make this contact transparent, let us expand the universal coupling function in Taylor series around the point $(\tau_R, \{c_i^R\})$:

$$\begin{aligned} a_S &= a(\tau_S, \{c_i^S\}) = a(\tau_R + \overline{\tau}, \{c_i^R + \overline{c}_i\}) \\ &= a_R + \left(\frac{\delta a}{\delta \tau}\right)_R \overline{\tau} + \left(\frac{\delta a}{\delta c_n}\right)_R \overline{c}_n \\ &+ \frac{1}{2!}\left[\left(\frac{\delta^2 a}{\delta \tau^2}\right)_R \overline{\tau}^2 + 2\left(\frac{\delta^2 a}{\delta \tau \delta c_n}\right)_R \overline{\tau}\overline{c}_n + \left(\frac{\delta^2 a}{\delta c_n \delta c_m}\right)_R \overline{c}_n \overline{c}_m\right] \\ &+ \frac{1}{3!}\left[\left(\frac{\delta^3 a}{\delta \tau^3}\right)_R \overline{\tau}^3 + \cdots\right] + \cdots \ , \end{aligned} \tag{54}$$

where

$$\begin{aligned} \overline{\tau} &= \tau_S - \tau_R \ , \\ \overline{c}_n &= c_n^S - c_n^R \ , \end{aligned} \tag{55}$$

and the subscript R next to the partial derivatives means they are evaluated at the point $(\tau_R, \{c_i^R\})$. To order a^4, we only need the following partial derivatives:

$$\begin{aligned} \left(\frac{\delta a}{\delta \tau}\right) &= \beta = -a^2 - a^3 - c_2 a^4 + O(a^5) \ , \\ \left(\frac{\delta a}{\delta c_2}\right) &= \beta_{(2)} = a^3 + O(a^5) \ , \\ \left(\frac{\delta a}{\delta c_3}\right) &= \beta_{(3)} = \frac{1}{2} a^4 + O(a^5) \ , \\ \left(\frac{\delta^2 a}{\delta \tau^2}\right) &= 2a^3 + 5a^4 + O(a^5) \ , \\ \left(\frac{\delta^2 a}{\delta \tau \delta c_2}\right) &= -3a^4 + O(a^5) \ , \\ \left(\frac{\delta^3 a}{\delta \tau^3}\right) &= -6a^4 + O(a^5) \ . \end{aligned} \tag{56}$$

After grouping all the terms in powers of $a = a_R$, we obtain:

$$\begin{aligned} a_S = a_R &- \overline{\tau} a_R^2 + \left(\overline{c}_2 - \overline{\tau} + \overline{\tau}^2\right) a_R^3 \\ &+ \left(\frac{1}{2}\overline{c}_3 - (c_2^R + 3\overline{c}_2)\overline{\tau} + \frac{5}{2}\overline{\tau}^2 - \overline{\tau}^3\right) a_R^4 \\ &+ O(a_R^5) \ , \end{aligned} \tag{57}$$

where $\overline{\tau}$ and $\overline{c}_n$ are as given in Eq. (55). The coefficients of this formula have been previously obtained by Maxwell and Stevenson in a slightly different notation.[123,124] Notice the occurrence of $\overline{\tau}$ and $\overline{c}_i$ in all higher order coefficients. By using the evolution equations, we are effectively performing a partial resummation of the perturbative series to all orders. By matching this last equation with Eq. (53), we can

identify the scale and scheme parameters of a_S order by order. For instance,

$$\begin{aligned} \tau_S &= \tau_R - f_2 \ , \\ c_2^S &= c_2^R - f_2 - f_2^2 + f_3 \ , \\ c_3^S &= c_3^R - 2f_2 c_2^R + f_2^2 + 4f_2^3 - 6f_2 f_3 + 2f_4 \ . \end{aligned} \tag{58}$$

Let us summarize here the necessary steps to evolve a_R to a_S.

1) Obtain the scheme parameters of a_R by calculating the coefficients of its fundamental beta equation. (In the case of $\overline{\rm MS}$ scheme these parameters are known. See Eq. (41).)
2) By Feynman diagram calculation, obtain the expansion series of a_S in terms of a_R. (See Eq. (53).)
3) Identify the scale and scheme parameters of a_S in terms of those of a_R. (See Eq. (58).)
4) Evolve a_R to a_S by using the Stückelberg-Peterman evolution Eqs. (42) and (48). The final result will not depend on the choice of the evolution path.

The application of this procedure to $R(e^+e^-\to\text{hadrons})$ will be presented later. But first, let us explain the meaning of the 't Hooft scheme and the 't Hooft scale.

The t' Hooft Scheme and Scale

The universal coupling function adopts a particularly simple form when all the scheme parameters are zero. In fact, the 't Hooft scheme[125] coupling constant $a_{\rm 'tH}(\tau) \equiv a(\tau, \{0\})$ is exactly given by the solution of:

$$\frac{1}{a_{\rm 'tH}} + \log\left(\frac{a_{\rm 'tH}}{1 + a_{\rm 'tH}}\right) = \tau \ . \tag{59}$$

(The optimization of QCD perturbative series in this scheme has been studied by C. J. Maxwell.[123]) Notice that due to the boundary condition $a(0, \{0\}) = \infty$, the 't Hooft coupling constant presents a singularity at $\tau = 0$.

For any single-scale effective charge $a_R(\mu)$ there exists a scale $\mu = \Lambda_R^{'\mathrm{tH}}$ for which the scale parameter $\tau_R = 2\beta_0^2\beta_1^{-1}\log(\mu/\Lambda_R^{'\mathrm{tH}})$ vanishes. We will call $\Lambda_R^{'\mathrm{tH}}$ the 't Hooft scale of the R-scheme. To understand the meaning of the 't Hooft scale, let us consider the $\overline{\mathrm{MS}}$ scheme coupling constant as an example:

$$a_{\overline{\mathrm{MS}}}(\mu) = a\left(\frac{2\beta_0^2}{\beta_1}\log(\mu/\Lambda_{\overline{\mathrm{MS}}}^{'\mathrm{tH}}), \{c_i^{\overline{\mathrm{MS}}}\}\right) . \tag{60}$$

Notice that *a priori* we do not know the behavior of $a_{\overline{\mathrm{MS}}}(\mu)$ at $\mu = \Lambda_{\overline{\mathrm{MS}}}^{'\mathrm{tH}}$: it could be infinite, finite, or simply not well-defined. However, $\mu = \Lambda_{\overline{\mathrm{MS}}}^{'\mathrm{tH}}$ is the pole in the 't Hooft scheme associated with the $\overline{\mathrm{MS}}$ scheme:

$$a_{'\mathrm{tH}-\overline{\mathrm{MS}}}(\mu) \equiv a\left(\frac{2\beta_0^2}{\beta_1}\log(\mu/\Lambda_{\overline{\mathrm{MS}}}^{'\mathrm{tH}}), \{0\}\right) , \tag{61}$$

because $a(0, \{0\}) = \infty$ by boundary condition. Since the 't Hooft scheme is completely free of higher-order corrections, this provides a precise definition for $\Lambda_{\overline{\mathrm{MS}}}$. (There are an infinite number of 't Hooft schemes, differing only by the value of the 't Hooft scale $\Lambda^{'\mathrm{tH}}$. The word "associated" here means we are choosing the particular 't Hooft scheme that shares the same 't Hooft scale with the $\overline{\mathrm{MS}}$ scheme: $\Lambda^{'\mathrm{tH}} = \Lambda_{\overline{\mathrm{MS}}}^{'\mathrm{tH}}$.)

As stated before, an experimental measurement of a_R leads us to the measurement of τ_R, which in turn gives a value for $\Lambda_R^{'\mathrm{tH}}$. In Fig. 17 we show the various experimental and theoretical errors involved in the analysis. For the measurement of $\Lambda_R^{'\mathrm{tH}}$, the input experimental error must be combined with the scheme uncertainty to give the error estimate for $\Lambda_R^{'\mathrm{tH}}$. Similarly, for the prediction of $a_R(\tau)$ the error from $\Lambda_R^{'\mathrm{tH}}$ must be combined with the scheme uncertainty in order to give the prediction error.

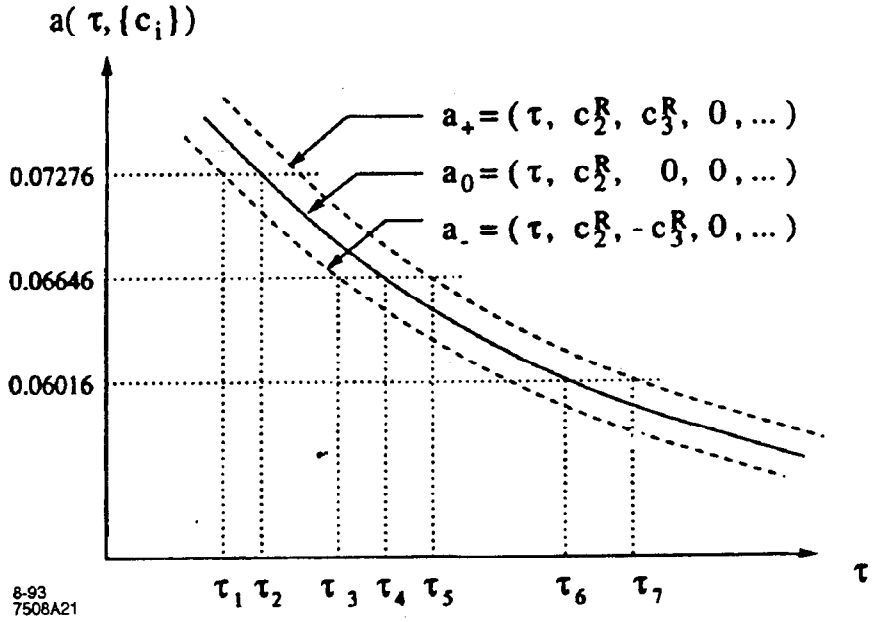

Figure 17. Graphical representation of the various errors involved. For the measurement of $\Lambda^{\prime tH}_{\overline{\rm MS}}$ (or equivalently $\Lambda^{\prime tH}_{R}$) the input experimental error must be combined with the scheme uncertainty. For the prediction of $a_R(\tau)$, the error in $\Lambda^{\prime tH}_{\overline{\rm MS}}$ must be combined with the scheme uncertainty.

Application to R($e^+e^- \to$ Hadrons)

In this section we present the application to the total hadronic cross section in e^+e^- annihilation $R(Q) = R(e^+e^- \to \text{hadrons})$ recently calculated to order α^3 in Refs. 115, and 117. (See also the recent analyses in Refs. 126 and 127]. From Refs. 115, and 117, for five light-quark flavors we have

$$R(Q) = \frac{11}{3}\left[1 + \frac{\alpha_{\overline{\rm MS}}(Q)}{\pi} + 1.4092\left(\frac{\alpha_{\overline{\rm MS}}(Q)}{\pi}\right)^2 - 12.8046\left(\frac{\alpha_{\overline{\rm MS}}(Q)}{\pi}\right)^3\right] \equiv \frac{11}{3}\left[1 + \frac{\alpha_R(Q)}{\pi}\right] . \tag{62}$$

By rescaling the effective charges appropriately (see Eq. (39)), we obtain the relation:

$$a_R(Q) = a_{\overline{\rm MS}}(Q) + 1.1176\, a^2_{\overline{\rm MS}}(Q) - 8.05426\, a^3_{\overline{\rm MS}}(Q) . \tag{63}$$

Notice that in the right-hand side the scale argument of $a_{\overline{\rm MS}}(\mu)$ has been set to be $\mu = Q$. In general, this needs not to be the case. When μ is left to be free, the relation between $a_R(Q)$ and $a_{\overline{\rm MS}}(\mu)$ is given by:

$$a_R(Q) = a_{\overline{\rm MS}}(\mu) + (1.1176 - 3.0402\ell n(Q/\mu))\ a^2_{\overline{\rm MS}}(\mu) + (-8.05426 - 9.8358\ell n(Q/\mu) + 9.2430\ell n^2(Q/\mu))\ a^3_{\overline{\rm MS}}(\mu)\ . \tag{64}$$

Applying the formulas in Eq. (58) and knowing that $\tau_R = 2\beta_0^2\beta_1^{-1} \times \ell n(Q/\Lambda_R^{'\rm tH})$ and $\tau_{\overline{\rm MS}} = 2\beta_0^2\beta_1^{-1}\ell n(\mu/\Lambda_{\overline{\rm MS}}^{'\rm tH})$, we arrive at the relations:

$$\Lambda_R^{'\rm tH} = 1.4443\ \Lambda_{\overline{\rm MS}}^{'\rm tH}\ , \qquad c_2^R = -9.4932\ . \tag{65}$$

Notice that, as one would expect, these results are independent of the scales Q and μ that we started with. In fact, we could use any scale and scheme in the right-hand side of Eq. (64), and always arrive to the same values of scale parameters for a_R and a consistent ratio of the 't Hooft scales.

Experimentally[128] we have

$$\frac{3}{11}R(31.6\ {\rm GeV}) = 1.0527 \pm 0.0050\ , \tag{66}$$

which gives

$$a_R(31.6\ {\rm GeV}) = 0.0665 \pm 0.0063\ . \tag{67}$$

We will now use this information to obtain values for $\Lambda_{\overline{\rm MS}}^{'\rm tH}$. We have to take into account the scheme uncertainty in addition to the experimental error in order to quote a correct error estimate for $\Lambda_{\overline{\rm MS}}^{'\rm tH}$ (see Fig. 18). The scheme uncertainty of R can be quantified by a reasonable estimate of its next scheme parameter: c_3^R. G. B. West[129] has put an estimate $r_4 = -158.6$ for the coefficient of $(\alpha_{\overline{\rm MS}}(Q)/\pi)^4$ in Eq. (62). After rescaling, this leads to a value $\bar{c}_3 = c_3^R - c_3^{\overline{\rm MS}} = -99.474$. Assuming $c_3^{\overline{\rm MS}}$ is of order unity, we conclude that $|c_3^R| \sim 100$. Although we have some reservation on West's estimate (see Ref. 130), we shall

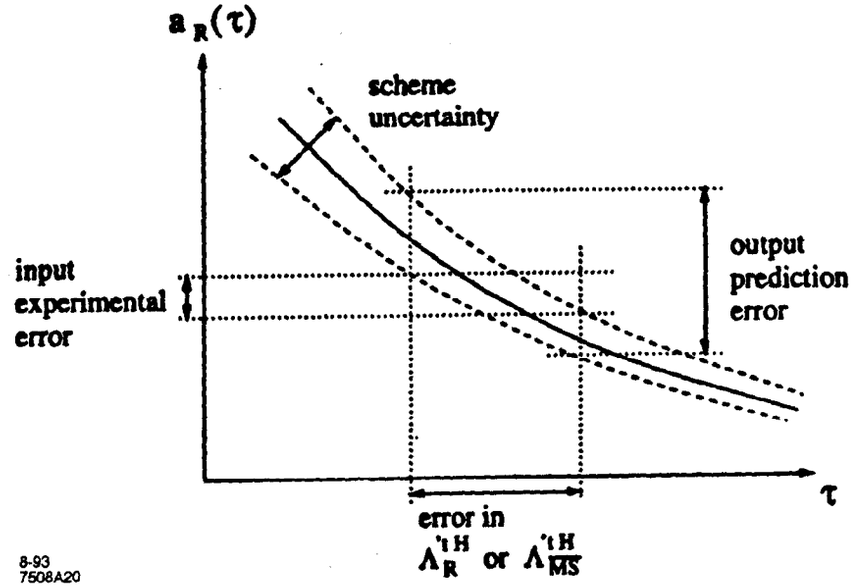

Figure 18. Measurement of $\Lambda_{\overline{\rm MS}}^{'\rm tH}$ from the experimental result of $a_R(31.6\ \text{GeV})$. We have parametrized the scheme uncertainty with a value $c_3^R = 100$. The scheme, experimental and total errors are respectively given by $\Delta_{\rm sch} = (\tau_5 - \tau_3)/2$, $\Delta_{\rm exp} = (\tau_6 - \tau_2)/2$ and $\Delta_{\rm tot} = (\tau_7 - \tau_1)/2$. There is a one-to-one relationship between τ and $\Lambda_{\overline{\rm MS}}^{'\rm tH}$ given by $\tau = 2\beta_0^2\beta_1^{-1}\log(31.6\ \text{GeV}/1.4443\ \Lambda_{\overline{\rm MS}}^{'\rm tH})$.

nonetheless use it to illustrate our procedure. A better estimate of c_3^R will lead to a better error estimate for $\Lambda_{\overline{\rm MS}}^{'\rm tH}$.

In Fig. 18 we show the universal charge for $a_0(\tau) = a(\tau, \{c_2 = c_2^R, c_3 = c_4 = \ldots = 0\})$ and its evolution under a scheme uncertainty $c_3 = \pm 100$ to $a_\pm(\tau) = a(\tau, \{c_2 = c_2^R, c_3 = \pm 100, c_4 = c_5 = \ldots = 0\})$.

The evolution in the scheme parameters are dictated by:

$$\begin{aligned} \frac{\delta a}{\delta c_2} &= \beta_{(2)} = -\beta \int_0^a dx \frac{x^4}{\beta^2} \sim a^3 + O(a^5)\ , \\ \frac{\delta a}{\delta c_3} &= \beta_{(3)} = -\beta \int_0^a dx \frac{x^5}{\beta^2} \sim \frac{1}{2}a^4 + O(a^5)\ , \end{aligned} \tag{68}$$

For our region of interest ($a \sim 0.07$) the first term in each expansion series suffices. But we should use the full integro-differential equation

whenever we want to evolve a to a higher-value region. This will not only improve the accuracy of our result, but also will respect the commutativity of the second-order partial derivatives of a and thus ensure the independence of the result on the choice of integration path.

To obtain the various scale parameters in Fig. 18, we can evolve their corresponding values of a_R to the 't Hooft scheme (switching off all scheme parameters) and then use Eq. (59) to get the value for the particular τ. Let us illustrate the procedure for τ_7. If we denote

$$\begin{aligned} a_+ &= a(\tau_7, c_2^R, c_3^R, 0, \cdots) = 0.06016 \ , \\ a_0 &= a(\tau_7, c_2^R, 0, 0, \cdots) \ , \\ a_{'\mathrm{tH}} &= a(\tau_7, 0, 0, 0, \cdots) \ , \end{aligned} \tag{69}$$

then the solutions to the evolution equations in (68) are given by:

$$\begin{aligned} a_0 &= \frac{a_+}{\left(1 + \frac{3}{2}\, c_3^R\, a_+^3\right)^{1/3}} \ , \\ a_{'\mathrm{tH}} &= \frac{a_0}{\left(1 + 2\, c_2^R\, {a_0}^2\right)^{1/2}} \ . \end{aligned} \tag{70}$$

Using these equations and Eq. (59), we obtain a value of $\tau_7 = 13.379$. Other scale parameters can be calculated in a similar way. In Fig. 18 we show the various errors involved in this analysis. Numerically we find the experimental, scheme, and total errors for τ to be:

$$\begin{aligned} \Delta\tau_{\mathrm{exp}} &= (\tau_6 - \tau_2)/2 = 1.41 \ , \\ \Delta\tau_{\mathrm{sch}} &= (\tau_5 - \tau_3)/2 = 0.22 \ , \\ \Delta\tau_{\mathrm{tot}} &= (\tau_7 - \tau_1)/2 = 1.63 \ . \end{aligned} \tag{71}$$

These errors can be translated into uncertainties in $\Lambda_{\overline{\mathrm{MS}}}^{'\mathrm{tH}}$ since there is a one-to-one correspondence between τ and $\Lambda_{\overline{\mathrm{MS}}}^{'\mathrm{tH}}$. (The ratio between $\Lambda_R^{'\mathrm{tH}}$ and $\Lambda_{\overline{\mathrm{MS}}}^{'\mathrm{tH}}$ is given in Eq. (65).) We can see that most error comes from the experimental error in a_R. We can also see that the experimental error and the scheme error are highly uncorrelated since

$\Delta\tau_{\rm tot} \sim \Delta\tau_{\rm exp} + \Delta\tau_{sch}$. Numerically we obtain $\tau_1 = 10.129, \tau_4 = 11.666$ and $\tau_7 = 13.379$. Knowing that

$$\tau = \frac{2\beta_0^2}{\beta_1} \log\left(\frac{31.6 \text{ GeV}}{1.4443\ \Lambda_{\overline{\rm MS}}^{'\rm tH}}\right) , \tag{72}$$

we arrive at the following result for $\Lambda_{\overline{\rm MS}}^{'\rm tH}$:

$$\Lambda_{\overline{\rm MS}}^{'\rm tH} = 472^{+310}_{-204} \text{ MeV} . \tag{73}$$

If there were no experimental error, the estimated scheme uncertainty would lead to $\Lambda_{\overline{\rm MS}}^{'\rm tH} = 472^{+35}_{-33}$ MeV . (In terms of the definition of $\Lambda_{\overline{\rm MS}}$ as given in the Review of Particle Properties[131], the corresponding values are $\Lambda_{\overline{\rm MS}} = 411^{+270}_{-178}$ MeV and $\Lambda_{\overline{\rm MS}} = 411^{+30}_{-29}$ MeV.)

As a second application of our formalism, we will show next how to use the experimental result of $a_R(31.6 \text{ GeV})$ to predict other effective charges. Specifically, we will give a prediction for $a_{\overline{\rm MS}}(M_Z)$, where $M_Z = 91.173$ GeV is the mass of the Z-boson. The evolution of $a_R(31.6 \text{ GeV})$ to $a_{\overline{\rm MS}}(M_Z)$ is illustrated in Fig. 19. Notice that the experimental and the scheme uncertainties confine the correct result for a_R into an approximate parallelogram $ABCD$. We can then evolve this parallelogram into any other scheme and scale. We will use $c_3^R = \pm 100$ and $c_3^{\overline{\rm MS}} = \pm 1$ to estimate the scheme uncertainties in a_R and $a_{\overline{\rm MS}}$. For $a_{\overline{\rm MS}}(M_Z)$, the parallelogram $ABCD$ is evolved into the parallelogram $A'B'C'D'$. Notice the inversion of the orientation of the new parallelogram due to the opposite signs of c_2^R and $c_2^{\overline{\rm MS}}$. Notice also the absence of scheme uncertainty in the 't Hooft scheme.

From $\tau_A = 10.129$ and $\tau_C = 13.379$ and knowing that $\tau_{\overline{\rm MS}} = \tau_R - \overline{\tau}$ with $\overline{\tau} = 2\beta_0^2\beta_1^{-1}\left[\log(M_Z/\Lambda_{\overline{\rm MS}}^{'\rm tH}) - \log(31.6 \text{ GeV}/\Lambda_R^{'\rm tH})\right] = 4.339$, we find $\tau_{A'} = 14.468$ and $\tau_{C'} = 17.718$. To evaluate $a_{A'} = a(\tau_{A'}, c_2^{\overline{\rm MS}} = 0.92766, c_3^{\overline{\rm MS}} = 1, 0, \ldots)$ and $a_{C'} = a(\tau_{C'}, c_2^{\overline{\rm MS}} = 0.92766, c_3^{\overline{\rm MS}} = -1, 0, \ldots)$ we can use the following steps. We will show the procedure for $a_{A'}$.

1.– Generate the 't Hooft scheme coupling $a_{'\rm tH} = a(\tau_{A'}, 0, \ldots)$ by

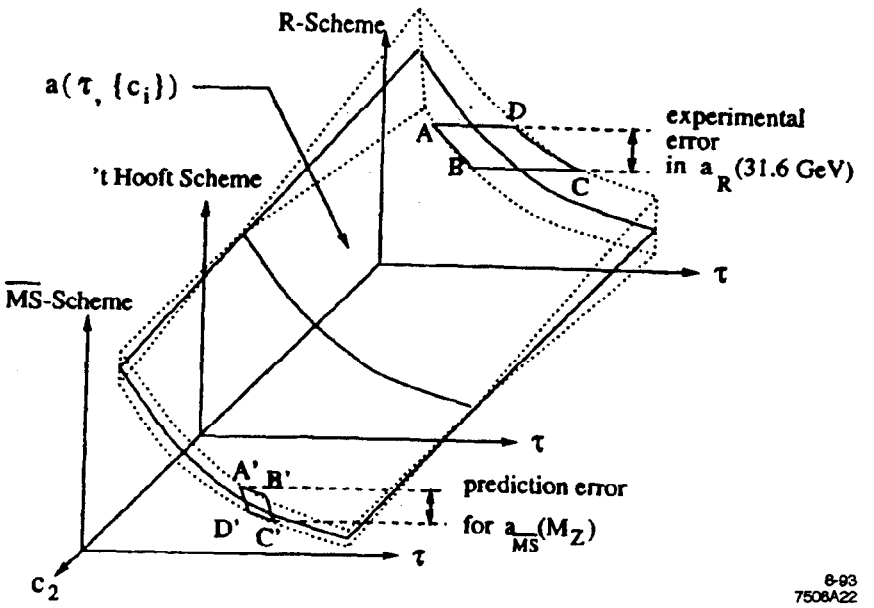

Figure 19. Prediction of $a_{\overline{\rm MS}}(M_Z)$ from the experimental result of $a_R(31.6\ {\rm GeV})$. By using the extended renormalization group equations, the quasi-parallelogram $ABCD$ is evolved into the quasi-parallelogram $A'B'C'D'$. Notice the inversion of the orientation of the parallelograms due to the opposite signs of c_3^R and $c_3^{\overline{\rm MS}}$. Notice also the absence of scheme uncertainty in the 't Hooft scheme.

solving iteratively

$$a_{'{\rm tH}} = \frac{1}{\tau_{A'} + \log\left(1 + 1/a_{'{\rm tH}}\right)} \ . \tag{74}$$

2.– Evolve $a_{'{\rm tH}}$ to $a_0 = a(\tau_{A'}, c_2^{\overline{\rm MS}}, 0, \ldots)$ by displacing in c_2.

$$a_0 = \frac{a_{'{\rm tH}}}{\left(1 - 2\ c_2^{\overline{\rm MS}}\ a_{'{\rm tH}}{}^2\right)^{1/2}} \ . \tag{75}$$

3.– Evolve a_0 to $a_{A'} = a(\tau_{A'}, c_2^{\overline{\rm MS}}, c_3^{\overline{\rm MS}} = 1, 0, \ldots)$ by displacing in c_3.

$$a_{A'} = \frac{a_0}{\left(1 - \frac{3}{2}\ c_3^{\overline{\rm MS}}\ a_0^3\right)^{1/3}} \ . \tag{76}$$

From here we obtain $a_{A'} = 0.05772$ and $a_{C'} = 0.04818$. Hence,

we arrive at the prediction

$$a_{\overline{\rm MS}}(M_Z) = 0.0530 \pm 0.0048 \ , \tag{77}$$

or equivalently,

$$\alpha_{\overline{\rm MS}}(M_Z) = 0.132 \pm 0.012 \ . \tag{78}$$

This value is higher than the world average $\alpha_{\overline{\rm MS}}(M_Z) = 0.1134 \pm 0.0035$ quoted in the Review of Particle Properties[131] but is still consistent with other quoted values for $\alpha_{\overline{\rm MS}}(M_Z)$.

We can also apply the extended renormalization group technique to the effective BLM charge[39] defined in the following manner. Given two physical quantities R and R' computed in a particular scheme

$$\begin{aligned} R(Q) &= r_0(Q)\alpha^p(\mu) + \left(r_{10}(Q) + r_{11}(Q,\mu)\beta_0\right)\alpha^{p+1}(\mu) + \cdots \ , \\ R'(Q') &= r'_0(Q')\alpha^{p'}(\mu') + \left(r'_{10}(Q') + r'_{11}(Q',\mu')\beta_0\right)\alpha^{p'+1}(\mu') + \cdots \ , \end{aligned} \tag{79}$$

where $\beta_0 = 11 - \frac{2}{3}n_f$ is the first beta function coefficient, we can define their "effective BLM charges" by

$$\begin{aligned} R(Q) &= r_0(Q)\alpha^p_{R-BLM}(Q) + r_{10}(Q)\alpha^{p+1}_{R-BLM}(Q) + \cdots \ , \\ R'(Q') &= r'_0(Q')\alpha^{p'}_{R'-BLM}(Q') + r'_{10}(Q')\alpha^{p'+1}_{R'-BLM}(Q') + \cdots \ , \end{aligned} \tag{80}$$

with $\alpha_{R-BLM}(Q) = \alpha(\mu^*)$ where μ^* is the solution of $r_{11}(Q,\mu^*) = 0$, and similarly $\alpha_{R'-BLM}(Q') = \alpha(\mu'^*)$ where μ'^* is the solution of $r'_{11}(Q',\mu'^*) = 0$. With this choice of scale, vacuum polarization contributions are associated with the charge rather than the expansion coefficients, and the scale tends to reflect the mass of the virtual gluons. The BLM method is particularly advantageous for setting the scale when one only has low order calculations available since it automatically resums the higher order contributions associated with vacuum polarization insertions.

We can now apply the evolution equations to $\alpha_{R-BLM}(Q)$ and evolve it to $\alpha_{R'-BLM}(Q')$. The evolution in the scheme parameters maintains the BLM condition that the next-to-leading order coefficient is flavor-independent. In fact, both the FAC and BLM definitions are consistent with evolution in the scheme and scale parameters.

Finally, let us obtain the relation between $\Lambda^{'tH}_{\overline{MS}}$ and a commonly used definition of $\Lambda_{\overline{MS}}$. The expansion of $\alpha_{\overline{MS}}(\mu)$ can be obtained by inverting the above formula iteratively by using the scale and scheme parameters of $\alpha_{\overline{MS}}(\mu)$. Noting that $\tau_{\overline{MS}} = 2\beta_0^2\beta_1^{-1}\ell n(\mu/\Lambda^{'tH}_{\overline{MS}})$, we obtain:

$$\alpha_{\overline{MS}}(\mu) = \frac{4\pi}{\beta_0 \ell n(\mu^2/\Lambda^{'tH\ 2}_{\overline{MS}})}\left[1 - \frac{\beta_1 \ell n\left[\beta_0^2\beta_1^{-1}\ell n(\mu^2/\Lambda^{'tH\ 2}_{\overline{MS}})\right]}{\beta_0^2 \ell n(\mu^2/\Lambda^{'tH\ 2}_{\overline{MS}})}\right] + \cdots . \tag{81}$$

This differs from the definition as given in Review of Particle Properties[131], where $\Lambda_{\overline{MS}}$ is defined so to make the coefficient inside the double logarithm unitary:

$$\alpha_{\overline{MS}}(\mu) = \frac{4\pi}{\beta_0 \ell n(\mu^2/\Lambda^2_{\overline{MS}})}\left[1 - \frac{\beta_1 \ell n\left[\ell n(\mu^2/\Lambda^2_{\overline{MS}})\right]}{\beta_0^2 \ell n(\mu^2/\Lambda^2_{\overline{MS}})}\right] + \cdots . \tag{82}$$

The relation between $\Lambda_{\overline{MS}}$ and $\Lambda^{'tH}_{\overline{MS}}$ can be found to be:

$$\Lambda^{'tH}_{\overline{MS}} = \left(\frac{\beta_1}{\beta_0^2}\right)^{-\beta_1/2\beta_0^2} \Lambda_{\overline{MS}} . \tag{83}$$

For $n_f = 5$ we have $\Lambda^{'tH}_{\overline{MS}} = 1.1477\Lambda_{\overline{MS}}$, thus, the difference between the two definitions is small in practice.

The most distinctive feature of the universal coupling function approach is that the perturbative series of a physical observable only serves to identify the scale and scheme parameters. The final prediction is obtained by the evolution of a universal coupling function. The prediction is scale-scheme independent in the sense that given the initial perturbative series in any scheme at any scale, we will always obtain its correct scale and scheme parameter and hence arrive at the same prediction. We have also shown that $\Lambda_{\overline{MS}}$ can be unambiguously defined as the pole in the associated 't Hooft scheme.

In many practical problems it is useful to set the renormalization scale, particularly in physical processes that involve several invariant

mass scales, or in cases where only next-to-leading order calculations are available. As I shall discuss in the next section, it is essential that any scale-setting procedure be consistent with the extended renormalization group equations.

Self-Consistency Conditions for Scale-Setting in QCD

In practice any perturbative prediction in QCD has to be truncated to finite order in the coupling constant $\alpha_s(\mu)$. Given a specific renormalization scheme which defines α_s, PQCD predictions for a physical observable R have the form

$$R_N = r_0\alpha_s^p(\mu) + r_1(\mu)\alpha_s^{p+1}(\mu) + \ldots + r_N(\mu)\alpha_s^{p+N}(\mu). \qquad (84)$$

Although, the infinite series is renormalization-scale independent, the scale dependences from $\alpha(\mu)$ and $r_i(\mu)$ do not exactly cancel in finite series; thus, in practice, there is always a scale ambiguity.

In this section, I will address the question of whether there a reliable way to choose the renormalization scale μ in relation to the physical scales. This problem is particularly important in the case of processes in which only low order calculations are available and in processes with multiple physical scales.

The apparent freedom in the choice of the renormalization scale μ can be a serious source of confusion in finite-order analyses. Indeed, when working to first order, one can set $r_1(\mu)$ to any value simply by μ. This coefficient thus seems meaningless here. In particular, it seems to give no indication of the convergence of the expansion. This question is of critical importance in testing QCD, since α_s is rather large ($\sim 0.1 - 0.3$) at current energies. In fact for some processes, perturbation theory may not be convergent.

The potential difficulties are well illustrated in low-energy quantum electrodynamics (QED), where, for example, the electron anomaly has a very convergent expansion

$$\alpha_e = \frac{g_e - 2}{2} = \frac{\alpha}{2\pi}\left[1 - 0.657\,\frac{\alpha}{\pi} + 2.352\,\frac{\alpha^2}{\pi^2}\,\cdots\right], \qquad (85)$$

whereas the expansion for orthopositronium decay is much less conver-

gent:

$$\Gamma_{0-P_s} = \Gamma_0 \left[1 - 10.3 \frac{\alpha}{\pi} + \cdots\right] . \tag{86}$$

It must be emphasized that the different in convergence rate is not an artifact due to a bad choice of scheme or scale; the first-order coefficients in these expansions should not be absorbed into a redefinition of α since the running coupling constant for QED does not run at these energies. This example shows that there is no general principle that the optimum choice of scale μ is one that best approximates the full answer or improves the convergence of the perturbative expansion. The 10.3 coefficient in the orthopositronium decay rate reflects real physics, not scale choice.

Three different scale-setting procedures have been proposed in the literature:

1. *Fastest Apparent Convergence* (FAC).[114] This method chooses the renormalization scale μ that makes the next-to-leading order coefficient vanish:

$$r_1(\mu) = 0. \tag{87}$$

2. *The Principle of Minimum Sensitivity* (PMS)[114] This method chooses μ at the stationary point of R:

$$\frac{dR_N}{d\mu} = 0. \tag{88}$$

   (Beyond the next-to-leading order, PMS involves the optimization of scheme parameters in addition to the renormalization scale.)

3. *Brodsky-Lepage-Mackenzie*[39] In the BLM scale-fixing method, the scale is chosen such that the n_f term does not appear in the next-to-leading order coefficient, where n_f the number of light-quark flavors. That is, if

$$r_1(\mu) = r_{10}(\mu) + r_{11}(\mu) n_f, \tag{89}$$

   where $r_{10}(\mu)$ and $r_{11}(\mu)$ are n_f independent, then BLM chooses

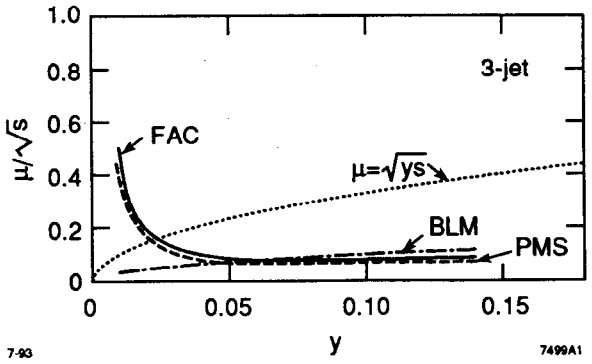

Figure 20. The scale $\mu/\sqrt{s}$ according to the BLM (dashed-dotted), PMS (dashed), FAC (full) and $\sqrt{y}$ (dotted) procedure for the three-jet rate in e^+e^- annihilation, as computed by Lampe and Kramer.[132] Notice the strikingly different behavior of the BLM method from the PMS and FAC methods at low y. In particular, the latter two methods predict increasing values of μ for small jet invariant mass cut.

the scale μ given by the condition

$$r_{11}(\mu) = 0. \tag{90}$$

This prescription ensures that, as in quantum electrodynamics, vacuum polarization contributions due to fermion pairs are associated with the coupling constant $\alpha(\mu)$ rather than the coefficients.

These setting methods can give strikingly different results in practical applications. In their study of jet production fractions in e^+e^- annihilation, Kramer and Lampe have analyzed[132] the application of the FAC, PMS and BLM methods. Jets are defined jets by clustering particles with invariant mass less than $\sqrt{ys}$, where y is the resolution parameter and $\sqrt{s}$ is the total center-of-mass energy. Physically one expects the renormalization scale μ to reflect the invariant mass of jets, that is, μ^2 of order ys. In particular, one expects μ to decrease as the resolution parameter $y \to 0$. However, in practice FAC and PMS do not reproduce this behavior (see Fig. 20). On the other hand, BLM gives a decreasing μ as $y \to 0$; thus, as expected, the perturbative QCD results cannot be used in the $y < 0.02$ domain, as pointed out in Ref. 132. The scales chosen by PMS and FAC give no sign that the perturbative expressions break down in the soft region.

In Ref. 133, Berger and Qiu have analyzed the application of the PMS method in their study of the prompt-photon production in QCD. They have shown that for some conditions on the factorization scale, PMS may not have a solution, or lead to unreasonable choices for the renormalization scale.

The Physics of the BLM Scale-Setting Prescription

In quantum electrodynamics, the running coupling constant $\alpha(Q)$ is defined to include all contributions due to vacuum-polarization insertions in the photon propagator. This is the only natural choice in any renormalization scheme since the variation of the effective coupling in QED is due to vacuum polarization alone. The coupling-constant scale Q^* best suited to a particular process in a given order can be determined simply by computing the vacuum-polarization insertions in the diagrams of that order. Expansion (84) is then replaced by

$$\mathcal{R} = C_0\alpha(Q_0^*)\left[1 + C_1^*\frac{\alpha(Q_1^*)}{\pi} + C_2^*\frac{\alpha^2(Q_2^*)}{\pi^2} + \cdots\right], \qquad (91)$$

where all photon self-energy corrections are absorbed into the effective coupling constants by an appropriate (and unique) choice of scales $Q_0^*, Q_1^*, \ldots$. Since all dependence upon the number of light-fermion flavors (n_f) usually enters through the photon self-energy in low orders, both the coupling-constant scales Q_i^* and the low-order coefficients C_i^* are independent of n_f. (Light-by-light scattering graphs leads to n_f dependence in higher orders.) The light-fermion loop corrections serve mainly to renormalized $\alpha(Q)$, as expected. Note also, that in a general process, the scales $Q_0^*, Q_1^*, \ldots$ can depend on the ratio of invariants, e.g., center-of-mass angles.

In QCD (*i.e.*, non-Abelian theories), it again is natural to absorb all vacuum-polarization corrections into $\alpha_s(Q)$. In particular, all vacuum polarization due to light fermions should be absorbed, leaving an expansion

$$\rho = C_0\alpha_s(Q^*)\left[1 + C_1^*\frac{\alpha_s(Q^*)}{\pi} + \ldots\right], \qquad (92)$$

where C_1^* and Q^* are defined to be n_f independent. (The calculation of C_1^* and Q^* are unambiguous since the dependence of α_s on n_F is determined to this order by $\beta_0 = 11 - \frac{2}{3}n_f$.)

The BLM procedure for fixing the scale is then straightforward, (at least for processes that do not have gluon-gluon interactions in lowest order.) For definiteness we assume the $\overline{\rm MS}$ scheme. To first order the prediction for observables has an expansion in

$$R = C_0 \alpha_{\overline{\rm MS}}(Q) \left[1 + \frac{\alpha_{\overline{\rm MS}}(Q)}{\pi} (A_{VP} n_f + B)\right] , \tag{93}$$

where the n_f term is all due to quark vacuum polarization. As in QED, the sole function of these light-quark insertions is to renormalize the coupling. Thus all such terms should be completely absorbed into the leading-order coupling by redefining the scale

$$\alpha_{\overline{\rm MS}}(Q) \to \alpha_{\overline{\rm MS}}(Q^*) = \alpha_{\overline{\rm MS}}(Q) \left[1 + \frac{\beta_0}{2\pi} \alpha_{\overline{\rm MS}}(Q) \ell n \frac{Q^*}{Q} + \cdots\right]^{-1} . \tag{94}$$

Furthermore, the new scale Q^* must be n_f independent if it is to retain any physical significance in relation to the momenta circulating in the leading-order diagrams. Thus we replace

$$R = C_0 \alpha_{\overline{\rm MS}}(Q) \left[1 + \frac{\alpha_{\overline{\rm MS}}(Q)}{\pi} \left(-\frac{3}{2}\beta_0 A_{VP} + \frac{33}{2} A_{VP} + B\right) + \cdots\right] \tag{95}$$

by

$$R = C_0 \alpha_{\overline{\rm MS}}(Q^*) \left[1 + \frac{\alpha_{\overline{\rm MS}}(Q^*)}{\pi} C_1^* + \cdots\right] , \tag{96}$$

where

$$Q^* = Q \exp(3A_{VP}) , \qquad C_1^* = \frac{33}{2} A_{VP} + B . \tag{97}$$

The term $33A_{VP}/2$ in C_1^* serves to remove that part of the constant B which renormalizes the leading-order coupling. The ratio of these gluonic corrections to the light-quark corrections is fixed by $\beta_0 = 11 - \frac{2}{3} n_f$.

Several features of this procedure are worth noting.

(*a*) Two schemes that differ only by an n_f-independent rescaling give identical expansions in $\alpha_s(Q^*)$. Thus the differences between MS and $\overline{\rm MS}$, for example, are irrelevant in this approach.

(*b*) If the $\overline{\rm MS}$ scheme is replaced by another for which

$$\begin{aligned}\alpha_s(Q) &= \alpha_{\overline{\rm MS}}(Q)\left[1+\frac{\alpha_{\overline{\rm MS}}}{\pi}(D\beta_0+E)+\cdots\right] \\ &= \alpha_{\overline{\rm MS}}(Qe^{-2D})\left[1+\frac{\alpha_{\overline{\rm MS}}}{\pi}E+\cdots\right],\end{aligned} \tag{98}$$

where D and E are n_f independent, then the first-order coefficients for all processes are shifted by $-E: C_1^* \to C_1^* - E$. Differences between first-order coefficients are scheme independent.

(*c*) The leading-order scale is determined solely by A_{VP}, which comes from quark vacuum-polarization insertions. This is usually all that need be computed to make a meaningful leading-order prediction.

(*d*) Equation (96) is a natural and convenient way to present perturbative results since all flavor dependence is implicit in the definition of $\alpha_{\overline{\rm MS}}$.

In many physical problems, one must also allow for multiple scales. For processes involving extremely dissimilar scales (as in scattering processes where $s \gg -t$), perturbative results are clearly not reliable and resummation techniques have to be used in order to resum an infinite set of contributions. Nonetheless, for processes involving relatively comparable scales (as in jet-fraction rates, where there are two scales: s and ys) perturbative calculations should be reliable, provided a reasonable treatment of the various scales. (As discussed by Kramer and Lampe, perturbative calculations for jet-rates using BLM are reliable down to $y \sim 0.02$.) In the case of $e^-e^- \to e^-e^-$ it is clear that both u and t appear as scales. In the case of $e^-e^+ \to e^-e^+$ the s channel annihilation amplitude has to have the correct scale ($\mu^2 = s$) in on-shell scheme; *i.e.*, $\alpha(s)$ so that the thresholds for lepton pair production occur exactly at the pair production threshold. The BLM prescription method is consistent with these principles and provides a direct method to analyze multiple scale problems.

We emphasize that any prescription for setting the scale of the coupling constant in a non-Abelian theory must agree with the known results for QED when specialized to the Abelian case.

Examples of the BLM Procedure

To illustrate our scale-fixing procedure and to explore its implications, we examine briefly a number of well known predictions of QCD.

$e^+e^- \to$ *hadrons*: The ratio of the total cross section into hadrons to the cross section for $e^+e^- \to \mu^+\mu^-$ is $(s = Q^2)$[134]

$$R_{e^+e^-}(Q^2) = 3\sum_q e_q^2 \left[1 + \frac{\alpha_{\overline{\rm MS}}(Q)}{\pi} + \frac{\alpha^2_{\overline{\rm MS}}}{\pi^2}(1.98 - 0.115 n_f) + \cdots\right]$$

$$\to 3\sum_q e_q^2 \left[1 + \frac{\alpha_{\overline{\rm MS}}(Q^*)}{\pi} + \frac{\alpha^2_{\overline{\rm MS}}(Q^*)}{\pi^2}\, 0.08 + \cdots\right] , \tag{99}$$

where from Eqs. (96) and (97), $Q^* = 0.708Q$. Notice that $\alpha_R(Q)$ differs from $\alpha_{\overline{\rm MS}}(Q^*)$ by only $0.08\ \alpha_{\overline{\rm MS}}/\pi$, so that $\alpha_R(Q)$ and $\alpha_{\overline{\rm MS}}(0.71\,Q)$ are effectively interchangeable (for any value of n_f).

Deep-inelastic scattering. The moments of the non-singlet structure function $F_2(x, Q^2)$ obey the evolution equation[135]

$$Q^2\frac{d}{dQ^2}\,\ell n\, M_n(Q^2) = -\frac{\gamma_n^{(0)}}{8\pi}\,\alpha_{\overline{\rm MS}}(Q)\left[1 + \frac{\alpha_{\overline{\rm MS}}}{4\pi}\,\frac{2\beta_0\beta_n + \gamma_n^{(1)}}{\gamma_n^{(0)}} + \cdots\right]$$

$$\to -\frac{\gamma_n^{(0)}}{8\pi}\,\alpha_{\overline{\rm MS}}(Q_n^*)\left[1 - \frac{\alpha_{\overline{\rm MS}}(Q_n^*)}{\pi}\,C_n + \cdots\right] , \tag{100}$$

where, for example,

$$\begin{aligned} Q_2^* &= 0.48Q\ , \qquad & C_2 &= 0.27\ , \\ Q_{10}^* &= 0.21Q\ , \qquad & C_{10} &= 1.1\ . \end{aligned} \tag{101}$$

For n very large, the effective scale here becomes $Q_n^* \sim Q/\sqrt{n}$, which is exactly what was found in Ref. 136 by a detailed study of the kinematics of deep-inelastic scattering.

η_c decay. The ratio of the η_c width into hadrons to that into $\gamma\gamma$ is $(n_f = 3)$,[137]

$$\frac{\Gamma(\eta_c \to \text{hadrons}}{\Gamma(\eta_c \to \gamma\gamma)} = \frac{2}{9e_c^4} \frac{\alpha^2_{\overline{\rm MS}}(M)\eta_c)}{\alpha^2_{QED}} \left[1 + \frac{\alpha_{\overline{\rm MS}}}{\pi}(17.13 - \frac{8}{9}n_f)\cdots\right]$$

$$\to \frac{2}{9e_c^4} \frac{\alpha^2_{\overline{\rm MS}}(Q^*)}{\alpha^2_{QED}} \left[1 + \frac{\alpha_{\overline{\rm MS}}(M^*)}{\pi} 2.46 + \cdots\right] , \tag{102}$$

where $Q^* = 0.26\, M_{\eta_c}$.

Υ decay. The ratio of the hadronic to the leptonic widths of the Υ is $(n_f = 4)$,[138]

$$\frac{\Gamma(\Upsilon \to \text{hadrons})}{\Gamma(\Upsilon \to \mu^+\mu^-)} = \frac{10(\pi^2 - 9)}{81\pi e_b^2} \frac{\alpha^3_{\overline{\rm MS}}(M_\Upsilon)}{\alpha^2_{QED}}$$

$$\times \left[1 + \frac{\alpha_{\overline{\rm MS}}}{\pi}[2.770(7)\beta_0 - 14.0(5)] + \cdots\right]$$

$$\to \frac{10(\pi^2 - 9)}{81\pi e_b^2} \frac{\alpha^3_{\overline{\rm MS}}(Q^*)}{\alpha^2_{QED}} \left[1 + \frac{\alpha_{\overline{\rm MS}}(M^*)}{\pi} 14.0(5) + \cdots\right] , \tag{103}$$

where $Q^* = 0.157\, M_\Upsilon$. Thus the decay rate into gluons has a large negative correction with this physical definition of the coupling, just as do the rates for $\Upsilon \to \gamma\gamma\gamma$ and for orthopositronium decay into three photons, both of which are scheme and scale independent to this order. Such a correction implies large, positive terms in higher orders, and, in fact, these are necessary if we are to fit the data. further study is clearly necessary before Υ decay can be used as a reliable measure of α_s. We do note, however that the large corrections cancel[139] almost completely in the branching ratio for producing a direct photon plus hadrons:[140]

$$\frac{\Gamma(\Upsilon \to \gamma_D + \text{hadrons})}{\Gamma(\Upsilon \to \text{hadrons})} = \frac{36e_b^2}{5} \frac{\alpha_{QED}}{\alpha_{\overline{\rm MS}}(Q^*)} \left[1 + \frac{\alpha_{\overline{\rm MS}}(Q^*)}{\pi} 2.2(6) + \cdots\right] , \tag{104}$$

where again $M^* = 0.157\, M_\Upsilon$. This cancellation occurs because the leading-order amplitudes for $\Upsilon \to ggg$ and $\Upsilon \to \gamma gg$ are identical in

structure. Thus the branching ratio for direct photons could be used to determine $\alpha_{\overline{\rm MS}}$.

Exclusive processes. Exclusive processes involving large transverse momentum are given by the convolution of distribution amplitudes $\psi(x,Q)$, representing the wave functions of each initial- and final-state hadrons, with (collinear irreducible) hard-scattering amplitudes $T_H(x_i,Q)$ in which each hadron is replaced by collinear on-shell quarks (or gluons).[8] The procedure given above allows us trivially to include the vacuum-polarization corrections to the (skeleton) tree graphs contributing to T_H, and thus set the coupling-constant scale for the leading-order results. For example, the hard-scattering amplitude required for the form factor of helicity-zero mesons is

$$T_H(x,y,Q) = \frac{64\pi}{3Q^2}\,\frac{\alpha_{\overline{\rm MS}}(e^{-5/6}[(1-x)(1-y)]^{1/2}Q)}{(1-x)(1-y)} \tag{105}$$

since the gluon's momentum transfer is $-(1-x)(1-y)Q^2$. If we estimate $\langle x\rangle \sim \langle y\rangle \sim \frac{1}{2}$, then the correct expansion parameter for T_H is $\sim \alpha_{\overline{\rm MS}}(Q/4.6)$ in agreement with the detailed analysis of Ref. 141.

$Q\overline{Q}$ potential. The interaction potential between two infinitely massive quarks is[142]

$$\begin{aligned} V(Q^2) &= -\frac{C_F 4\pi\alpha_{\overline{\rm MS}}(Q)}{Q^2}\left[1+\frac{\alpha_{\overline{\rm MS}}}{\pi}\left(\frac{5}{12}\beta_0-2\right)+\cdots\right] \\ &\to -\frac{C_F 4\pi\alpha_{\overline{\rm MS}}(Q^*)}{Q^2}\left[1-\frac{\alpha_{\overline{\rm MS}}(Q^*)}{\pi}2+\cdots\right], \end{aligned} \tag{106}$$

where $Q^* = e^{-5/6}$, $Q \cong 0.43\,Q$. This result shows that the effective scale of the $\overline{\rm MS}$ scheme should generally be about half of the true momentum transfer occurring in the interaction. In parallel to QED, the effective potential $V(Q^2)$ gives a particularly intuitive scheme for defining the QCD coupling constant

$$V(Q^2) \equiv -\frac{4\pi C_F \alpha_v(Q)}{Q^2}\,, \tag{107}$$

with $\alpha_v(Q) = \alpha^{\overline{\rm MS}}(e^{-5/6}Q)(1-2\alpha_{\overline{\rm MS}}/\pi\ldots)$. The perturbative QCD prediction can be tested empirically—without scheme or scale ambiguities—if the prediction for two processes are consistent with experiment.

The automatic scale-fixing procedure can be summarized as follows. Given a renormalization scheme for α_s, the QCD perturbative expansion for the processes of interest takes the form

$$\rho = C_0 \alpha_s(Q^*)(1 + C_1^* \alpha_s/\pi + \cdots) \; . \tag{108}$$

The scale Q^* should then be chosen such that Q^* and C_1^* are independent of n_f, the number of "light" fermions (*i.e.*, with $m_q \ll Q^*$). Most importantly, this implies that the expansion is unchanged in low orders as the important momenta vary across a quark threshold—all vacuum-polarization effects due to a new quark are automatically absorbed into the effective coupling constant. Clearly this is where such effects belong. For the processes of interest, the low-order expansions well below and well above such a threshold differ only by gluon self-energy corrections due to the new quark, provided, of course, the argument of α_s is rescaled with the momenta. Such self-energy contributions are then correctly absorbed into the coupling constant, leaving the expansion unchanged across the threshold. Whatever scheme is employed, this criterion of n_f independence uniquely determines the scale appropriate to that scheme for both Abelian and non-Abelian theories.

A striking feature of each of the perturbative QCD predictions discussed here is that—except for Υ decay—the first-order correction in $\alpha_{\overline{\rm MS}}$ is only 10 to 20 percent of the leading term at typical Q^2 after the scale has been fixed. [This is despite the fact that the coefficient $A_{VP} n_f + B$ is replaced by $16.5 A_{VP} + B$, as in Eqs. (96) and (97).] Perturbation theory seems to work rather well—the leading term in $\alpha_{\overline{\rm MS}}(Q^*)$ for these processes is by itself quite accurate. The main effect of the higher-order corrections is in setting the correct scale Q^*, and for this only the fermionic vacuum-polarization corrections are needed. In effect, the BLM scale-fixing prescription uses the fermionic loops to probe the momentum flowing in the leading-order diagrams. The remainder of the higher-order corrections, *i.e.*, the $[(\frac{33}{2})A_{VP} + B]\alpha_s/\pi$ correction, must of course be computed to obtain predictions with precision better than 10 to 20 percent.

For Υ decay into three gluons [Eq. (103)], the higher-order corrections are quite large, calling into question the possibility of a perturbative analysis of this reaction. The fact that the higher-order corrections

for the corresponding decay of orthopositronium in QED are large indicates that this effect is not due to ambiguities in the renormalization scale.

Self-Consistency of Scale-Setting Procedures

Recently, Hung Jung Lu and I have discussed additional criteria which bear on the self-consistency of the scale setting methods.

1. *Existence and Uniqueness of* μ.
2. *Reflexivity.* Given a coupling constant (or an effective charge defined in terms of an observable[114]) $\alpha(\mu)$ specified at a scale μ, we can express it in terms of itself, but specified at another scale μ':

$$\alpha(\mu) = \alpha(\mu') - \frac{\beta_0}{4\pi} \log(\mu^2/\mu'^2)\alpha^2(\mu') + \cdots, \qquad (109)$$

   where $\beta_0 = 11 - 2n_f/3$ is the first coefficient of the QCD beta function.

   If a scale-setting prescription is self-consistent, it should choose the unique value $\mu' = \mu$ on the right-hand side. Notice that when μ' is chosen to be μ, the above equation reduces to a trivial identity. This is a very basic requirement, since if $\alpha(\mu)$ is known (say, experimentally measured for a range of scale μ), and then we try to use the above equation to "predict" $\alpha(\mu)$ from itself, any deviation of μ' from μ would lead to an inaccurate result due to the truncation of the expansion series.
3. *Symmetry.* Given two different coupling constants (or effective charges,[114] or renormalization schemes) $\alpha_1(\mu_1)$ and $\alpha_2(\mu_2)$, we can express one of them in terms of the other:

$$\begin{aligned} \alpha_1(\mu_1) &= \alpha_2(\mu_2) + r_{12}\ (\mu_1, \mu_2)\alpha_2^2(\mu_2) + \cdots, \\ \alpha_2(\mu_2) &= \alpha_1(\mu_1) + r_{21}\ (\mu_2, \mu_1)\alpha_1^2(\mu_1) + \cdots. \end{aligned} \qquad (110)$$

   If a scale-setting method gives

$$\mu_2 = \lambda_{21}\ \mu_1 \qquad (111)$$

for the first series and

$$\mu_1 = \lambda_{12}\ \mu_2 \tag{112}$$

for the second series, then this method is said to be symmetric if

$$\lambda_{12}\ \lambda_{21} = 1. \tag{113}$$

This feature is desirable since it gives us a unique ratio between μ_1 and μ_2, irrelevant of which way we choose to expand the coupling constants.

4. *Transitivity.* Given three different coupling constants $\alpha_1(\mu_1)$, $\alpha_2(\mu_2)$, and $\alpha_3(\mu_3)$, we can establish the relation between μ_1 and μ_3 in two ways:
Going through the extra scheme $\alpha_2(\mu_2)$. That is, we can fix the relative scales in the two series

$$\begin{aligned} \alpha_1(\mu_1) &= \alpha_2(\mu_2) + r_{12}(\mu_1,\mu_2)\ \alpha_2^2(\mu_2) + \cdots, \\ \alpha_2(\mu_2) &= \alpha_3(\mu_3) + r_{23}(\mu_2,\mu_3)\ \alpha_3^2(\mu_3) + \cdots,\ cr \end{aligned} \tag{114}$$

to obtain

$$\mu_1 = \lambda_{12}\ \mu_2, \qquad \mu_2 = \lambda_{23}\ \mu_3, \tag{115}$$

and combine the last two expressions to get

$$\mu_1 = \lambda_{12}\lambda_{23}\ \mu_3. \tag{116}$$

Directly setting μ_1 in terms of μ_3 in the series

$$\alpha_1(\mu_1) = \alpha_3(\mu_3) + r_{13}(\mu_1,\mu_3)\alpha_3^2(\mu_3) + \cdots \tag{117}$$

to get

$$\mu_1 = \lambda_{13}\ \mu_3. \tag{118}$$

A scale-setting method is transitive if the two paths of substitution give the same result. That is,

$$\lambda_{12}\ \lambda_{23} = \lambda_{13}. \tag{119}$$

A scale-setting method that satisfies reflexivity, symmetry, and transitivity effectively establishes an equivalent relation among all the

effective charges. This is a necessary feature since it guarantees that no matter how we move from one effective charge to another, we will always keep a consistent choice of scale.

It is straightforward to verify that the FAC and BLM criteria satisfy all the consistency requirements outlined above.

Before analyzing the self-consistency relations for PMS, let us perform first some preliminary calculations. In what follows we will consider the case of QCD with N_f massless quarks.

Given the QCD beta function for an effective charge α_1:

$$\beta(\alpha_1) = \frac{d}{d\log\mu_1^2}\left(\frac{\alpha_1}{4\pi}\right) = -\beta_0\left(\frac{\alpha_1}{4\pi}\right)^2 - \beta_1\left(\frac{\alpha_1}{4\pi}\right)^3 - \cdots, \qquad (120)$$

where $\beta_0 = 11 - \frac{2}{3}n_f$ and $\beta_1 = 102 - \frac{38}{3}n_f$. To the next-to-leading order, α_1 is implicitly given by the following equation:

$$\frac{1}{a_1} + \log\left(\frac{a_1}{1+a_1}\right) = \tau_1 \qquad (121)$$

where $a_1 = \beta_1\beta_0^{-1}\alpha_1/4\pi$, and $\tau_1 = \beta_0^2\beta_1^{-1}\log(\mu_1^2/\Lambda_1^2)$.

Two effective charges α_1 and α_2 are related by the perturbative series

$$a_1(\tau_1) = a_2(\tau_2) + (\tau_2 - \tau_1)a_2^2(\tau_2) + \cdots, \qquad (122)$$

where $a_2 = \beta_1\beta_0^{-1}\alpha_2/4\pi$, and $\tau_2 = \beta_0^2\beta_1^{-1}\log(\mu_2^2/\Lambda_2^2)$. This is an equation of the form of Eq. (1) where the scale μ_2 is to be chosen. PMS proposes the choice of μ_2 (or equivalently, τ_2) at the stationary point, *i.e.*:

$$\frac{da_1}{d\tau_2} = 0 = \frac{d}{d\tau_2}\left[a_2(\tau_2) + (\tau_2 - \tau_1)a_2^2(\tau_2)\right]. \qquad (123)$$

From here we obtain the condition:

$$1 + a_2 = \frac{1}{2(\tau_1 - \tau_2)}. \qquad (124)$$

In order to obtain τ_2 in terms of τ_1, we must solve the last equation in

conjunction with

$$\frac{1}{a_2} + \log\left(\frac{a_2}{1+a_2}\right) = \tau_2. \tag{125}$$

Notice that in the large momentum region ($\tau_1, \tau_2 \gg 1$) we have

$$\tau_2 \sim \tau_1 - \frac{1}{2}. \tag{126}$$

In terms of μ_1 and μ_2, the relation becomes

$$\frac{\mu_2}{\Lambda_2} \sim \frac{\mu_1}{\Lambda_1} \exp(-\beta_1/4\beta_0^2). \tag{127}$$

Let us now check the self-consistency relations for PMS. For simplicity we will consider the large momentum kinematic region where the above approximation holds, although none of our conclusions will rely on this approximation.

Reflexivity is violated in PMS. When the PMS method is applied to Eq. (109), from Eq. (127) we obtain:

$$\mu' \sim \mu \exp(-\beta_1/4\beta_0^2) \neq \mu. \tag{128}$$

Unlike the cases of FAC and BLM, when we apply PMS to predict an effective charge from itself, an inaccurate result is obtained.

Symmetry and transitivity are also violated in PMS. Since

$$\lambda_{ij} = \frac{\mu_i}{\mu_j} \sim \frac{\Lambda_i}{\Lambda_j} \exp(-\beta_1/4\beta_0^2). \tag{129}$$

This would mean that

$$\begin{aligned} &\lambda_{12}\lambda_{21} \sim \exp(-\beta_1/2\beta_0^2) \neq 1, \\ &\lambda_{12}\lambda_{23} \sim \frac{\Lambda_1}{\Lambda_3} \exp(-\beta_1/2\beta_0^2) \neq \lambda_{13} \sim \frac{\Lambda_1}{\Lambda_3} \exp(-\beta_1/4\beta_0^2). \end{aligned} \tag{130}$$

That is, PMS does not satisfy the symmetry and transitivity conditions Hence, when we successively express one effective charge or observable in terms of others, PMS would lead to inconsistent scale choices.

The transitivity condition can be best illustrated in Fig. 21. Let A, B, C be three different physical observables or their effective charges. (For instance, A could represent the $\overline{\rm MS}$ coupling constant, B the total hadronic rate in e^+e^- annihilation, and C the value of the Bjorken sum rule.) QCD allows one to relate these three quantities. One can obtain C directly in terms of A, or one can obtain C in terms of B, and then B in terms of A. The transitivity of the FAC and BLM methods means that one obtains the same prediction for C either way. A scale setting method that is non-transitive can lead to incompatible results. This is usually not noticed due to the biased preference for the $\overline{\rm MS}$ scheme. That is, one often expresses perturbative QCD results only in terms of the $\overline{\rm MS}$ scheme, hence bypassing the potential inconsistency that would be present when physical quantities are related.

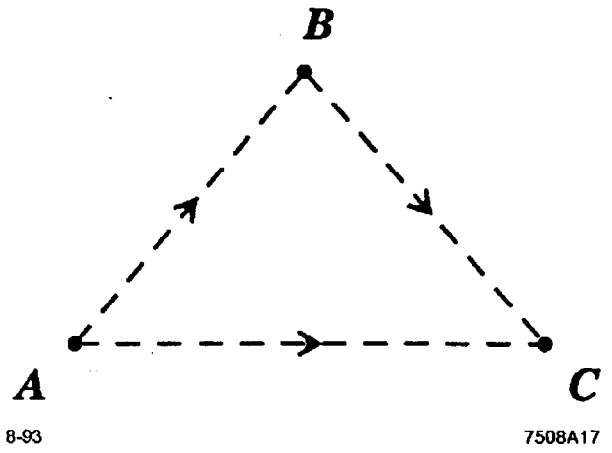

Figure 21. A triangle representing the transitivity condition. The quantity C can be obtained directly from A, or it can be obtained from B, and B obtained from A.

The reason that PMS does not meet these self-consistency requirements is that the minimization operations in general do not commute with the operations of reflexivity, symmetry and transitivity. The highly non-linear nature of the optimization method has been pointed out by Politzer.[143] For the PMS method, the result obtained directly and the result obtained through the use of an intermediate scheme in

general will differ. This non-commutativity is contrary to the Peterman-Stückelberg's full renormalization group invariance,[122] which states that physical predictions should not depend on the intermediate renormalization procedure. In this formalism, the effective charges of two physical observables can be related by an evolution path on the hypersurface defined by the QCD universal coupling function $a(\tau, \{c_i\})$,[144] where τ is the scale parameter and $\{c_i\}$ are the scheme parameters. Given a initial effective charge a_{init} at the point $(\tau_{init}, \{c_i^{init}\})$, we can use the evolution equations[113,144]

$$\begin{aligned} \frac{\delta a}{\delta \tau} &= \beta(a, \{c_i\}) = -a^2(1 + a + c_2 a^2 + c_3 a^3 + \cdots), \\ \frac{\delta a}{\delta c_n} &= \beta_{(n)}(a, \{c_i\}) = -\beta(a, \{c_i\}) \int_0^a dx \frac{x^{n+2}}{\beta^2(x, \{c_i\})}. \end{aligned} \tag{131}$$

to evolve a_{init} into a final effective charge a_{final} at the point $(\tau_{final}, \{c_i^{final}\})$. As long as we stay inside an analytical region where the second partial derivatives exist and commute, the predicted value of a_{final} will not depend on the path chosen for the evolution.

In Fig. 22 we illustrate the paths that represent the operations of reflexivity, symmetry and transitivity. We can pictorially visualize that the evolution paths satisfy all these three self-consistency properties. A closed path starting and ending at the point A represents the operation of identity. Since the predicted value does not depend on the chosen path, if the effective charge at A is a_A, after completing the path we will also end up with an effective charge a_A. Similarly, if we evolve a_B at B to a value a_C at C, we are guaranteed that when we evolve a_C at C back to the point B, the result will be a_B. Hence, the evolution equations also satisfy symmetry. Transitivity follows in a similar manner. Going directly from D to F gives the same result as going from D to F through a third point E.

In conclusion, we have shown that the BLM procedure chooses a scale well matched to the physics of the process. The BLM scale also indicates the cases where perturbative QCD is inapplicable such as at very small jet invariant masses. Unlike BLM, the FAC and PMS methods give no indication of the convergence of perturbation theory;

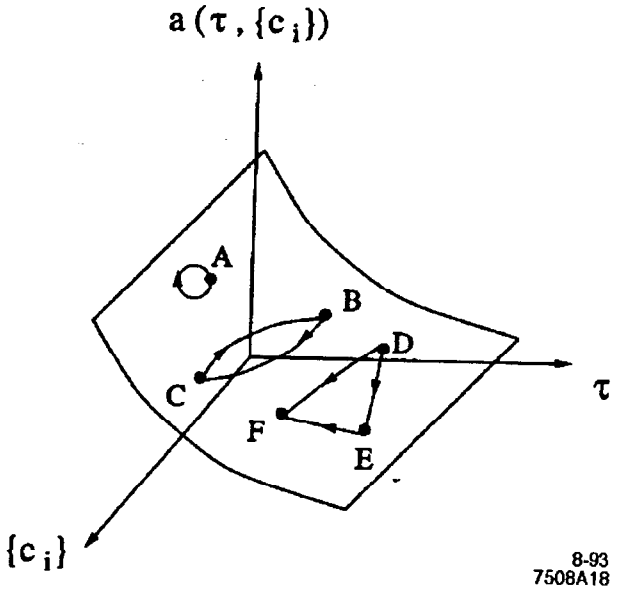

Figure 22. Pictorial representation of the universal coupling function. The point A with a closed path represents the operation of reflexivity. The paths $\overline{BC}$ and $\overline{CB}$ represent the operation of symmetry, and the paths $\overline{DE}$,$\overline{EF}$ and $\overline{DF}$ represent the operation of transitivity.

$C_1(Q^*)$ is by definition small and process independent for both of the methods mentioned above. Such methods will also be wrong when applied to processes, like Υ decay, for which the higher-order corrections are very large; worse, they give no warning of such situations.

We have also discussed several self-consistency conditions for setting the scale in QCD perturbative expansions which follow from the full renormalization group invariance proposed by Peterman and Stückelberg. We have shown that the FAC and BLM scale-setting procedures satisfy these self-consistency conditions, but that the scale-setting method based on the principle of Minimum Sensitivity (PMS) does not satisfy these criteria. In particular, we have shown that PMS is not transitive, *i.e.*, when one relates physical observables or coupling constants to each other, the predicted value of the physical quantity will depend on the path one uses to apply PMS. When we relate many physical observables or coupling constants to each other, the application of PMS will thus lead to a chaotic situation, where the predicted value of a physical quantity depend on how we arrive to it. This danger is usually not fully appreciated because traditionally one obtains perturbative QCD

results only in the $\overline{\rm MS}$ scheme, rather than relate physical observables directly to each other.

5 ACKNOWLEDGEMENTS

I wish to thank Professor T. D. Lee for organizing this workshop and his outstanding hospitality at CCAST. I also wish to thank my collaborators for many helpful discussions, especially Hung Jung Lu, Hans Christian Pauli, Peter Lepage, and Kent Hornbostel. Section 4 was written in collaboration with Hung Jung Lu. I also thank Kai Wong for helpful suggestions. Portions of the paper were also given as lectures at the 10th International Symposium on High Energy Spin Physics, Nagoya (1992) and the workshop "QCD—20 Years Later," Aachen (1992). This work was supported by the U.S. Department of Energy under Contract No. DE-AC03-76SF00515.

REFERENCES

1. For a recent review of the light-cone quantization of gauge theories see S. J. Brodsky, G. McCartor, H. C. Pauli, S. S. Pinsky, SLAC-PUB-5811, (1992).
2. For further discussions on many of the topics of this chapter and further references, see S. J. Brodsky and H. C. Pauli in *Recent Aspects of Quantum Fields*, H. Mitter and H. Gausterer, Eds.; Lecture Notes in Physics, Vol. 396, Springer-Verlag, Berlin, Heidelberg, (1991).
3. W. A. Bardeen, R. B. Pearson, and E. Rabinovici, *Phys. Rev.* **D21**, 1037 (1980); P. A. Griffin, *Nucl. Phys.* **B372**, 270 (1992).
4. D. Mustaki, S. Pinsky, J. Shigemitsu, K. Wilson *Phys. Rev.* **D43**, 3411 (1991); S. Glazek, A. Harindranath, S. Pinsky, J. Shigemitsu, K. Wilson, Ohio State University preprint OHSTPY-HEP-T-92-004, and references therein.

5. V. L. Chernyak and A. R. Zhitnitskii, *Phys. Rept.* **112**, 173 (19854); V. L. Chernyak, A. A. Oglobin, and I. R. Zhitnitskii, *Sov. J. Nucl. Phys.* **48**, 536 (1988); I. D. King and C. T. Sachrajda, *Nucl. Phys.* **B297**, 785 (1987); M. Gari and N. G. Stefanis, *Phys. Rev.* **D35**, 1074 (1987); and references therein.
6. A. S. Kronfeld and D. M. Photiadis, *Phys. Rev.* **D31**, 2939 (1985).
7. G. Martinelli and C. T. Sachrajda, *Phys. Lett.* **B217**, 319 (1989). Equal-time Fock state Coulomb gauge position space wavefunctions have been computed in quenched approximation lattice QCD in M. W. Hecht and T. DeGrand, *Phys. Rev.* **D46**, 2155 (1992).
8. G. P. Lepage and S. J. Brodsky, *Phys. Rev.* **D22**, 2157 (1980); *Phys. Lett.* **87B**, 359 (1979); *Phys. Rev. Lett.* **43**, 545, 1625E (1979).
9. See P. Kroll, Wuppertal University preprint WU-B-90-17 (1990), and references therein.
10. For a review, see S. J. Brodsky, SLAC-PUB 5529 (1991), published in the *Proceedings of the Lake Louise Winter Institute* (1991).
11. G. Bertsch, S. J. Brodsky, A. S. Goldhaber, J. F. Gunion, *Phys. Rev. Lett.* **47**, 297 (1981); S. J. Brodsky, P. Hoyer, *Phys. Rev. Lett.* **63**, 1566 (1989); S. J. Brodsky, P. Hoyer, A. H. Mueller, W. - K. Tang, *Nucl. Phys.* **B369**, 519 (1992). H. Heiselberg, G. Baym, B. Blaettel, L. L. Frankfurt, M. Strikman *Phys. Rev. Lett.* **67**, 2946 (1991).
12. P.A.M. Dirac, *Rev. Mod. Phys.* **21**, 392 (1949).
13. S. J. Brodsky, R. Roskies, and R. Suaya, *Phys. Rev.* **D8**, 4574 (1973). See also S. J. Brodsky and A. Langnau, SLAC-PUB-5667 (1991), and references therein.
14. H. C. Pauli and S. J. Brodsky, *Phys. Rev.* **D32**, 1993 (1985); *Phys. Rev.* **D32**1, 2001 (1985).
15. T. Eller, H. C. Pauli, S. J. Brodsky, *Phys. Rev.* **D35**, 1493 (1987).
16. A. Harindranath and J. P. Vary, *Phys. Rev.* **D36**, 1141 (1987).
17. K. Hornbostel, S. J. Brodsky, H. C. Pauli, *Phys. Rev.* **D41**, 3814 (1990). S. J. Brodsky and K. J. Hornbostel, to be published.

18. M. Burkardt, *Nucl. Phys.* **A504**, 762 (1989).
19. J. R. Hiller, University of Minnesota preprints (1990), and *Phys. Rev.* **D43**, 2418 (1991).
20. A. C. Tang, S. J. Brodsky, and H. C. Pauli, *Phys. Rev.* **D44**, 1842 (1991).
21. M. Kaluza and H. C. Pauli, *Phys. Rev.* **D45**, 2968 (1992).
22. M. Krautgartner, H. C. Pauli, F. Wolz *Phys. Rev.* **D45**, 3755 (1992).
23. S. D. Drell and T. M. Yan, *Phys. Rev. Lett.* **24**, 181 (1970).
24. For reviews of the theory of exclusive processes in QCD and further references see S. J. Brodsky and G. P. Lepage in *Perturbative Quantum Chromodynamics*, edited by A. Mueller (World Scientific, Singapore, 1989). A comprehensive comparison of baryon form factors with PQCD is given in P. Stoler, Rensselaer Polytechnic Institute preprint (1992), to be published in Physics Reports.
25. S. J. Brodsky and A. H. Mueller, *Phys. Lett.* **206B**, 685 (1988).
26. General QCD analyses of exclusive processes are given in Ref. 8, S. J. Brodsky and G. P. Lepage, SLAC-PUB-2294, presented at the Workshop on Current Topics in High Energy Physics, Cal Tech (Feb. 1979), S. J. Brodsky, in the *Proceedings of the La Jolla Institut Summer Workshop on QCD*, La Jolla (1978), A. V. Efremov and A. V. Radyushkin, *Phys. Lett.* **B94**, 245 (1980), V. L. Chernyak, V. G. Serbo, and A. R. Zhitnitskii, *Yad. Fiz.* **31**, 1069 (1980), S. J. Brodsky, Y. Frishman, G. P. Lepage, and C. Sachrajda, *Phys. Lett.* **91B**, 239 (1980), and A. Duncan and A. H. Mueller, *Phys. Rev.* **D21**, 1636 (1980).
27. QCD predictions for the pion form factor at asymptotic Q^2 were first obtained by V. L. Chernyak, A. R. Zhitnitskii, and V. G. Serbo, *JETP Lett.* **26**, 594 (1977), D. R. Jackson, Ph.D. Thesis, Cal Tech (1977), and G. Farrar and D. Jackson, *Phys. Rev. Lett.* **43**, 246 (1979). See also A. M. Polyakov, *Proceedings of the International Symposium on Lepton and Photon Interactions at High Energies*, Stanford (1975), and G. Parisi, *Phys. Lett.* **84B**, 225 (1979). See also S. J. Brodsky and G. P. Lepage, in *High Energy Physics–1980*, proceedings of the XXth International Conference, Madison, Wisconsin, edited by L. Durand and L. G.

Pondrom (AIP, New York, 1981), p. 568. A. V. Efremov and A. V. Radyushkin, Rev. Nuovo Cimento **3**, 1 (1980) and Ref. 26. V. L. Chernyak and A. R. Zhitnitskii, *JETP Lett.* **25**, 11 (1977); M. K. Chase, *Nucl. Phys.* **B167**, 125 (1980).

28. N. Isgur and C. H. Llewellyn Smith, *Phys. Rev. Lett.* **52**, 1080 (1984); *Phys.Lett* **B217**, 535 (1989).
29. A. V. Radyushkin, *Nucl. Phys.* **A532**, 141 (1991).
30. J. Botts and G. Sterman, *Nucl. Phys.* **B325**, 62 (1989); *Phys. Lett.* **B224**, 201 (1989); J. Botts, J.-W. Qiu, and G. Sterman, *Nucl. Phys.* **A527**, 577 (1991). H. N. Li and G. Sterman, Stony Brook preprint ITP-SB-92-10 (1991); H. N. Li, Stony Brook preprint ITP-SB-92-25 (1991).
31. A. N. Kronfeld and B. Nizic, *Phys. Rev.* **D44**, 3445 (1991). B. Nizic *Phys. Rev.* **D35**, 80 (1987).
32. S. J. Brodsky and G. R. Farrar, *Phys. Rev.* **D11**, 1309 (1975).
33. P. Stoler, *Phys. Rev.* **D44**, 73 (1991) *Phys. Rev. Lett.* **66**, 1003 (1991).
34. Higher twist amplitudes in the factorized PQCD formalism are computed in S. J. Brodsky, E. L. Berger, and, G. Peter Lepage, published in proceedings of the Drell Yan Workshop, Fermilab (1982); E. L. Berger and S. J. Brodsky, *Phys. Rev. Lett.* **42**, 940 (1979). For a recent analysis and additional references see S. S. Agaev, Baku State University preprint BSU HEP-0003 (1992).
35. See, *e.g.*, J. S. Conway *et al.*, *Phys. Rev.* **D39**, 92 (1989).
36. S. J. Brodsky and G. P. Lepage, *Phys. Rev.* **D24**, 1808 (1981).
37. B. Nizic, *Fizika* **18**, 113 (1986).
38. For a recent review of exclusive two-photon processes, see S. J. Brodsky, SLAC-PUB-5088 in the Proceedings of the *Tau-Charm Workshop*, Stanford, CA (1989).
39. S. J. Brodsky, G. P. Lepage, and P. B. Mackenzie, *Phys. Rev.* **D28**, 228 (1983).
40. G. R. Farrar, *et al. Nucl. Phys.* **B311**, 585 (1989).
41. D. Millers and J. F. Gunion, *Phys. Rev.* **D34**, 2657 (1986).
42. T. Hyer, SLAC-PUB-5889 (1992).

43. S. J. Brodsky, F. E. Close, J. F. Gunion, *Phys. Rev.* **D6**, 177 (1972).

44. M. A. Shupe, *et al.*, *Phys. Rev.* **D19**, 1921 (1979).

45. G. P. Lepage and S. J. Brodsky, *Phys. Rev.* **D24**, 2848 (1981).

46. See e.g., S. J. Brodsky and J. F. Gunion, *Phys. Rev. Lett.* **37**, 402 (1976).

47. A. Duncan, and A. H. Mueller, *Phys. Lett.* **90B**, 159 (1980).

48. A. Szczepaniak and L. Mankiewicz, *Phys. Lett.* **B266**, 153 (1991).

49. S. J. Brodsky and G. F. de Teramond, *Phys. Rev. Lett.* **60**, 1924 (1988).

50. M. Luke, A. V. Manohar, M. J. Savage, *Phys. Lett.* **B288**, 355 (1992).

51. S. J. Brodsky, and G. F. de Teramond, and I. A. Schmidt, *Phys. Rev. Lett.* **64**, 1011 (1990).

52. S. J. Brodsky, G. Kopp, and P. Zerwas, *Phys. Rev. Lett.* **58**, 443 (1987).

53. W. Bartel, *et al.*, *Phys. Lett.* **184B**, 288 (1987).

54. A. Szczepaniak, E. M. Henley, S. J. Brodsky, *Phys. Lett.* **B243**, 287 (1990).

55. P. Stoler, Ref. 33; and to be published in *Phys. Rev. D.*

56. S. J. Brodsky, G. P. Lepage, and S.A.A. Zaidi, *Phys. Rev.* **D23**, 1152 (1981).

57. S. J. Brodsky, C. Greub, C. Munger, and D. Wyler, to be published.

58. G. D. Date, Y. Frishman, J. Sonnenschein, *Nucl. Phys.* **B283**, 365 (1987); Y. Frishman, J. Sonnenschein WIS-92-54-PH, (1992).

59. For a recent discussion and further references, see C. S. Kim, *Nucl. Phys.* **B353**, 87 (1991).

60. J. J. Aubert, *et al.*, *Nucl. Phys.* **B213**, 31 (1983). See also E. Hoffmann and R. Moore, *Z. Phys.* **C20**, 71 (1983).

61. K. Hornbostel, private communication; S. J. Brodsky and K. Hornbostel, to be published.

62. S. J. Brodsky and I. A. Schmidt, *Phys. Lett.* **B234**, 144 (1990); *Phys. Rev.* **D43**, 179 (1991).

63. G. P. Lepage, S. J. Brodsky, T. Huang, P. B. Mackenzie, published in the *Proceedings of the Banff Summer Institute*, 1981.
64. S. J. Brodsky and P. Hoyer, SLAC-PUB-5422, (1991).
65. It also should be noted that in Gribov's approach to quark confinement, Pauli-Villars or dimensional regulation cannot even be used in principle for strong coupling problems in QCD because of the way it eliminates the negative energy sea.
66. S. J. Brodsky, Y. Frishman, G. P. Lepage and C. Sachrajda, Ref. 26. M. E. Peskin, *Phys. Lett.* **88B**, 128 (1979).
67. M. Burkardt, A. Langnau, SLAC-PUB-5394, (1990), and to be published.
68. T. Heinzl, S. Kruschke, E. Werner, *Phys. Lett.* **272B**, 54 (1991).
69. D. G. Robertson, SMUHEP/92-03 (1992); G. McCartor, *Z. Phys.* **C52**, 611 (1992); G. McCartor and D. G. Robertson, **Z. Phys. C53**, 679 (1992).
70. P. A. Griffin, University of Florida preprint UFIFT-HEP-92-17.
71. K. Hornbostel, *Phys. Rev.* **D45**, 3781 (1992).
72. J. J. Wivoda and J. R. Hiller, University of Minnesota Preprint (1992).
73. D. Soper, to be published.
74. A. Bassetto, Padova preprint PDFPD/91/TH/19 (1991).
75. See R. Jaffe, Invited talk given at 10th International Symposium on High Energy Spin Physics, Nagoya, Japan (1992).
76. For references to the data and a review, see A. Krisch, talk presented at the 10th International Symposium on High Energy Spin Physics, Nagoya, Japan (1992).
77. S. J. Brodsky, G. P. Lepage, in "Perturbative Quantum Chromodynamics", Edited by A. H. Mueller, World Scientific Publ. Co. (1989).
78. S. J. Brodsky, P. Hoyer, A. H. Mueller, W. K. Tang, Ref. 11.
79. By S. J. Brodsky, T. A. DeGrand, R. Schwitters, *Phys. Lett.* **79B**, 255 (1978).
80. V. D. Burkert and B. L. Ioffe, CEBAF-PR-92-018, (1992).
81. S. J. Brodsky, S. D. Drell, *Phys. Rev.* **D22**, 2236 (1980).
82. S. J. Brodsky, J. R. Hiller, *Phys. Rev.* **D46**, 2141 (1992).

83. S. J. Brodsky, J. R. Primack, *Annals Phys.* **52**, 315 (1969).
84. S. J. Brodsky, M. Burkardt, I. A. Schmidt, in preparation; S. J. Brodsky and I. A. Schmidt, Ref. 62.
85. V. N. Gribov and L. N. Lipatov, *Sov. J. Nucl. Phys.* **15**, 438 and 675 (1972).
86. P. Aurenche, *et al.*, *Phys. Rev.* **D39**, 3275 (1989).
87. J. D. Bjorken, *Phys. Rev.* **D1**, 1376 (1970).
88. C. Biino, *Phys. Rev. Lett.* **58**, 2523 (1987).
89. J. G. Heinrich, *et al.*, *Phys. Rev.* **D44,** 1909 (1991); M. Gusanziroli, *et al.*, Z. Phys. **C37**, 545 (1988).
90. S. J. Brodsky, W. Tang, P. Hoyer, and M. Vanttinen, in preparation.
91. J. Badier, *et al.*, Z. Phys. **C20**, 101 (1983).
92. D.M. Alde, *et al. Phys. Rev. Lett.* **66**, 133 (1991).
93. R. Vogt, S. J. Brodsky, P. Hoyer, *Nucl. Phys.* **B360**, 67 (1991).
94. S. J. Brodsky, E. L. Berger, G. P. Lepage, SLAC-PUB-3027, published in the proceedings of the Workshop on Drell-Yan Processes, Batavia, IL, (1982).
95. J. Botts, *Phys. Rev.* **D44**, 2768 (1991); H. Li, G. Sterman, *Nucl. Phys.* **B381**, 129 (1992).
96. P. Bosted, *et al.*, *Phys. Rev. Lett.* **68**, 3841 (1992).
97. V. D. Burkert, CEBAF-PR-87-006. P. Stoler, Ref. 33.
98. A.S. Kronfeld B. Nizic, Ref. 31 and *Phys. Rev.* **D46**, 2272 (1992). T. Hyer, Ref. 42.
99. S. J. Brodsky, G. P. Lepage, and San Fu Tuan, *Phys. Rev. Lett.* **59**, 621 (1987).
100. M. Chaichian, N. A. Tornqvist, *Nucl. Phys.* **B323**, 75 (1989).
101. S. S. Pinsky, *Phys. Lett.* **B236**, 479 (1990).
102. Wei-Shou Hou and A. Soni, *Phys. Rev. Lett.* **50**, 569 (1983).
103. P. G. O. Freund and Y. Nambu, *Phys. Rev. Lett.* **34**, 1645 (1975).
104. A. S. Carroll, *et al.*, *Phys. Rev. Lett.* **61**, 1698 (1988).
105. G. C. Blazey *et al.*, *Phys. Rev. Lett.* **55**, 1820 (1985).
106. J. F. Gunion, R. Blankenbecler, and S. J. Brodsky, *Phys. Rev.* **D6**, 2652 (1972).

107. A. W. Hendry, *Phys. Rev.* **D10**, 2300 (1974).

108. J. P. Ralston and B. Pire, *Phys. Rev. Lett.* **57**, 2330 (1986); Phys. Lett. **117B**, 233 (1982); University of Kansas preprint 5-15-92, (1992). See also G. P. Ramsey and D. Sivers, *Phys. Rev.* **D45**, 79 (1992); and C. E. Carlson, M. Chachkhunashvili, and F. Myhrer, *Phys. Rev.* **D46** 2891 (1992).

109. G. Alexander *et al.*, *Phys. Rev.* **154**, 1284 (1967).

110. S. J. Brodsky and H. J. Lu, *Phys. Rev. Lett.* **64**, 1342 (1990).

111. V. Del Duca, S. J. Brodsky, P. Hoyer, *Phys. Rev.* **D46**, 931 (1992).

112. N. N. Nikolaev, talk given at the 10th International Symposium on High Energy Spin Physics, Nagoya, Japan (1992).

113. P. M. Stevenson, *Phys. Lett.* **B100,** 61 (1981); *Phys. Rev.* **D23,** 2916 (1981); *Nucl. Phys.* **B203,** 472 (1982); *Nucl. Phys.* **B231,** 65 (1984).

114. G. Grunberg, *Phys. Lett.* **B95,** 70 (1980); *Phys. Lett.* **B110,** 501 (1982); *Phys. Rev.* **D29,** 2315 (1984).

115. S. G. Gorishny, A. L. Kataev and S. A. Larin, *Phys. Lett.* **B259,** 144 (1991).

116. J. Chýla, A. L. Kataev and S. A. Larin, *Phys. Lett.* **B267,** 269 (1991), J. Chýla and A. L. Kataev, preprint CERN-TH-6604/92.

117. L. R. Surguladze and M. A. Samuel, *Phys. Rev. Lett.* **66,** 560 (1991), erratum: *ibid.* **66,** 2416 (1991).

118. S. A. Larin, F. V. Tkachov and J. A. M. Vermaseren, *Phys. Rev. Lett.* **66,** 862 (1991), S. A. Larin and J. A. M. Vermaseren, *Phys. Lett.* **B259,** 345 (1991), S. A. Larin, F. V. Tkachov and J. A. M. Vermaseren, *Phys. Lett.* **B272,** 121 (1991).

119. E. L. Berger, R. Meng, and W. Tung, *Phys. Rev.* **D46,** 1895 (1992).

120. A. Dhar, *Phys. Lett.* **B128,** 407 (1983), A. Dhar and V. Gupta, *Pramana* **21,** 207 (1983) and *Phys. Rev.* **D29,** 2822 (1984), V. Gupta, D. V. Shirkov and O. V. Tarasov, *Int. J. Mod. Phys.* **A6,** 3381 (1991).

121. O. V. Tarasov, A. A. Vladimirov and A. Yu. Zharkov, *Phys. Lett.* **B93,** 429 (1980).

122. E. C. G. Stückelberg and A. Peterman, *Helv. Phys. Acta* **26,** 499 (1953), A. Peterman, *Phys. Rept.* **53 C,** 157 (1979).

123. C. J. Maxwell, *Phys. Rev.* **D29,** 2884 (1984).

124. P. M. Stevenson, *Phys. Rev.* **D33,** 3130 (1986).

125. G. 't Hooft in The Whys of Subnuclear Physics, Proc. Intern. School of Subnuclear Physics (Erice, 1977), ed. A. Zichichi (Plenum, New York, 1979), p. 943.

126. M. Haruyama, *Phys. Rev.* **D45,** 930 (1992).

127. V. Branchina, M. Consoli, D. Zappala and R. Fiore, *Phys. Rev.* **D46,** 75 (1992).

128. R. Marshall, *Z. Phys.* **C43,** 595 (1989).

129. G. B. West, *Phys. Rev. Lett.* **67,** 1388 (1991), erratum: *ibid.* **67,** 3732 (1991).

130. D. T. Barclay and C. J. Maxwell, preprint DTP-91/72 (Durham, UK 1991), M. A. Samuel and E. Steinfeld, OSU preprint RN-256, 1992, L. S. Brown and L. G. Yaffe, *Phys. Rev.* **D45,** 398 (1992).

131. Particle Data Group, Review of Particle Properties, *Phys. Rev.* **D45,** S1 (1992).

132. G. Kramer and B. Lampe, *Zeit. Phys.* **A339,** 189 (1991).

133. E. L. Berger and J.-W. Qiu, *Phys. Rev.* **D44,** 2002 (1991).

134. M. Dine and J. Sapirstein, *Phys. Rev. Lett.* **43,** 668 (1979); K. C. Chetyrkin, A. L. Kataev, and F. V. Tkachov, *Phys. Lett.* **85B,** 277 (1979); *Phys. Rev.* **D21,** 3312 (1980). For a recent discussion of the three-loop calculation and further references, see L. R. Surguladze, and Mark A. Samuel, *Phys. Lett.* **B309,** 157 (1993).

135. For a review, see A. J. Buras, *Rev. Mod. Phys.* **52,** 1 (1980).

136. S. J. Brodsky and G. P. Lepage, in *Quantum Chromodynamics, Proceedings of the Summer Institute on Particle Physics*, SLAC, 1979, edited by Anne Mosher (SLAC, Stanford, 1980); D. Amati *et al.*, *Nucl. Phys.* **B173,** 429 (1980).

137. R. Barbieri *et al.*, *Nucl. Phys.* **B154,** 535 (1979).

138. P. B. Mackenzie and G. P. Lepage, *Phys. Rev.* **47,** 1244 (1981).

139. In general, our scale-fixing procedures should be applied to each process separately, not to ratios, as in Eq. (104). Each process will usually have its own optimal scale Q^*. However, in the case of $\Upsilon \to ggg$ and $\Upsilon \to \gamma gg$, the scale Q^* is identical, so Eq. (104) is valid.

140. P. B. Mackenzie and G. P. Lepage, in *Perturbative Quantum Chromodynamics*, proceedings of the conference, Tallahasse, 1981, edited by D. W. Duke and J. F. Owens (AIP, New York, 1981).

141. R. D. Field *et al.*, *Nucl. Phys.* **B186,** 429 (1981); F.-M. Dittes and A. V. Radyushkin, *Yad. Fiz.* **34,** 529 (1981) [*Sov. J. Nucl. Phys.* **34,** 293 (1981)].

142. W. Fischler, *Nucl. Phys.* **B129,** 157 (1977); A. Billoire, *Phys. Lett.* **92B,** 343 (1980); W. Buchmuller, G. Grunberg, and S.-H.H. Tye, *Phys. Rev. Lett.* **45,** 103 (1980); **45,** 587(E) (1980).

143. H. D. Politzer, *Nucl. Phys.* **B194,** 493 (1982).

144. H. J. Lu and S. J. Brodsky, preprint SLAC-PUB-5938R (1993).